DEVELOPMENT OF THE NEW YEAST-BASED ASSAYS FOR PRION PROPERTIES

A Dissertation
Presented to
The Academic Faculty

By

Meng Sun

In Partial Fulfillment
Of the Requirements for the Degree
Doctor of Philosophy in Biology

Georgia Institute of Technology

December, 2011

DEVELOPMENT OF THE NEW YEAST-BASED ASSAYS FOR PRION PROPERTIES

Approved by:

Dr. Yury Chernoff, Advisor
School of Biology
Georgia Institute of Technology

Dr. Kirill Lobachev
School of Biology
Georgia Institute of Technology

Dr. Roger Wartell
School of Biology
Georgia Institute of Technology

Dr. Francesca Storici
School of Biology
Georgia Institute of Technology

Dr. John Cairney
President and Scientific Director
NanoBiotechnologies

Date approved: August 5, 2011

DEDICATION

I dedicate this thesis to my parents, and my family. This work would not exist

without your constant love, faith, support and encouragement.

ACKNOWLEDGEMENTS

I thank my advisor Dr. Yury Chernoff for wise advisement, guidance and discussion throughout my research and thesis.

I thank my thesis committee members, Dr. Kirill Lobachev, Dr. Roger Wartell, Dr. John Cairney and Dr. Francesca Storici, for support, encouragement, feedback and suggestions.

I thank our lab manager, Gary Newnam, for technical support, and the grammar checking for my thesis.

I thank research scientist Andrey Romanyuk, for his help and advice in my biochemical research.

I thank graduate student Katy Bruce, for the grammar checking for my thesis.

I thank all Chernoff lab members, past and present.

TABLE OF CONTENTS

LIST OF TABLES

LIST OF FIGURES

CHAPTER 4

SUMMARY

Prion is an infectious isoform of a normal cellular protein which is capable of converting the non-prion form of the same protein into the alternative prion form. Mammalian prion protein PrP is responsible for prion formation (PrP^{Sc}) in mammals, causing a series of fatal and incurable prion diseases. (1) We constructed, for the first time, a two-component system to phenotypically monitor the conformational status of PrP in the yeast cells. In this system, the prion domain of Sup35 (Sup35N) was fused to PrP$_{90-230}$, and the initial formation of the PrP^{Sc}-like conformation stimulated prion formation of Sup35N, which in turn converted soluble Sup35 into the prion isoform, leading to a detectable phenotype. Prion-like properties of PrP were studied in this novel yeast model system. Additionally, we employed this system to study amyloidogenic protein Aβ42 aggregation in the yeast model.

It has been suggested that the ability to form transmissible amyloids (prions) is widespread among yeast proteins and is likely intrinsic to proteins from other organisms. However, the distribution of yeast prions in natural conditions is not yet clear, which prevents us from understanding the relationship between prions and their adaptive roles in various environmental conditions. (2) We modified and developed sequence and phenotype-independent approaches for prion detection and monitoring. We employed these approaches for prion-profiling among yeast strains of various origins.

(3) Lastly, we found a prion-like state [MCS^+] causing nonsense suppression in the absence of the Sup35 prion domain. Our results suggested that [MCS^+] is determined by both a prion factor and a nuclear factor. The prion-related properties of [MCS^+] were studied by genetic and biochemical approaches.

CHAPTER 1
INTRODUCTION

1-1 Prions and amyloids

A prion (proteinaceous infectious particle) is an infectious isoform of a normal cellular protein which is capable of converting the non-prion form of the same protein into the alternative prion form (Figure 1-1). Prion conversion is always associated with a conformational change of the secondary structure of the native protein which forms a highly a stable β-sheet-rich structure termed "amyloid". Prions are self-propagating amyloids and the β-sheet-rich structure can be precisely reproduced and transmitted solely by the prion protein itself. The prion concept was first proposed by Prusiner in 1982 (Prusiner et al., 1982), and explains a series of mammalian neurodegenerative disorders caused by an abnormal isoform of the prion protein PrP. Prions have also been identified in fungi, although the responsible proteins are not homologous in sequence to mammalian PrP.
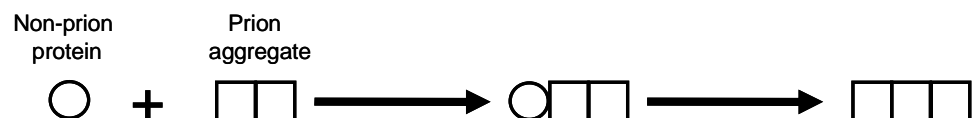
Figure 1-1. The prion model: Prion is an infectious or heritable agent made only of protein. A prion protein can convert a non-prion protein of the same amino acid sequence into a prion
.

1-2 Prion diseases

Prion diseases, also known as transmissible spongiform encephalopathies (TSE), are fatal neurodegenerative disorders which occur in humans and animals (Table 1-1). No treatments for prion diseases are currently available. Prion diseases are characterized by the transformation of a cellular prion protein of normal conformation, PrP^C, into a β-sheet-rich and protease-resistant conformation, PrP^{SC}.

Table 1-1. Prion diseases in mammals

Affected species	Diseases
Sheep, goat	Scrapie
Cattle	Bovine spongiform encephalopathy ("mad cow" disease)
Deer, elk, mule, moose	Chronic wasting disease
Mink	Transmissible mink encephalopathy
Feline	Feline spongiform encephalopathy
Human	Creutzfeldt–Jakob disease (CJD), Gerstmann–Sträussler–Scheinker syndrome (GSS), Fatal familial insomnia (FFI), Kuru

Scrapie was the first recognized prion disease and affects sheep and goats (Kimberlin et al., 1981). Scrapie has been recognized in European countries for centuries and is present worldwide. Other identified prion diseases which affect animals include bovine spongiform encephalopathy (BSE) (Wells et al., 1987), chronic wasting disease of mule deer and elk (Williams and Young , 1980), transmissible mink encephalopathy (Marsh et al., 1992), feline spongiform encephalopathy of domestic cats (Wyatt et al., 1991), and spongiform encephalopathies of a number of zoo animals (Jeffrey and Wells et al., 1988; Kirkwood et al., 1990)

The human prion diseases have been classified into Creutzfeldt-Jakob disease (CJD), Gerstmann-Sträussler-Scheinker syndrome (GSS), fatal insomnia (FI) and kuru. Human prion diseases occur via sporadic, acquired, and inherited ways, and the most common is the sporadic form of CJD, which accounts for approximately 85% of all cases (Will et al., 1996). Sporadic CJD occurs in all countries with a random case distribution and an annual incidence of ~one per million. The pathogenesis of sporadic CJD remains unclear, and epidemiological studies have failed to identify any specific risk factors for sporadic CJD. Characteristically, the disease affects elderly individuals with a peak onset at 60–69 years of age, with a wide age range from 14 to over 90 years (Brown et al., 1986).

About 10-15% of human prion disease is inherited, and so far all cases have been associated with mutations in the PrP coding gene (*PRNP*) (Collinge et al., 1997; Collinge et al., 2001). To date, GSS has only been described in association with *PRNP* gene mutations and is inherited in an autosomal dominant manner. Histologically, the hallmark of GSS is the presence of multicentric PrP-amyloid plaques, while in most cases of CJD and FI, PrP^{Sc} accumulates in brain parenchyma without significant amyloid deposition. Acquired prion diseases include iatrogenic CJD and kuru and arise from accidental exposure to human prions through medical or surgical procedures or participation in cannibalistic feasts.

To understand the prion mechanism, two major issues need to be addressed: the initiation of prion formation and prion propagation. Unfortunately, neither of them is well understood. The initial prion conversion process remains a mystery. In fact *de novo*

formation of a prion is a rare event, and the majority of prion-associated diseases are sporadic. Although a number of disease-promoting mutations in PrP have been identified (van der Kamp et al., 2009; Solomon et al., 2009), systematic studies of the mechanisms by which mutations influence a prion are difficult due to a high complexity of the experimental animal models and long incubation times employed. Nevertheles, prion propagation, in other words, the conformational transmission from PrP^{Sc} to PrP^{C}, is being extensively studied using animal models. The likely mechanism of prion propagation is immobilization of the monomeric protein into amyloidogenic polymers, accompanied by conversion into the β-sheet-rich conformation (Lansbury et al., 1995).

Besides prion diseases, there are other human neurodegenerative diseases associated with formation of amyloids or amyloid-like polymers (Aguzzi et al., 2010). Two well known amyloidosis diseases are Huntington's disease (HD) and Alzheimer's disease (AD). Huntington's disease is an inherited neurodegenerative disorder caused by polyglutamine (polyQ) expansions in the huntingtin (Ht) protein, which leads to formation of fibrous polymers (Shao et al., 2007). Alzheimer's disease is another fatal neurodegenerative disease, affecting approximately 50% people by age 85 (Kidd et al., 2008). It is associated with accumulation of polymers of the amyloid β (Aβ) peptide, produced by proteolytic cleavage of amyloid protein precursor (APP) (Goedert et al., 2006; Roberson et al., 2006). Less that 1% of AD cases are associated with mutations; the rest are sporadic. Although AD is not known to be infectious from person to person, transmission of Aβ amyloids by injection has been observed in experimental models (Kane et al., 2000).

In summary, human prion diseases and other amyloidosis diseases are fatal and incurable. These diseases occur sporadically and their incidence increases with age. These diseases pose an enormous threat to human health and limit the human life span. It is very important to study the mechanism of prion and amyloid formation in order to achieve treatment or disease prevention.

1-3 Mammalian prion protein

Compelling evidence demonstrate that TSEs are transmitted by the mammalian prion protein (PrP) in an abnormal PrP^{Sc} (prion) conformation. Propagation occurs by converting the PrP^{C} cellular protein of the same sequence into a prion (Prusiner et al., 1982; Prusiner et al., 1998). Compared with wild type mouse, the PrP knockout mouse showed a complete resistance to prion disease and did not replicate prions (Bueler et al., 1993).

Prion protein PrP is highly conserved in mammals and may be present in all vertebrates. It is expressed during early embryogenesis and is found in most tissues in adults (Manson et al., 1992). However, the highest level of expression is detected in the central nervous system, and particular, in association with synaptic membranes. As a glycosylphosphatidylinositol (GPI) anchored cell-surface glycoprotein, it has been speculated that prion protein may have a role in cell adhesion or signaling processes, but its precise cellular function remains unclear.

Prion protein encoded by a single gene, *PRNP*, consists of about 250 residues (254 aa for mouse PrP) (Figures 1-2). With posttranslational processing, the 22 aa N-terminal signal peptide is removed, and the 23 aa C-terminal peptide is replaced with a GPI-anchor peptide. There is an unstructured copper binding octarepeats in the N-terminal region of PrP residues which is rich in glycine (Prusiner et al., 1998). NMR studies of the remaining protein (residues 90-230) show that the N-terminus is largely unstructured (Donne et al., 1997), and the C-terminus is an ordered globular domain. The structures of the C-terminal region of PrP^C from three species (mouse, hamster, and human) show that they each consist of three α helices and two short antiparallel β-strands (Riek et al., 1996; Riek et al., 1997; James et al., 1997; Donne et al.,1997; Zahn et al., 2000). The Mouse PrP_{90-230} region is essential and sufficient for prion transmission, while the N-terminus 90-120 region is especially required for prion formation. (Peretz et al., 1997) The prion form PrP^{Sc} has a highly stable β-sheet-rich conformation, which distinguishes it from the α-helix-rich, protease-sensitive PrP^C (Pan KM, 1993). Electron microscopy study suggests a parallel β-helix structure in PrP^{Sc} (Wille et al., 2002).
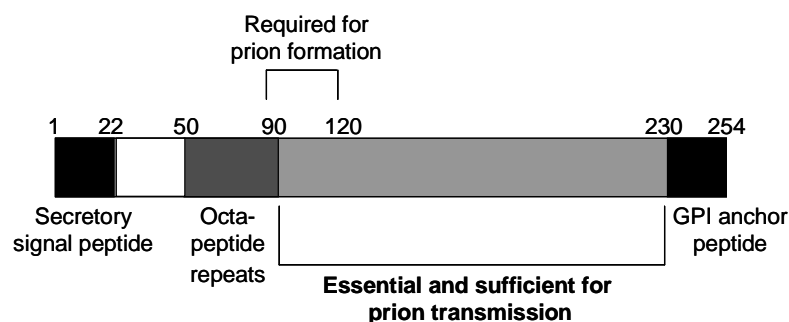
Figure 1-2: Structural and functional organization of mouse prion protein PrP The PrP protein consists of N terminal secretory signal peptide which is removed after maturation, octa-peptide repeats, and C terminal glycosylphosphatidyl inositol (GPI)

anchor peptide. The region emcompassing redisues 90-230 is essential and sufficient for the prion conversion and transmission. Numbers correspond to amino acid positions.

1-4 Yeast Prions

A numbers of prions have been found in yeast (in most cases *Saccharomyces cerevisiae*) which share many similarities with mammalian prions (Chien et al., 2004) (Table 1-2). Yeast prions manifest themselves as non-Mendelian heritable states transmitted via the cytoplasm, and are usually associated with a partial loss of the cellular function of a prion-forming protein. This partial loss of cellular function has enabled researchers to develop rapid and simple prion detection tools. Because of the ease of genetic manipulation and fast growth rate of yeast, yeast prions serve as a good model for the study of prions.

Table 1-2. Proven yeast prions

Protein	Prion state	Non-prion state	Cellular function
Sup35	[*PSI*⁺]	[*psi*⁻]	Translation termination factor
Ure2	[URE3]	[ure3-0]	Regulator in nitrogen metabolism
Rnq1	[*PIN*⁺]	[*pin*⁻]	Unknown
Swi1	[*SWI*⁺]	[*swi*⁻]	Chromatin remodeler
Mca1	[*MCA*⁺]	[*mca*⁻]	Metacaspase
Cyc8	[*OCT*⁺]	[*oct*⁻]	Transcriptional corepressor
Mot3	[*MOT3*⁺]	[*mot3*⁻]	Transcriptional repressor

As one of the most extensively studied yeast prions, [PSI^+] is the prion isoform of translational termination factor Sup35 (eRF3) (Cox et al., 1980, True et al., 2000). Sup35 protein is essential for cell viability, and it works with Sup45 to indentify stop codons and to terminate translation. Prion conversion of Sup35 results in a decreased translation termination function, due to its conformational change and amyloid formation. Another well characterized yeast prion is [URE3], whose functional isoform is Ure2, a posttranslational regulator in the nitrogen metabolism pathway (Shorter et al., 2005). The prion formation of [URE3] causes cells to constitutively utilize poor nitrogen sources. The [PIN^+] prion was initially detected by its ability to promote *de novo* formation of the [PSI^+] prion (Derkatch et al., 1997) and was then discovered to be an isoform of the Rnq1 protein of unknown cellular function called Rnq1 (Sondheimer and Lindquist, 2000, Derkatch et al., 2001).

There have been several more yeast prions identified in recent years, including [$MOT3^+$], [SWI^+], [OCT^+] and [MCA^+]. [$MOT3^+$] is a prion formed by the transcription factor Mot3, an environmentally responsive regulator of yeast cell wall composition and pheromone signaling (Abramova et al., 2001). Cells with the [$MOT3^+$] prion show increased resistance to certain cell wall stressors. [SWI^+] and [OCT^+] are formed by the globally acting transcriptional regulators, Swi1 and Cyc8, respectively (Du et al., 2008; Patel et al., 2009). [SWI^+] cells are resistant to the microtubule disruptor, benomyl; and [OCT^+] induces flocculation, a growth form that has been shown to protect cells from various stresses. [MCA^+] is a prion formed by Mca1, a metacaspase which has been proposed to

be involved in yeast programmed cell death processes (Nemecek et al., 2009). The physiological consequence of the [MCA^+] prion is not yet clear.

Yeast prion proteins contain prion domains (PrDs) which are responsible for both *in vivo* prion formation and propagation, and *in vitro* amyloid aggregation (Chernoff et al., 2004). For all the proven yeast prions (Table 1-2), the prion domains are glutamine (Q) and asparagine (N)- rich, and are always separate from the domains responsible for the major cellular function of the respective proteins. Unlike the mammalian prion PrP^{Sc}, yeast prions are not pathogenic. Prion infected yeast cells do not show apparent growth defects compared with wild-type, and they show even better growth in some unfavorable conditions. Thus it has even been proposed that yeast prions might have some adaptive roles in evolution (True et al., 2000, Chernoff et al., 2007; Chernoff et al., 2008).

1-5 Sup35 and the [PSI^+] prion

Sup35 is the protein responsible for the [PSI^+] prion; it contains 685 amino acids and can be divided into three domains (Figure 1-3 A). The 123 residue N-terminal domain (N) is the prion domain (PrD), which is essential for prion formation and propagation (Figure 1-3 B). The Sup35 N domain contains a Q/N rich stretch and five imperfect oligopeptide repeats. Experimental data suggest that [PSI^+] formation is driven primarily by the amino acid composition, but not by the sequence, of the Sup35 prion domain. In addition, Sup35p oligopeptide repeats are not required for prion maintenance (Ross et al., 2005; Toombs et al., 2010). The prion domain is dispensable for the cellular function of normal Sup35 protein.
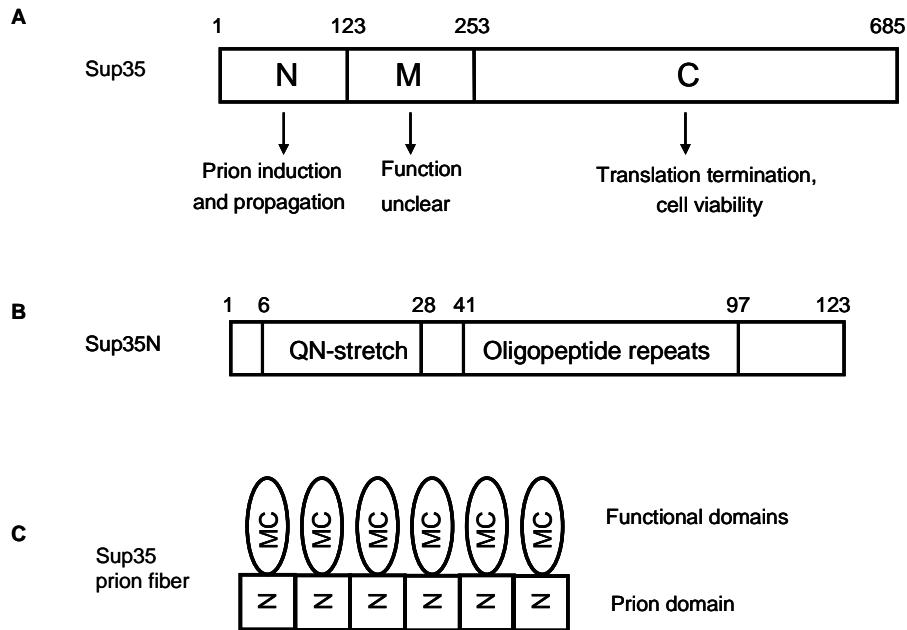
Figure 1-3. Structure of Sup35 and Sup35 prion fiber. N, M and C refer to Sup35N, Sup35M and Sup35C regions respectively. Numbers correspond to amino acid positions. **A**- Structural and functional organization of the Sup35 protein. **B**- Structure of the Sup35N region (prion domain). **C**- Structure of the Sup35 prion fiber. Sup35N domains form the core of the fiber, Sup35C (and possibly M) domains are exposed on the side. The ends of the fiber are active sites for immobilization of new sup35 molecules

The middle domain (M) (aa 124–253) is highly charged and is dispensable for both cell viability and [*PSI* $^+$] propagation (Derkatch et al., 1996; Kushnirov et al., 1990; Ter-Avanesyan et al., 1993). The M region is thought to promote protein solubility. *In vivo*, the fragment containing the Sup35N and M regions (NM) is soluble in yeast cells with no Sup35 prion ([*psi*$^-$]). In contrast, Sup35N alone is insoluble in the *[psi$^-$]* strain (Paushkin et al., 1996). The C-terminal domain (C) (aa 254–685) of Sup35 is the functional domain, which is responsible for the translation termination function. It is dispensable for [*PSI* $^+$] induction and propagation but is essential for viability (Derkatch et al., 1996; Ter-Avanesyan et al., 1994).

The prion conversion of Sup35 is associated with extensive conformational change of the prion domain to form a β-sheet enriched structure. Prion domains are connected together via β – β interactions and form the axis of the amyloid fiber (Krishnan et al., 2005; Nelson et al., 2005). The M and C domains are exposed on the side of the fiber and may retain the proper fold (Figure 1-3 C). The amyloid fiber is highly ordered and very stable, and it is protease-resistant and detergent insoluble (Kryndushkin et al., 2003; Bagriantsev et al., 2004).

1-6 Nonsense suppression system is used to assay [*PSI*$^+$]

In the [*PSI*$^+$] yeast strain, most of the Sup35 protein is sequestered as an amyloid, which in turn decreases its normal cellular function in translation termination. Based on this phenotypic character, a nonsense suppression assay is used to detect the [*PSI*$^+$] prion. (Figure 1-4) (Chernoff et al., 2000; Derkatch et al., 1996)

For the nonsense mutation allele *ade1-14* $_{UGA}$, the [*PSI*$^+$] strain has partial translational readthough, caused by the decreased translation termination function of Sup35. Therfore, there is still adenine produced and [*PSI*$^+$] cells can grow on the synthetic medium lacking adenine (-Ade). In [*psi*$^-$] cells, the nonsense mutation is not suppressed and cells can not grow on –Ade media. Also [*psi*$^-$] colonies show a red color on rich YPD medium while [*PSI*$^+$] colonies show a white color.
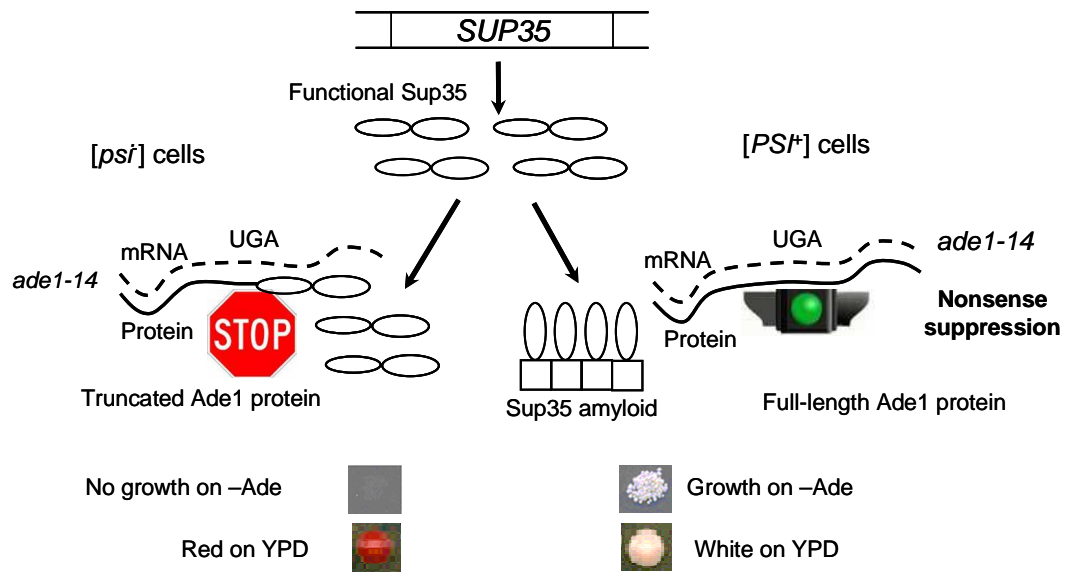
Figure 1-4. Nonsense suppression system is used to assay [*PSI*⁺] In [*PSI*⁺] strain, nonsense mutation *ade1-14* ₍UGA₎ was suppressed, cells can grow on –Ade medium sicnce adenine was produced. In [*psi*⁻] strain no functional adenine was produced, cells can not grow on –Ade medium. [*PSI*⁺] colonies show white color on YPD medium, while [*psi*⁻] colonies show red color on YPD medium.

1-7 *De novo* prion induction in yeast

Transient overproduction of Sup35 protein or its prion domain can induce *de novo* appearance of [*PSI*⁺] prion in a [*psi*⁻] cell (Chernoff et al., 1993), but the induction is only efficient in the presence of other Q/N rich yeast prions such as [*PIN*⁺] (Derkatch et al., 1997; Derkatch et al., 2000). The increased amount of Sup35 protein presumably enhances the chance that a prion seed will form *de novo*, and the [*PIN*⁺] amyloid is proposed to provide an initial nuclei facilitating [*PSI*⁺] appearance (Figure 1-5) (Bradley et al., 2002). Notably, the [*PIN*⁺] prion is only needed for [*PSI*⁺] induction, and it is dispensable for [*PSI*⁺] propagation (Derkatch et al., 2000).

Sup35/Sup35N overproduction

Sup35N

N

N

N

N MC

N MC

Sup35

MC

N N N N

[*PSI+*]
formation

MC MC MC MC

Z Z Z Z

[*PSI+*]

Z Z Z Z

Another QN-rich prion
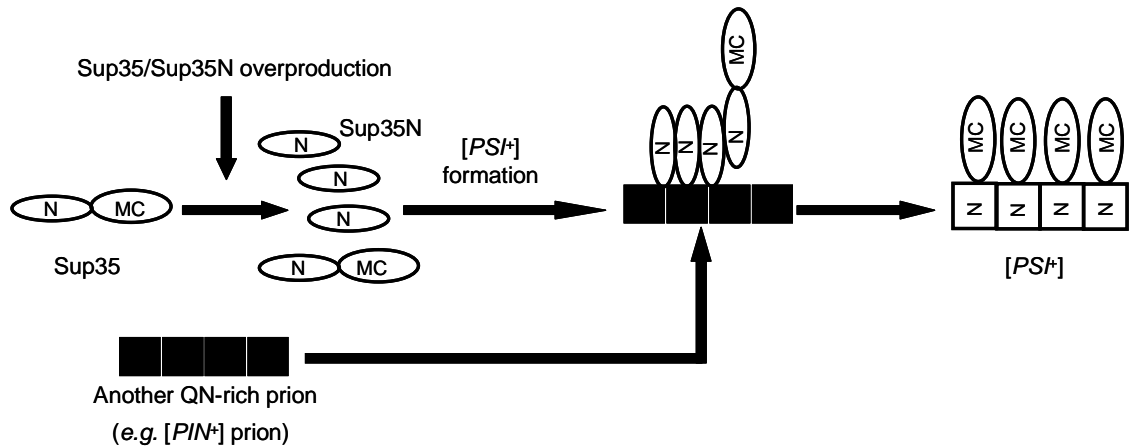
(*e.g.* [*PIN+*] prion)

 Figure 1-5. *De novo* **induction of [*PSI*+] by excess Sup35 or Sup35N**. Overproduction of Sup35 or Sup35N can induce *de novo* formation of [*PSI*$^+$] facilitated by another prion (e. g. [*PIN*+], prion isoform of Rnq1). The [*PSI*$^+$] induction is not efficient without other pre-formed prion.

1-8 Role of molecular chaperone Hsp104 in prion propagation

Molecular chaperones are proteins which can recognize and bind to misfolded polypeptides and facilitate their folding into native states that are specified by their primary sequences (Wickner et al., 1999). Hsp104 is a heat shock protein which is required for induced thermotolerance (Sanchez and Lindquist, 1990; Parsell et al., 1994). However, this chaperone is also important for yeast prion propagation.

The expression level of Hsp104 is crucial for [*PSI*$^+$] propagation; either overproduction or deletion of Hsp104 will eliminate the [*PSI*$^+$] prion (Figure 1-6) (Chernoff et al., 1995; Patino et al., 1996; Newman et al., 1999). Notably, only transient overproduction of Hsp104 is sufficient to eliminate the [*PSI*$^+$] prion, and when the Hsp104 level is returned to normal, the prion state does not reappear.

The mechanism of Hsp104 curing effects is not yet clear. One model suggests that Hsp104 can break the [*PSI*[+]] amyloid fibers into smaller prion "seeds", which would more efficiently promote prion conversion of newly synthesized Sup35 (Kushnirov and Ter-Avanesyan, 1998; Paushkin et al., 1996). Depletion of Hsp104 results in insufficient prion "seeds" as well as larger amyloid fibers, which would be inefficiently transmitted to daughter cells. Conversely, excess Hsp104 may disaggregate the amyloid fiber to such a high degree that all or most of the Sup35 is disassociated into monomer and can be easily refolded into the native conformation or be degraded with the help of the Ubiquitin/Proteasome system (Kushnirov and Ter-Avanesyan, 1998; Patino et al., 1996) (Figure 1-6).
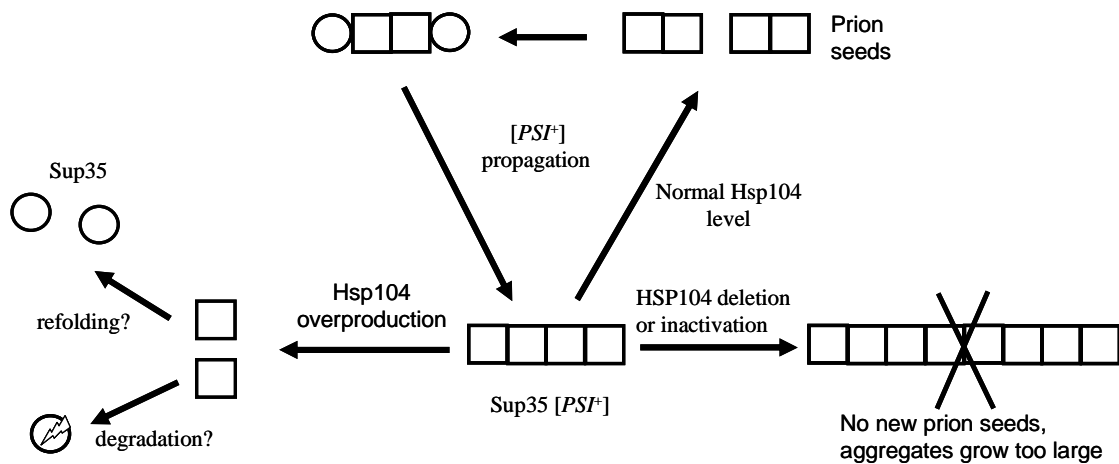
Figure 1-6. Model of Hsp104 modulated [*PSI*[+]] propagation and elimination. Excess Hsp104 will disaggregate the prion polymers into monomers. The prion monomers will either be refolded into soluble Sup35 facilitated by other chaperon systems such as Hsp70/Hsp40, or be degraded via ubiquitin-proteasome system. On the other hand, if Hsp104 is eliminated or inactivated, the prion aggregate may not be sheared properly and can not initiate new round of polymerization; the prion aggregate may also grow too big to transmit efficiently to the daughter cells.

14

Hsp104 is also required for the propagation of other yeast prions, such as [URE3] and [*PIN*$^+$]. Interestingly overproduction of Hsp104 does not eliminate [URE3] (Moriyama et al., 2000) or [*PIN*$^+$] (Derkatch et al., 1997; Sondheimer and Lindquist, 2000). The activity of Hsp104 can be inhibited by millimolar concentrations of guanidine (Grimminger et al., 2004), which is therefore employed as a yeast prion-curing agent (Tuite et al., 1981).

CHAPTER 2
A YEAST MODEL FOR PRION-RELATED PROPERTIES OF MAMMALIAN PRION PROTEIN

2-1 Introduction:

Prion diseases are fatal and presently, incurable. Both incubation periods and the late appearance of symptoms make it difficult to study the prion mechanism directly in animal models. Also, animal-based infectivity assays are laborious and difficult to apply to initial prion formation, which occurs at low frequency. *In vitro* systems have been developed to study the propagation of the protease-resistant PrP^{res} conformation (resembling PrP^{Sc}) (Caughey et al., 1995; Castilla et al., 2005). However their role remains limited since the *in vitro* conditions can not reproduce those existing in the cell.

Yeast prions have been extensively studied, and the availability of powerful genetic approaches using the yeast model led to rapid progress in the prion field. However, yeast prion proteins are non-homologous to mammalian PrP and to other mammalian amyloidogenic proteins. Ultimately, mammalian PrP has been studied in the yeast model. Thus, utilizing this powerful system, a greater understanding of *de novo* PrP^{Sc} was achieved.

One of the pioneering works to study the aggregation properties of mammalian PrP in the yeast system was done by Ma and Lindquist (Ma and Lindquist, 1999). They found that a PrP^{Sc}-like conformation could be generated by the high-level expression of mouse PrP$_{23-231}$ in the yeast cytoplasm. The PrP^{Sc}-like structure is detergent insoluble and proteinase K

16

resistant (two hallmarks of PrP^{Sc}), and the proteinase K resistant fragment of PrP from yeast is the same as that from PrP^{Sc}. In mammalian cells PrP^C is cotranslationally translocated into the secretory pathway, of which two features distinguish it from cytoplasm: N-linked glycosylation and the oxidation of sulphydryl bonds (Weissmann et al., 1994; Prusiner et al., 1998). Thus, the *de novo* formed PrP^{Sc}-like conformation in the yeast cytoplasm may be due to the less glycoylated and greater reducing environment. This hypothesis is supported by the finding that blocking glycosylation and providing a reducing environment promotes conversion of PrP^C to a PrP^{Sc}-like form in mammalian cells (Ma and Lindquist, 1999). Further studies have revealed that the AGAAAAGA palindrome within the N-terminal region of PrP (aa 112-119) is crucial for PrP to adopt the PrP^{Sc}-like conformation in the yeast cytoplasm, as well as for prion propagation in prion infected mammalian cells (Norstrom et al., 2005). In the following study, it was found that PrP partially purified from the yeast cytoplasm can form amyloid fiber-like structures, and the PrP^{Sc}-like conformation is able to convert normal PrP^C from mouse brain homogenate to a proteinase K-resistant conformation *in vitro (*Yang et al., 2006). These results suggest that the yeast originated PrP^{Sc}-like conformation has a self-propagating property similar to that of a prion.

Other mammalian amyloidogenic proteins have also been tested in the yeast model system. Aβ42 and expanded polyglutamine repeats, 2 protein/peptides responsible for Alzheimer's disease and Huntington's disease, respectively, were tagged with green fluorescent protein (GFP) and expressed in the yeast cytoplasm. Both can form aggregates spontaneously (Caine et al., 2007; Krobitsch and Lindquist, 2000; Meriin et

17

al., 2002). Also, a chimeric Aβ42-Sup35 protein was constructed by replacing most or the entire Sup35 prion domain with Aβ42, and was tested in the yeast model system. It was found that the chimeric protein can form SDS stable oligomers, and the translation termination function of Sup35 is disturbed, presumably caused by the Aβ42 aggregation (Bagriantsev and Liebman, 2006; von der Haar et al., 2007).

The major obstacle for monitoring PrP^{Sc} formation in non-mammalian environments has been a lack of reliable phenotypic detection assays. Biochemical techniques are not sufficient for differentiation between the amyloidogenic complexes and other forms of aggregates. In this work, we attempt to overcome this obstacle by employing a [*PSI*$^+$] *de novo* induction system to monitor the formation of the PrP^{Sc}-like conformation. Overproduction of Sup35 or Sup35N can induced *de novo* [*PSI*$^+$] formation, in the presence of other yeast prions such as [*PIN*$^+$]. Previous results showed that the fusion of Sup35 or Sup35N to the expanded polyQ stretch, associated with HD (~50Q or more), enables overproduction of the chimeric construct to induce [*PSI*$^+$] in the [*pin*$^-$] strain (Goehler et al., 2010). Based on this finding, we constructed, for the first time, a two-component system to phenotypically monitor the conformational status of PrP in the yeast cell. In this system, Sup35N was fused to PrP$_{90-230}$, and the initial formation of PrP^{Sc}-like conformation stimulated prion formation of Sup35N, which in turn converted soluble Sup35 into [*PSI*$^+$], leading to a detectable phenotype. Prion-like properties of PrP were studied in this novel yeast model system. Additionally, we employed this system to study Aβ42 aggregation in the yeast model, and, potentially, other amyloidogenic proteins could be examined.

<u>Objectives</u>

The main goal of this work is to establish a yeast-based model for studying the mechanism of prion and amyloid formation by mammalian proteins. The mechanism of the prion-inducing effect of mammalian PrP in yeast was investigated. The amino acids sequence elements or chemical compounds influenceing the prion inducing ability of mammalian PrP can be screened in this yeast-based system, which will help us develop the anti-prion or anti-amyloid therapeutic treatments.

2-2 Materials and methods

<u>2-2-1 Materials</u>

Yeast strains

All *S. cerevisiae* yeast strains used in this chapter are listed in table 2-1. The most commonly used set of isogenic strains in these studies are derived from the strong [PSI^+ PIN^+] diploid parent GT81 (Chernoff et al., 2000). GT81 is an autodiploid that is heterozygous by the *MAT* locus and homozygous for all other genes. GT81-1C is a haploid, meiotic segregant derived from GT81. GT409 is a [$psi^- pin^-$] strain obtained by curing GT81-1C with GuHCl, while GT159 is [$psi^- PIN^+$] strain obtained by curing *[PSI^+]* from GT81-1C with excess Hsp104. GT564 is a [psi^-] Δrnq1 strain obtained by disrupting the *RNQ1* gene from GT159. GT953 is a cytoduction recipient strain derived from 1B-D910 (*MAT**a** ade1-14$_{SC}$ his3 leu2 trp1 ura3 cyh^R kar1-1* [rho^- psi^- pin^-]), kindly

provided by A. Galkin (St. Petersburg University, Russia), with the *sup35Δ::HIS3*

deletion on the chromosome and containing a plasmid expressing Sup35 [*SUP35 LEU2*].

Table 2-1: Yeast strains used in this study

Strain name	Prion Background	Genotype
GT81-1C	[*PSI⁺PIN⁺*]	*MATa ade1-14$_{SC}$ his3-Δ200 lys2 leu2-3,112 trp1-Δ ura3-52*
GT409	[*psi⁻pin⁻*]	*MATa ade1-14$_{SC}$ his3-Δ200 lys2 leu2-3,112 trp1-Δ ura3-52*
GT159	[*psi⁻PIN⁺*]	*MATa ade1-14$_{SC}$ his3-Δ200 lys2 leu2-3,112 trp1-Δ ura3-52 [psi⁻][PIN⁺]*
GT564	[*psi⁻*]	*MATa ade1-14$_{SC}$ his3- Δ200 lys2 leu2-3,112 trp1- Δ, ura3-52 ,rnq1 Δ::HIS3*
GT953	[*psi⁻PIN⁺*]	*MATa ade1-14$_{SC}$ his3Δ leu2-3,112 trp1-289 ura3 kar1 cyhᴿ sup35::HIS3 [rho⁻] [CEN LEU2 SUP35$_{SC}$]*
GT1535	[*PSI⁺*]	*MATa ade1-14 his3Δ (or 11,15) lys2 ura3-52 leu2-3,112 trp1 sup35::HIS3 [CEN LYS2 SUP35]*

Plasmids

Plasmids used and constructed in this study are listed and briefly described in table 2-2.
All PCR-generated fragments were verified by sequencing.

pcDNA3.1 (+) plasmids containing N-PrP$_{90-230}$, PrP$_{90-230}$, NM-PrP$_{90-230}$, M-PrP$_{90-230}$,
NM-HA constructs were kindly provided by I. Vorberg. To express them in yeast, the
constructs were excised with BamHI and XbaI/SacI and the desired fragment was put
under the copper inducible promoter in vector pMCUP1. The resulting plasmids are:
pMCUP1-N-PrP$_{90-230}$, pMCUP1-PrP$_{90-230}$, pMCUP1-NM-PrP$_{90-230}$, and pMCUP1-M-
PrP$_{90-230}$ and $_{pMCUP1}$-NM-HA respectively.

pMCUP1-N-PrPΔ90-119 was constructed based on the NM-PrPΔ90-119 fragment in plasmid pcDNA3.1 (+), from I. Vorberg. The NM-PrPΔ90-119 fragment was cut out with BamHI and XbaI, and inserted into pMCUP1 vector, and then the NM fragment was removed with EcoRI and replaced with Sup35N.

Plasmids pMCUP1-N-PrPΔ160-230 and pMCUP1-N-PrPΔ172-230 were constructed in the following way. N-PrP90-159 and N-PrP90-171 were PCR amplified from pMCUP1-N-PrP$_{90-230}$, adding BamHI and XbaI restriction sites to the end of the fragment. The common forward primer was: ATTAGGATC CGTCGCCACCATGTCC. The reverse primer for N-PrPΔ160-230 was TAATTCTAGATCATTGGTTAGGGTAGCGGTACATG. The reverse primer for N-PrPΔ172-230 was: TAATTCTAGATCACTGGTTGCTGTACTGATCCACTGG. Those two DNA fragments were then digested with BamHI and XbaI and inserted into pMCUP1 under the *CUP1* promoter.

The pcDNA3.1 (+) plasmid containing the human Aβ42 gene was kindly provided from K.E. Ugen lab (Kutzler et al., 2006). Plasmid pMCUP1-N-Aβ42, expressing the chimeic protein N-Aβ42 was constructed in the following way. The open reading frame (ORF) region of Aβ42 was PCR amplified using the primers CAAGAATTCGATGCAGAATTCCGACATGAC and TTGTCTAGATTACGCTAT GACAACACCGCC. EcoRI and XbaI restriction sites are added on the ends. The Aβ42 fragment was then inserted into pcDNA3.1 (+) and linked with SUP35N by EcoRI. Then the SUP35N-Aβ42 fragment was cut with BamHI and XbaI and inserted into pMCUP1

under the *CUP1* promoter. Plasmid pMCUP1-NM-Aβ42 was constructed by cutting SUP35N in pMCUP1-N-Aβ42 with EcoRI and replacing with SUP35NM. The plasmid pMCUP1-NM-Aβ42$_{TM}$ was constructed using plasmid pMCUP1-NM-Aβ42 and generating the triple mutations F19S/F20S/I31P in the Aβ42 portion (triple mutations were generated by Emory University facilities).

The plasmids pMCUP1-Sup35N-HA and pMCUP1-N-PrP$_{90-230}$-HA were constructed in the following way. Sup35N and N-PrP$_{90-230}$ were each amplified from plasmid pMCUP1-N-PrP$_{90-230}$, adding the HA tag on the C-terminal end. The common forward primer, containing the BamHI site, was: GCGTGGATCCGTCGCCACCATGTCC. The reverse primer, containing the SacI site, for Sup35N-HA was: AGTCGAGCTCTCAAGCGT AATCTGGTACGTCGTATGGGTAACCTTGAGACTGTGGTTGGAA. The reverse primer, containing the SacI site, for PrP$_{90-230}$-HA is: AGTCGAGCTCTCAAGCGT AATCTGGTACGTCG TATGGGTAGGATCTT CTCCCGTCGTAATA. The two DNA fragments were digested with BamHI and SacI and inserted into pMCUP1 vector under the *CUP1* promoter.

Table 2-2: Plasmids used in this study

Plasmid name	Protein	Yeast marker	Promoter	Source
pMCUP1	no	URA3	*CUP1*	Lindquist Lab
pMCUP1-PrP$_{90\text{-}230}$	PrP$_{90\text{-}230}$	URA3	*CUP1*	
pMCUP1-N-PrP$_{90\text{-}230}$	N-PrP$_{90\text{-}230}$	URA3	*CUP1*	
pMCUP1-SUP35N	Sup35N	URA3	*CUP1*	
pMCUP1-NM-PrP$_{90\text{-}230}$	NM-PrP$_{90\text{-}230}$	URA3	*CUP1*	
pMCUP1-NM-HA	NM-HA	URA3	*CUP1*	
pMCUP1-M-PrP$_{90\text{-}230}$	M-PrP$_{90\text{-}230}$	URA3	*CUP1*	
pMCUP1-N-PrP$_{90\text{-}230}$-HA	N-PrP$_{90\text{-}230}$-HA	URA3	*CUP1*	
pMCUP1-Sup35N-HA	Sup35N-HA	URA3	*CUP1*	
pMCUP1-N-PrP Δ 90-119	N-PrP Δ 90-119	URA3	*CUP1*	
pMCUP1-N-PrP Δ 172-230	N-PrP Δ 172-230	URA3	*CUP1*	
pMCUP1-N-PrP Δ 160-230	N-PrP Δ 160-230	URA3	*CUP1*	
pMCUP1-N-A β 42	N-A β 42	URA3	*CUP1*	
pMCUP1-NM-A β 42	NM-A β 42	URA3	*CUP1*	
pMCUP1-NM-A β 42$_{TM}$	NM-A β 42$_{TM}$	URA3	*CUP1*	
pCUP-SUP35	Sup35	URA3	*CUP1*	This study
pZTD104	Hsp104	TRP1	GPD	Lindquist Lab
pLH105	Hsp104	LEU2	GPD	
pRS315-SUP35 del3ATG	Sup35C	LEU2	P_{SUP35}	
pRS315-SUP35MC	Sup35MC	LEU2	P_{SUP35}	
pLA1-SUP35	Sup35	HIS3	GAL	Chernoff lab
pLA1	no	HIS3	GAL	Lindquist lab
pLA1-PrP$_{90\text{-}230}$	PrP$_{90\text{-}230}$	HIS3	GAL	
pLA1-N-PrP$_{90\text{-}230}$	N-PrP$_{90\text{-}230}$	HIS3	GAL	
pLA1-Sup35N	Sup35N	HIS3	GAL	This study
pRS315/P$_{CUP}$-Sup35NM-sGFP	Sup35NM-GFP	LEU2	CUP1	Chernoff lab

(Note: NM-Aβ42$_{TM}$ refers to NM-Aβ42 with triple mutations F19S/F20S/I31P in Aβ42 part.)

Antibodies

Antibodies and their corresponding dilution rates are listed in table 2-3.

Table 2-3: Antibodies used in this study

Antibody	Dilution rate	Secondary antibody	Dilution rate	Source
Anti-PrP(6H4)	1:3000	Anti-Mouse-HRP	1:8000	Prionics, Switzerland
Anti-Prp(4H11)	1:200	Anti-Mouse-HRP	1:6000	Vorberg lab
Anti-Rnq1	1:2000	Anti-Rabbit-HRP	1:3000	Lindquist lab
Anti-Sup35C	1:2000	Anti-Rabbit-HRP	1:6000	Chernoff lab
Anti-Sup35N	1:2000	Anti-Rabbit-HRP	1:8000	Chernoff lab
Anti-HA	1:5000	Anti-Mouse-HRP	1:8000	Chernoff lab

2-2-2 Methods

Molecular biology techniques

Standard protocols were used for DNA electrophoresis, restriction digestion, ligation, and bacterial transformation (Sambrook et al., 2001). Enzymes were purchased from New England Biolabs.

QIAGEN Gel Extraction protocol

Fragments of DNA generated by restriction digest or PCR reaction were separated using standard DNA electrophoresis (Sambrook and Russel, 2001). DNA bands corresponding to desired products were identified using a UV transilluminator (Fischer Biotech 312nm Variable Intensity Transilluminator) and bands were excised from EtBr-stained gels using a scalpel. Separation of DNA from gel was achieved using the QIAquick Gel Extraction Kit and protocols supplied by the manufacturer, QIAGEN.

E.coli plasmid DNA isolation

Small-scale plasmid DNA isolation was performed using the boiling prep method (Sambrook et al., 2001). Briefly, sterile wooden toothpicks were used to collect cells which were resuspended in STET buffer (5% Triton X-100, 8% sucrose, 20 mM ethylenediaminetetraacetic acid (EDTA), 50 mM Tris-HCl, pH 8.0) with lysozyme added to a final concentration of 1mg/ml. Suspensions were boiled for 90 seconds, followed by centrifugation at 16,000 g for 15 minutes. The viscous pellets were removed using sterile toothpicks, and DNA in the remaining supernatant was precipitated with isopropanol at -20 ℃ for 30 minutes. Precipitated DNA was collected by centrifugation at 16,000 g for 10 minutes, washed with 70 % ethanol, dried thoroughly, and was resuspended in TE+RNase (10 mM Tris-HCl, 1 mM EDTA, 0.1 mg/ml RNase, pH 7.4).

For large-scale isolation of plasmid DNA, sterile wooden toothpicks were used to collect cells from a quarter of the petri dish, and cells were resuspended in 200 μl of Solution I (25 mM Tris-HCl, 10 mM EDTA, 0.9% glucose, 2 mg/ml lysozyme, pH 8.0). Suspensions were incubated for 10 minutes, followed by adding 400 μl of Solution II (0.2 M NaOH, 1% sodium dodecyl sulfate (SDS)). The mixtures were incubated on ice for 15 minutes before 300 μl of Solution III (5 M CH_3COONa – 3 M Na, 5 M acetate, pH 4.8) was added, and the mixtures were incubated on ice for another 30 minutes. Cell debris was pelleted at 16,000 g for 15 minutes. The supernatant was moved to another tube that contains 600 μl isopropanol and mixed well. The mixtures were incubated for 20 minutes. Precipitated DNA was collected by centrifugation at 16,000 g for 15 minutes, washed with 70 % ethanol, dried thoroughly, and resuspended in 200 μl of TE+RNase.

Suspensions were incubated at 37 ℃ for 30 minutes, followed by adding 200 μl of 9 M lithium chloride (LiCl) and incubating at -20℃ for 20 minutes. The mixtures were pelleted at 16,000 g for 10 minutes, and supernatant was moved to another tube containing 800 μl of 95 % ethanol. DNA was precipitated for 40 minutes, and collected at 16,000 g for 10 minutes. DNA pellet was washed with 70 % ethanol and dried thoroughly. Finally, dry pellets were resuspended in 30-50 μl of 10 mM Tris-HCl, pH 8.0.

E. coli competent cells preparation

The DH5α *E. coli* strain was inoculated into 100 ml of SOB (20 g/l Bactotryptone, 5 g/l Yeast Extract, 0.584 g/l NaCl, 0.186 g/l KCl and 5 ml/l 2 M Mg^{2+} was added after autoclaving). The culture was incubated in a 37 ℃ shaker until an OD_{550} reached 0.45 to 0.55. Cells were incubated on ice for 15 minutes, and were collected by centrifugation at 2,000 g for 10 minutes at 4 ℃. Cells were resuspended in 33 ml of RF1 (100 mM Rubidium chloride (RbCl), 50 mM Manganese chloride (MnCl), 30 mM Potassium acetate, 10 mM Calcium Chloride ($CaCl_2$), 15% Glycerol, pH 5.8). The suspension was incubated on ice for 45 minutes and was collected by centrifugation at 2,000 g for 10 minutes at 4℃. Finally, cells were resuspended in 8 ml of RF2 (10 mM Morpholinopropanesulfonic acid (MOPS), 10 mM RbCl, 75 mM $CaCl_2$, 15% Glycerol), and were used immediately or were stored at -70 ℃.

Yeast and E.coli transformation procedures

All yeast transformations were performed according to the standard lithium-treatment procedure (Ito et al., 1983; Kaiser et al., 1994). All *E.coli* transformations were prepared using chemically competent *E. coli* cells according to standard laboratory protocols (Sambrook et al., 2001).

Standard yeast media and growth conditions

Yeast cultures were grown at 30 °C. Standard yeast media and standard procedures for yeast cultivation, phenotypic and genetic analysis, transformation, sporulation and dissection were used (Kaiser et al., 1994). Sporulating cultures were dissected using a micromanipulator (Ergaval Series 10 from Carl Zeiss or the Singer MSM System 300). Cell counts were performed using a hemacytometer (Brightline). Synthetic media lacking adenine, leucine, or uracil are designated as –Ade, -Leu, and -Ura, respectively. In all cases when the carbon source is not specifically indicated, 2% glucose (Glu) was used. The synthetic medium containing 2% galactose (Gal) or 2% galactose and 2% raffinose (Gal+Raf) instead of glucose was used to induce the *GAL* promoter. 10 or 50 µM copper sulfate ($CuSO_4$) was used to induce overproduction of proteins under control of the *CUP1* promoter. Liquid cultures were grown with at least a 1/5 liquid/flask volumetric ratio in a shaking incubator (200-250 rpm). Yeast transformants were checked in all cases on YPG (medium containing glycerol as carbon source). Petites that are respiratory deficient do not grow on YPG or on medium containing galactose as the sole carbon source and were not considered for future use.

Yeast DNA isolation

Plasmid and genomic DNA from yeast cultures was collected according to standard laboratory protocols (Kaiser et al., 1994). Briefly, cells from late log phase cultures were centrifuged at 7000 g, and cell pellets were resuspended in 500 µl of 1M Sorbitol, 0.1 M EDTA, pH 7.5 containing 4% of a 50 ug/ml lyticase solution and were incubated at 37° C for approximately 3 hours. Cells were briefly spun down at 12,000 x g, and pellets were resuspended in 500 µl of a 50 mM Tris-HCl (ph 7.4), 20 mM EDTA solution. SDS was added to a final concentration of 1%, and the samples were incubated at 65°C for 30 minutes. 2 ml of 5 M potassium acetate was added and samples were placed on ice for 1 hour. Following 12,000 g centrifugation, 0.75 ml isopropanol was added to the supernatants and samples were centrifuged at 12,000 g for 5 minutes. Supernatants were discarded, and pellets were dried, resuspended in 0.4 ml TE (pH 7.4) plus 22 µl of a 1 mg/ml solution of RNAse A, and incubated at 37°C for 30 minutes. DNA was precipitated with 2 volumes of 95% isopropanol. Samples were centrifuged at 12,000 g for 15 minutes, and pellets were washed with 70% ethanol. DNA pellets were dried and resuspended in 50 µl TE (pH 7.4).

Protein isolation and analysis

Yeast protein isolation and centrifugation analysis were conducted using standard yeast laboratory procedures (Kaiser et al., 1994; Sambrook et al., 2001). Yeast cultures were grown in liquid media selective for the protein expressing plasmid. Cells were collected by centrifugation at 2,000 g for 5 minutes at 4 °C, followed by washing cells with 300 µl of ice-cold lysis buffer (25 mM Tris PH 7.5, 0.1M Nacl, 10mM EDTA, 100ug/ml

cycloheximide, 2mM benzamidine, 20ug/ml leupeptin, 4ug/ml pepstatin A, 1mM NEM, 1X protease inhibitor cocktail form Roche Diagnostics GmbH, 2mM PMSF) Then the cells were resuspended in 2 volumes of ice-cold lysis buffer, and ~300 µl of acid washed glass beads were added. Cells were lysed by vortexing 6 times for 30seconds, with at least 1 minute on ice between vortexes. Cell debris was removed by centrifugation at 2,000 g for 5 minutes. To conduct the centrifugation analysis, the isolated total cell lysate was fractionated by centrifugation at 16,000 g for 30 minute at 4 °C. The supernatant was placed into a fresh tube, and the pellet was resuspended in an equal amount of the lysis buffer. SDS, glycerol, 2-mercaptoethanal and Tris-HCl (pH 6.8) were added to every sample to final concentrations of 2.5 %, 10 %, 5 % and 25 mM, respectively. Resulting samples were boiled for 10 minutes (or not boiled to keep the SDS-stable amyloid) to run on the standard SDS-polyacrylamide (SDS-PAGE) gel or stored at -70 °C. Western blot was used to detect the protein signal. Protein gels were transferred onto Hybond ECL nitrocellulose membranes and reacted to the appropriate antibodies.

In addition to Western blotting, the Dot blot was also used to detect the protein signal. The Dot-blot apparatus was purchased from Bio-Rad. Cell lysate (50 µl, diluted if required) with 2%SDS was loaded onto the Immobilon-P PVDF membrane (activated in methanol before use) and waspre-equilibrated on the dot blot apparatus. The membrane needed to be equilibrated with 3 washes of SDS wash buffer (10mM Tris Ph 8.0, 150mM NaCl, 01.% SDS) prior to loading the samples. Binding took place over 20 minutes, and the membrane was then washed twice with SDS wash buffer. Finally the membrane was removed and reacted to appropriate antibodies.

Quantitative assay for [PSI$^+$] de novo induction rate

Plasmids bearing target proteins (e.g. chimeric N-PrP proteins) under *CUP1* promoters were transformed into the [*psi$^-$pin$^-$*] strain GT409. Transformants were grown on media selective for the plasmid (e.g. –Ura) and tested on YPG media to rule out the respiratory deficient colonies. The pre-culture was grown in liquid selective media for up to 2 days until the OD_{600} reached 2.5. The numbers of cells were counted, and then used to inoculate liquid induction media (e.g. –Ura +10 µM CuSO4) to a concentration of $1X10^6$ cells/ml. The cells were then grown at 30°C with shaking. At the desired time points, 0, 12, 24, 48 and 72 hours, aliquots of the cell culture were taken, washed with water, and cells were counted and plated on both selective media (e.g. –Ura, in order to check the cell viability rate) and selective media without adenine (e.g. –Ura-Ade, in order to check the [*PSI$^+$*] *de novo* induction rate). The cell viability rate was obtained by dividing the viable colony number from selective medium bty the total number of cells plated. The final *de novo* [*PSI$^+$*] induction rate was obtained by dividing the Ade+ colony number from -Ura–Ade medium by the total number of cells plated, and then by dividing again by the cell viability rate. Approximately 500 cells were plated on selective media at each of the time points, and between $1X10^4$ to $1X10^6$ cells (depending on the induction ability of the protein) were plated on –Ura-Ade medium at each time points. To ensure accuracy, only plates containing fewer than 500 colonies were counted. The quantitative test was repeated 3 times for each construct.

GFP detection by fluorescence microscopy

GFP fluorescence images were taken using live cultures. An aliquot of cells was placed onto a glass slide; it was sealed with a coverslip using nail polish. Images were scanned using an Olympus BX41 microscope with a 100X objective, with a narrow band GFP filter. Typically, Cultures were grown overnight in the inducer containing medium (e. g. –Ura with copper sulfate medium for genes expressed under *CUP1* promoter). Only cells showing fluorescence were counted and grouped into different classes based on the patterns observed. The excitation wavelength was 543 nm for the helium-neon laser (rhodamine fluorescence), and 488 nm for the argon laser used to visualize GFP.

Secondary Immunofluorescence straining

A secondary immunofluorescence straining technique was used to visually detect the aggregation of certain proteins in living cells in cases when there was no fluorescence tag on the proteins. The cells were grown in media selective for the protein expressing plasmid and contained the proper promoter-inducing agent (e.g. -Ura+100 μM $CuSO4$ for plasmid pMCUP1-N-PrP$_{90-230}$). The cells were fixed by adding formaldehyde directly to the culture to a final concentration of 4% and cultures were incubated for 15 minutes at room temperature. To destroy the cell wall, cells were then gently spun down, washed twice in solution B, resuspended in 1 ml of the same solution. Cells were then treated by adding 2 µl of 2-mercaptoethanol and 20 µl of a 1mg/ml lyticase and were incubated for 30 minutes at 37°C. Cells were precipitated again and washed twice with solution B. For immunofluorescence staining, fixed cells with destroyed cell walls were resuspended in 100 µl of solution F (100 mM potassium phosphate buffer pH 7.4, 1 mg/ml BSA, 15 mM sodium azide, 15 mM NaCl) containing the appropriate antibody (to detect N-PrP, an

Anti-PrP 6H4, 1:500 dilution was used), incubated in the dark for 1 hour, washed 10 times with solution F, and resuspended in solution F containing the appropriate rhodamine-conjugated secondary antibodies (Alexa Fluor 488 goat anti-mouse, 1:500 dilution). Refer to Table 2.3 for appropriate antibody concentration used in each case. After a one hour incubation in the dark, cells were washed 10 times with solution F and resuspended in phenylenediamine mounting solution (1 mg/ml *p*-phenylenediamine, Sigma, in 1X PBS and 90% glycerol) to prevent bleaching of the rhodamine conjugates (Pringle et al., 1991). Preparation for imaging was accomplished by placing an aliquot of cells onto a glass slide, and sealing the coverslip to the slide with clear nail polish. Samples were visualized under fluorescence microscope with a 488nm excitation wavelength. Only cells showing fluorescence were counted and analyzed.

Cytoduction

Cytoduction is the transfer of cytoplasm material from one strain of yeast to another, without transferring any nuclear genes (Conde et al., 1976). The recipient strain is respiratory-deficient and karyogamy-defective, and possesses a recessive mutation for cycloheximide resistance (cyhr). Since the *kar1-1* recipient strain is defective in nuclear fusion, and the nuclei segregate during mitosis by defective mating with the donor strain, only the cytoplasm material (e.g. mitochondria and prion amyloid) is transferred into the recipient strain. The respiratory-proficient cytoductants were selected on a synthetic medium containing 2% ethanol (instead of glucose). This counterselected against the respiratory-deficient recipient, and 5 mg/l cycloheximide, counterselected against donor cells and diploids (heterozygous by cyhr). (See figure 2-7, panels III-IV for the

cytoduction scheme). The experimental procedures is described in (Borchsenius et al., 2006), with slight modification for this work. The donor strain was mated with the recipient strain GT953 on a YPD plate, was incubated at 30 $^{\circ}$C for 12 hours, and the cytoductants were then obtained by velveteening to selective media as described above. The presence of [PSI^+] in cytoductants was tested by monitoring the growth on selective media lacking adenine.

2-3 Results

2-3-1 Development of a yeast assay for prion induction by mammalian amyloidogenic protein

The mammalian prion protein PrP tends to form a PrP^{Sc}-like conformation in yeast cytoplasm upon overproduction, presumably due to the less glycosylated and greater reducing environment (Ma and Lindquist, 1999). The yeast model can serve as a powerful system to study the initial steps of *de novo* PrP^{Sc} formation. However, there is no reliable phenotypic assay to monitor the formation of the PrP^{Sc}-like conformation in a yeast system.

 In order to overcome this obstacle, we developed a *de novo* [PSI^+] induction system to phenotypically monitor PrP aggregation in yeast. The PrP$_{90-230}$ fragment, a region essential and sufficient for prion transmission (Peretz et al., 1997) was fused to the C-terminal end of the Sup35 prion domain (N). (Figure 2-1) The chimeric N-PrP protein was shown to aggregate in the cytoplasm of mammalian cells and displayed increased resistance to proteinase K (Krammer et al., 2008). We proposed that overproduction of

33

N-PrP in yeast cells can induce the *de novo* formation of [*PSI*$^+$] in the absence of other pre-existing yeast prions. This can ultimately serve as a phenotypic assay for PrP^{Sc} formation in a yeast model.
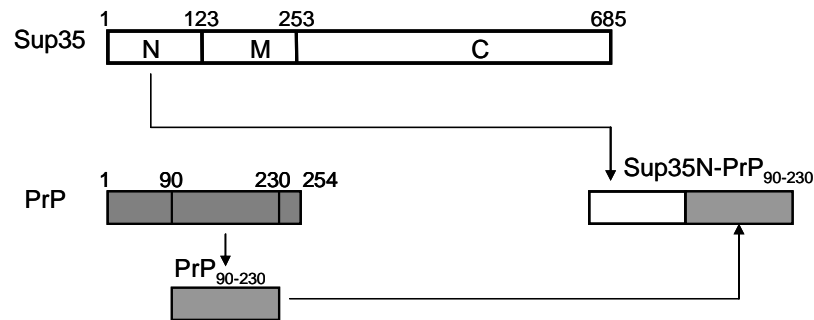
Figure 2-1. Construction of Sup35N-PrP chimeric protein. The Sup35N-PrP was constructed by fusing the PrP$_{90-230}$ region to the C-terminal end of Sup35N.

Sup35N-PrP induced *de novo* formation of [*PSI*$^+$] in the absence of other prions

In order to test the [*PSI*$^+$] *de novo* induction ability of the chimeric protein N-PrP, the plasmid pMCUP1-N-PrP$_{90-230}$ was transformed into the [*psi$^-$pin$^-$*] strain GT409. Plasmids pMCUP1, pMCUP1-PrP$_{90-230}$ and pMCUP1-SUP35N were also tested as controls. With transient overproduction (2 days on selective media –Ura with 10 µM CuSO4), nonsense suppression was detected in the strain containing N-PrP (Figure 2-2 A), indicating the formation of [*PSI*$^+$]. The Ade$^+$ colonies were cured by GuHCl, an agent eliminating all known yeast prions. In contrast, overproduction of Sup35N did not induce [*PSI*$^+$] formation efficiently in [*pin$^-$*] strain. Notably, overproduction of PrP itself did not induce [*PSI*$^+$], indicating that the physical link with Sup35N is important. Without overproduction, N-PrP did not induce [*PSI*$^+$] efficiently (data not shown), corresponding

to the finding that PrP only aggregates in the yeast cytoplasm upon overproduction (Ma

and Lindquist, 1999). A quantitative test was performed in order to accurately check the

[*PSI*⁺] induction rate of N-PrP (Figure 2-2 B). After transient overproduction (24 hours in

–Ura medium with10 μM $CuSO_4$), N-PrP induced [*PSI*⁺] in a rate as high as 86 per 10^5

cells, comparing with 2.6 per 10^5 cells from Sup35N and 0.6 per 10^5 cells from empty

vector control.

G Vector N-PrP PrP N

H N-PrP [*PIN⁺*] [*pin⁻*]

I 3 passages on GuHCl

3 passages on YPD

YPD
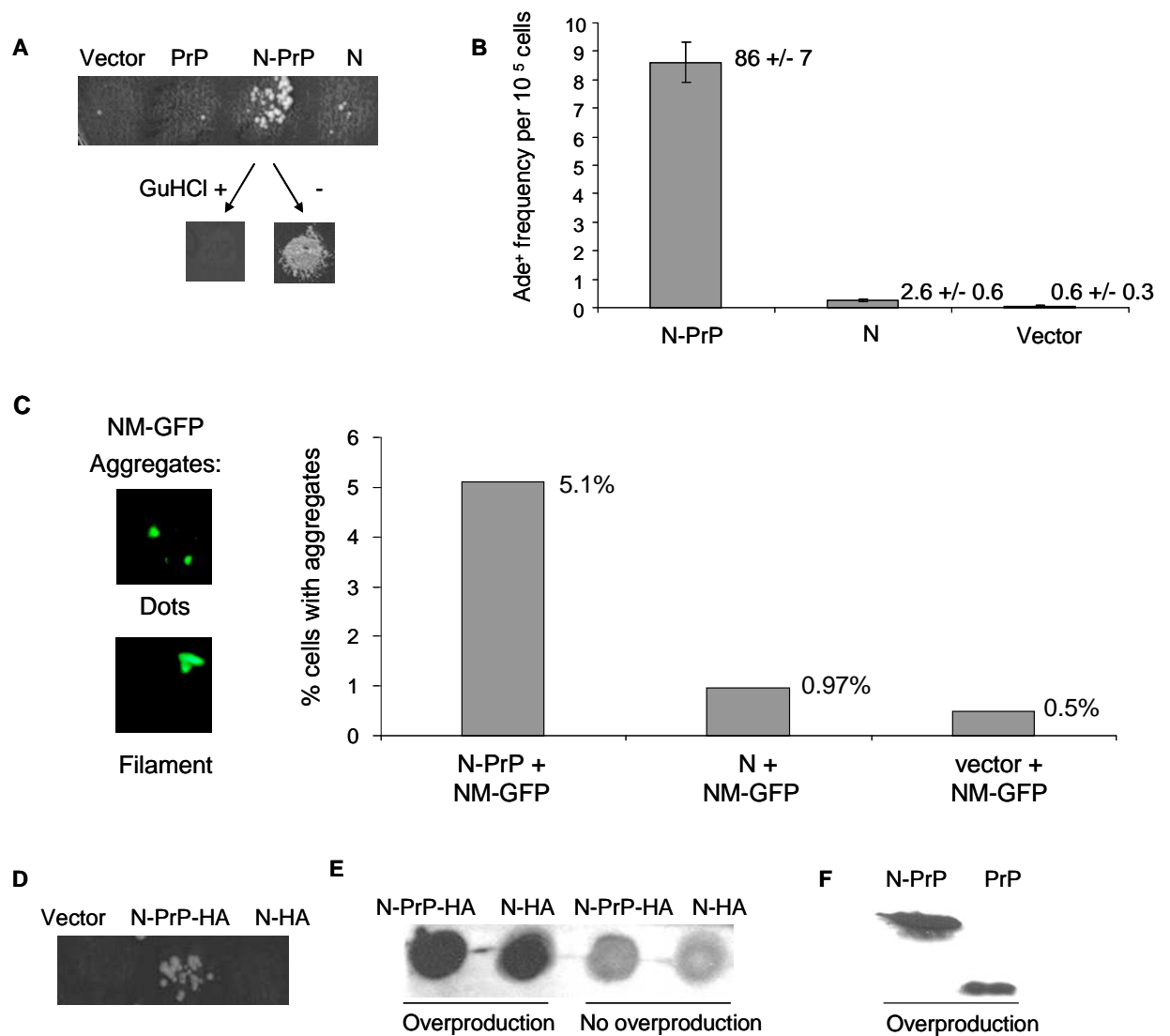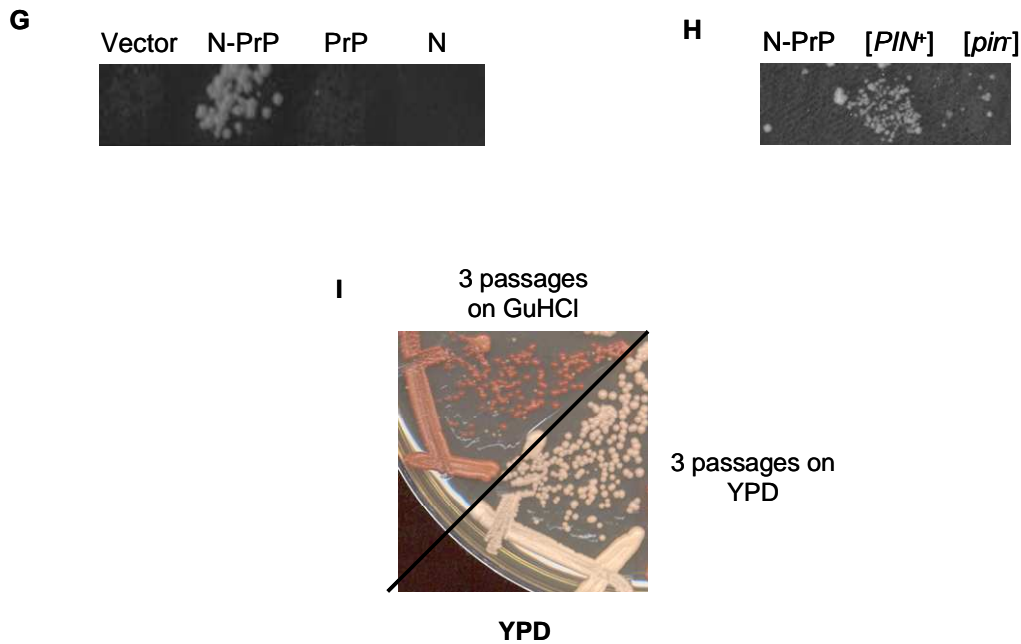
Figure 2-2. Transient overproduction of Sup35N-PrP induced *de novo* formation of [*PSI⁺*] in the absence of other prions. "N-PrP", "N", "PrP", and "vector" refer to Sup35N-PrP, Sup35N, PrP$_{90\text{-}230}$ and empty vector respectively. Nonsense suppression of [*PSI⁺*] is checked on –Ade media. **A**- Transient overproduction of N-PrP in a [*psi⁻pin⁻*] strain induced *de novo* formation of [*PSI⁺*], while overproduction of PrP$_{90\text{-}230}$, Sup35N or empty vector induced no or little [*PSI⁺*]. The Ade⁺ colonies induced by Sup35N-PrP was GuHCl curable. **B**- Quantitative test of the [*PSI⁺*] induction rate of Sup35N-PrP, Sup35N and empty vector in [*psi⁻pin⁻*] strain. The proteins were overprocued in liquid –Ura Meida containing 10 µM CuSO$_4$ for 24 hours, numbers of *de novo* induced Ade⁺ colonies were counted on –Ura-Ade plates. Each group was tested 3 times. Check the method section for detailed description. **C**- *De novo* [*PSI⁺*] induction by N-PrP can be visually monitored by Sup35NM-GFP (NM-GFP). After overproduction in liquid –Ura meida containing 100 µM CuSO$_4$ for 24 hours, aggregation of NM-GFP was monitored by fluorescence microscopy. Cells with NM-GFP aggregates were counted and the aggregation rate was calculated. **D**- With transient overproduction, N-PrP-HA induced de novo [*PSI⁺*] formation while N-HA did not. **E**- Protein expression levels of N-PrP-HA and N-HA in [*psi⁻PIN⁺*] strain (cells were incubated in liquid –Ura meida containing 0 or 10 µM CuSO$_4$ for 2 days) were checked with dot blot assay. HA antibody was used for the immunostaining. **F**- Protein expression levels of Sup35N-PrP and PrP90-230 in [*psi⁻pin⁻*] strain (cells were incubated in liquid –Ura meida containing 10 µM CuSO$_4$ for 2 days) were checked by SDS-PAGE and western blot. Anti-PrP (4H11) was used for the immunostraing. **G**- The checked proteins were expressed under GAL promoter. By galactose-induced overproduction, N-PrP still induced de novo [*PSI⁺*] formation in [*psi⁻pin⁻*] strain, while other proteins did not. **H-** Cured by Hsp104, the N-PrP induced [*PSI⁺*] strain was mated with PIN tester strain. No [*PSI⁺*] was induced in the diploid strain, indicating no [*PIN⁺*] existed. Known [*PIN⁺*] and [*pin-*] strains were tested as controls. **I-** After loss of the N-PrP expressing plasmid from the *de novo* induced [*PSI⁺*] strain, the

prion was stably maintained after 3 passages of growth on YPD, while GuHCl efficiently eliminated the prion state.

[*PSI*$^+$] formation can also be visually detected by monitoring the Sup35NM-GFP aggregates with a fluorescent microscope. To do this, pMCUP1-N-PrP$_{90-230}$ and pRS315/P$_{CUP}$-Sup35NM-sGFP plasmids were co-transformed into the [*psi*$^-$*pin*$^-$] strain GT409. The strain was inoculated into induction medium (liquid –Ura+100 µM CuSO$_4$) which promotes the overproduction of N-PrP and NM-GFP, and the GFP signal was monitored using fluorescence microscopy. Sup35NM-GFP aggregated in [*PSI*$^+$] cells (Paushkin et al., 1996) and formed dots or filamentous structures (Figure 2-2 C). When overproduced together with N-PrP, the frequency of cells with NM-GFP aggregates was 5.1%, which was much higher than that of Sup35N or the empty vector. Notably, the NM-GFP aggregation rate was higher than the [*PSI*$^+$] *de novo* induction rate, because only a portion of the cells having NM-GFP aggregation turned into [*PSI*$^+$].

N-PrP and Sup35N were tagged with HA for the purpose of assessing protein levels. It was shown that the HA tag does not affect the [*PSI*$^+$] induction ability of N-PrP (Figure 2- 2 D). In the yeast strain GT159, protein expression of N-PrP-HA and Sup35N-HA is of the same level, either with or without overproduction (Figure 2-2 E). In the yeast strain GT409, the protein expression level of N-PrP and PrP are comparable after overproduction (Figure 2-2 F).

Since we induced N-PrP overproduction with CUP1 promoter, it is possible that the [*PSI*$^+$] inducibility is promoter-dependent or copper-dependant. To rule out this possibility, we constructed N-PrP, PrP and Sup35N plasmids under the galactose-inducible promoter GAL (pLA1-N-PrP$_{90-230}$, pLA1-PrP$_{90-230}$, pLA1-Sup35N). In the [*psi$^-$pin$^-$*] strain GT409, after transient overproduction on galactose media, N-PrP induced [*PSI*$^+$] *de novo* formation as well (Figure 2-2 G). Thus, the prion induction ability of N-PrP is directly associated with its overproduction, and it is not promoter dependent.

Overproduction of Sup35 or Sup35N can induce *de novo* [*PSI*$^+$] formation facilitated by other yeast prions such as [*PIN*$^+$] (Derkatch, et al., 1997). It is possible that the [*PSI*$^+$] formation is due to the acquisition of [*PIN*$^+$] or other yeast prions, but not to N-PrP overproduction. To rule out this possibility, we monitored the presence of [*PIN*$^+$] in the *de novo* induced [*PSI*$^+$] colonies. 6 individual [*PSI*$^+$] colonies were cured by transient overproduction of Hsp104, without affecting [*PIN*$^+$] in the cells. The existence of [*PIN*$^+$] or other yeast prions was tested by mating cells with a [*psi$^-$pin$^-$*] strain that contained a Sup35 over-expressing plasmid. The diploid strain will have [*PSI*$^+$] induced if [*PIN*$^+$] or other yeast prions existed. The result (Figure 2-2 H) showed no [*PIN*$^+$] or other yeast prions existing in the [*PSI*$^+$] colonies, indicating overproduction of N-PrP induces *de novo* [*PSI*$^+$] formation in the absence of other yeast prions.

In order to check if N-PrP is required for propagation of the *de novo* induced [*PSI*$^+$] prion, the N-PrP expressing plasmid was lost from the strain. After 3 passages of growth on rich

YPD medium, [*PSI*⁺] was still stably maintained in the strain (Figure 2-2 I). Thus, N-PrP was only required for [*PSI*⁺] *de novo* formation but not for [*PSI*⁺] propagation.

2-3-2 Effects of PrP deletions on the [*PSI*⁺] induction ability of N-PrP

We proposed that in the N-PrP chimeric protein, PrP spontaneously forms PrP^{Sc}-like structure and polymerized, which provides an initial nucleus. This facilitates prion formation of the Sup35N portion. Then the Sup35 protein is converted to the [*PSI*⁺] state via the prion isoform of Sup35N. Based on this hypothesis, elimination of the PrP^{Sc} forming ability of PrP will result in the failure of the [*PSI*⁺] induction by the chimeric protein N-PrP. To test this hypothesis, we constructed deletions in the PrP portion of the chimeric protein, and tested their [*PSI*⁺] induction abilities.

It was shown that the N-terminal region of PrP (from residue 90 to 120) is critical for PrP^{Sc} formation (Muramoto et al., 1996; Peretz et al., 1997). Deletion of the PrP palindrome region (aa 112-119) prevents the formation of the PrP^{Sc}-like structure in the yeast cytoplasm (Norstrom et al., 2005). We deleted the N-terminal residues 90-119 from PrP and constructed the N-PrPΔ90-119 plasmid under the *CUP1* promoter (pMCUP1-N-PrPΔ90-119). After transient overproduction in the [*psi⁻pin⁻*] strain GT409, no apparent [*PSI*⁺] induction by N-PrPΔ90-119 was detected (Figure 2-3 A). A quantitative assay indicated that the [*PSI*⁺] induction rate of N-PrPΔ90-119 was decreased dramatically when compared with that of N-PrP (Table 2-4). In the yeast strain GT409, the protein expression levels are similar for N-PrP and N-PrPΔ90-119, either with or without overproduction (Figure 2-3 B). In these results, the [*PSI*⁺] induction ability of N-PrP was

lost when the prion formation ability of PrP region was eliminated. It strongly indicates

that the formation of PrP^{Sc}-like structure promotes the *de novo* [*PSI*$^+$] formation.

A

N-PrP Δ90-119	N-PrP	N	vector	N-PrP Δ172-230	N-PrP Δ160-230

B

N-PrP	N-PrPΔ90-119	N-PrP	N-PrPΔ90-119

No overproduction   Overproduction

C

N-PrP	N-PrP Δ160-230	N-PrP Δ172-230
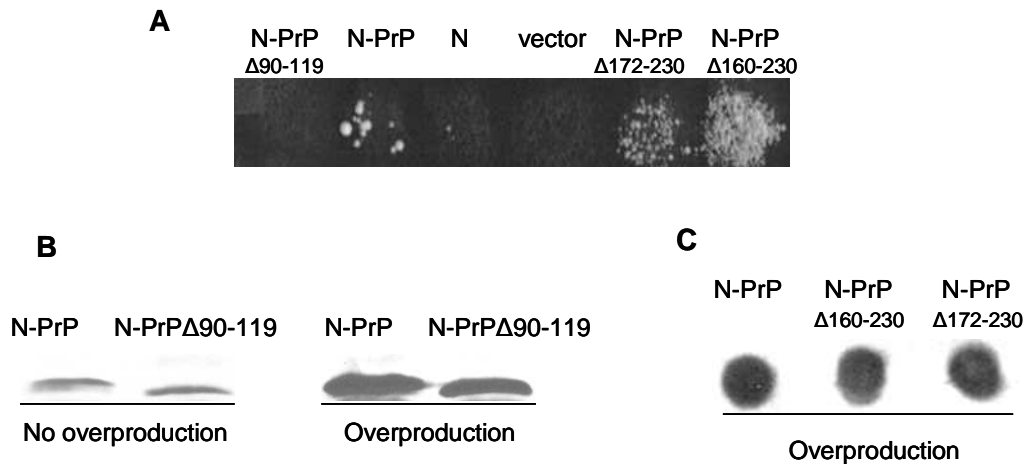
Overproduction

Figure 2-3. Effects of PrP deletions on the [*PSI*$^+$] induction ability of Sup35N-PrP. The respective proteins were overproduced in -Ura media containing 10 µM CuSO$_4$ for 2 days. Nonsense suppression was tested on –Ade medium. **A**- After transient overproduction in [*psi*$^-$*pin*$^-$] strain, Sup35N-PrPΔ90-119 did not induce [*PSI*$^+$] formation, while Sup35N-PrPΔ172-230 and Sup35N-PrPΔ160-230 induced [*PSI*$^+$] formation more efficiently than Sup35N-PrP. **B**-Protein expression levels of Sup35N-PrP and Sup35N-PrPΔ90-119 were checked by SDS-PAGE and western blot. Anti-PrP (4H11) was used for the immunostaining. **C**- Protein expression level of Sup35N-PrP, Sup35N-PrPΔ172-230 and Sup35N-PrPΔ160-230 were checked by dot blot assay. Anti-PrP (6H4) was used for the immunostaining.

Table 2-4. Frequencies of [*PSI*$^+$] induced by Sup35N-PrP and the deletions

Chimeric constructs	Ade$^+$ frequency	Standard deviation
Sup35N-PrP	8.6×10^{-4}	7×10^{-5}
Sup35N-PrP *Δ90-119*	4.4×10^{-5}	1.3×10^{-5}
Sup35N-PrP *Δ*160-230	7.5×10^{-2}	4.96×10^{-3}

(The proteins were overproduced in –Ura liquid media containing 10 µM CuSO4 for 24 hours. Each group was tested 3 times; see the method section for detailed description)

During prion conversion, the C-terminal region of PrP^C is transformed from an α -helix rich structure into a β -sheet rich structure, and is included in the amyloid core (Cobb et al., 2008). In order to check how the C-terminal region affects PrP^{Sc} *de novo* formation, we constructed PrP C-terminal deletions in the chimeric protein N-PrP.

We deleted the C-terminal residues of 160-230 or 172-230 from PrP and constructed the N-PrPΔ160-230 and N-PrPΔ172-230 plasmids under the *CUP1* promoter (pMCUP1-N-PrPΔ160-230, pMCUP1-N-PrPΔ172-230). Interestingly, after transient overproduction in GT409, the [*PSI*$^+$] inductions by the C-terminal deletions were much stronger than that of the N-PrP wild type (Figure 2-3 A). Quantitative tests indicated that the [*PSI*$^+$] induction rate of N-PrPΔ160-230 was increased dramatically when compared to that of N-PrP (Table 2-4). In the yeast strain GT409, the protein expression of N-PrP, N-PrPΔ160-230 and N-PrPΔ172-230 were found to be similar after overproduction (Figure 2-3 C).

Based on these results, we concluded that the PrP C-terminal region has an anti-prion formation effect, whereas, deletion of this region promotes PrP^{Sc} *de novo* formation. This result is supported by some clinical evidences for human GSS disease. As a prion disease caused by PrP^{Sc} formation, one case of inheritable GSS disease was associated with a nonsense mutation at residue 160 in human PrP (corresponding to residue 159 in mouse PrP). Additionally, another human prion disease PrP-CAA (prion protein cerebral amyloid angiopathy) is associated with nonsense mutations at residues 145 or 163 in human PrP (corresponding to residues 144 and 162 respectively in mouse PrP). In all of these cases, the C-terminal truncated PrP promotes the PrP^{Sc} associated diseases,

implicating the anti-prion formation effect of the C-terminal region. The effect of N-PrPΔ160-230 in this study is closely related to the nonsense mutations (160/stop or 163/stop) occurring in certain prion diseases.

2-3-3 Mammalian Aβ42 protein induced [*PSI*⁺] in the yeast assay

Alzheimer's disease is a severe neurodegenerative disorder characterized by amyloid formation and accumulation of Aβ42 protein. The mechanism of Aβ42 structural conversion and amyloid assembly is not yet clear. It was found that Aβ42 can aggregate spontaneously in the yeast cytoplasm. Here, we wanted to check Aβ42 with the [*PSI*⁺] *de novo* induction system in a yeast model.
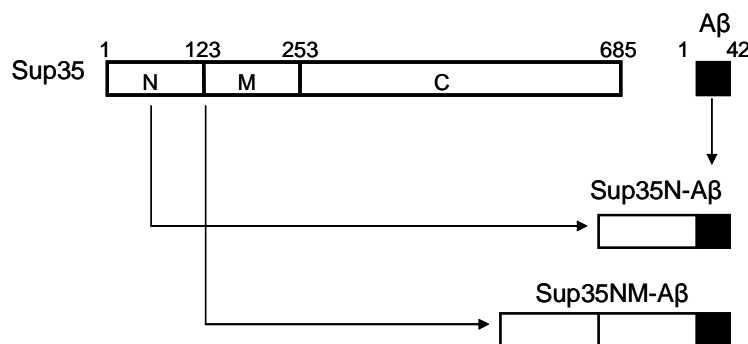
Figure 2-4. Construction of Sup35N-Aβ and Sup35NM-Aβ chimeric proteins. The Sup35N-Aβ and Sup35NM-Aβ were constructed by fusing the Aβ1-42 region to the C-terminal end of Sup35N or Sun35NM. Numbers correspond to amino acid positions.

We fused human Aβ42 to the C-terminal end of either Sup35N or Sup35NM to construct the chimeric proteins N-Aβ42 and NM-Aβ42 respectively (Figure 2-4). In order to test the [*PSI*⁺] *de novo* induction ability of the Aβ42 chimeric proteins, plasmids pMCUP1-N-

Aβ42 and pMCUP1-NM-Aβ42 were transformed into the [*psi⁻pin⁻*] strain GT409. Plasmids pMCUP1, pMCUP1-SUP35N and pMCUP1-NM-HA were also tested as controls. With transient overproduction (2 days on –Ura selective media with 10 μM CuSO4), nonsense suppression was detected in the strain containing N-Aβ42 and NM-Aβ42 (Figure 2-5 A), indicating the formation of [*PSI⁺*]. The [*PSI⁺*] colonies induced by N-Aβ42 and NM-Aβ42 were also GuHCl curable (Figure 2-6 B). Notably, the [*PSI⁺*] induction ability of NM-Aβ42 was weaker than that of N-Aβ42, presumably because of the solubility promoting effect of the Sup35M region (Paushkin et al., 1996). Sup35M may inhibit the aggregation of Aβ42 in the chimeric protein NM-Aβ42 and then consequently, weaken its [*PSI⁺*] induction ability. The same effect was detected for the chimeric protein NM-PrP, which could barely promote any [*PSI*+] induction when compared to N-PrP (date not shown).

As for N-PrP, N-Aβ42 and NM-Aβ42 are only needed for the [*PSI⁺*] *de novo* formation but are not required for [*PSI⁺*] propagation. After loss of the N-Aβ42 or NM-Aβ42 plasmids from the *de novo* induced [*PSI⁺*] strain, the prion state was still maintained well (Figure 2-5 C, D).

The *de novo* induced [*PSI⁺*] prion can be cured by transient overproduction of Hsp104, either with or without the N-Aβ42 or NM-Aβ42 plasmid in the strain.
After Hsp104 curing, the strain harboring the N-Aβ42 plasmid had a low level of [*PSI⁺*] re-induction, promoted N-Aβ42 on a normal expression level.
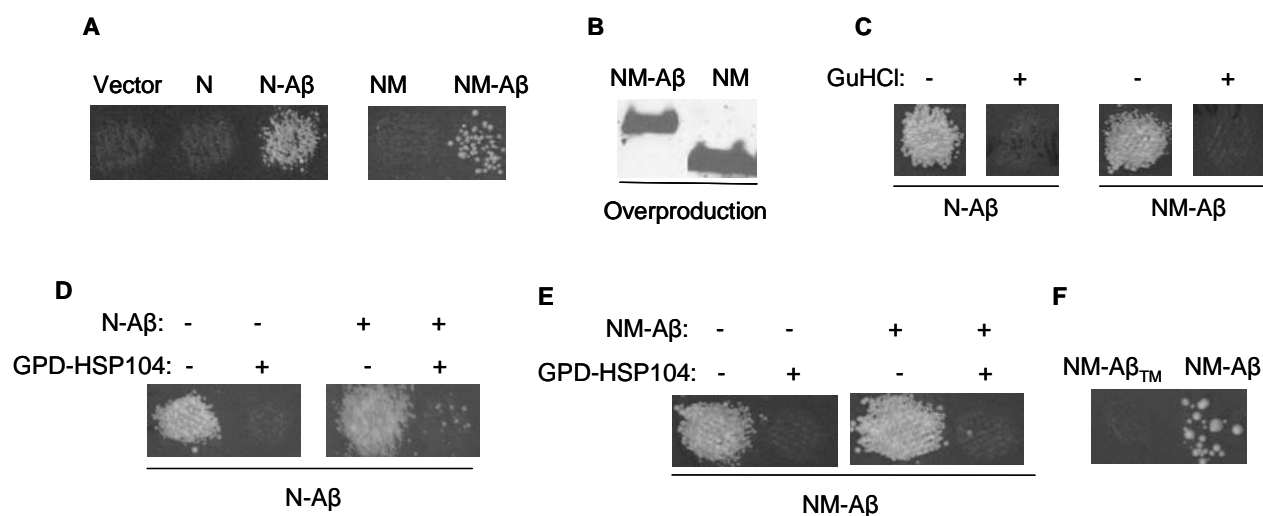
Figure 2-5. Transient overproduction of Sup35N-Aβ or Sup35NM-Aβ induced *de novo* formation of [*PSI*$^+$] in the absence of other prions. The respective proteins were overproduced in -Ura media containing 10 μM CuSO$_4$ for 2 days. Nonsense suppression was checked on –Ade media. GPD-HSP104 refers to Hsp104 over expressing plasmid which was lost from the cells after the overproduction process. NM-Aβ$_{TM}$ refers to NM-Aβ with triple mutations. **A-**Transient overproduction of Sup35N-Aβ (N-Aβ) or Sup35NM-Aβ (NM-Aβ) in a [*psi⁻pin⁻*] strain induced *de novo* formation of [*PSI*$^+$], while overproduction of Sup35N or Sup35NM did not induce [*PSI*$^+$] formation. **B-** Protein expression levels of NM-Aβ42 and Sup35NM-HA (after overproduction) in [*psi⁻pin⁻*] strain were checked by SDS-PAGE and western blot. Anti-Sup35N was used for the immunostraing. **C-**The Ade$^+$ colonies induced by N-Aβ or NM-Aβ were GuHCl curable. **D, E-** The prion state was maintained after loss of N-Aβ or NM-Aβ plasmid from the strain. Transient overproduction of Hsp104 cured the [*PSI*$^+$] strains with or with the plasmid. **F-**Transient overproduction of the NM-Aβ with triple mutations F19S/F20S/I31P did not induce de novo [*PSI*$^+$] formation in [*psi⁻pin⁻*] strain.

In order to prove that the aggregation of Aβ42 is required for the [*PSI*$^+$] induction ability, we designed NM-Aβ42$_{TM}$ with triple mutations F19S/F20S/I31P in the Aβ42 portion. Substitutions of Phe19, Phe20, and Ile31 were previously shown to inhibit aggregation of Aβ42 *in vitro* and to prevent its neurotoxic effects (Hilbich et al., 1992; Morimoto et al., 2004). It was inferred that Aβ42 aggregation is inhibited by the triple mutations in the chimeric protein, and so its effect on the [*PSI*$^+$] induction ability was then tested. The

result showed that after transient overproduction in the [*psi⁻pin⁻*] strain GT409, no [*PSI⁺*] was induced by NM-Aβ42$_{TM}$ (Figure 2-5 E). Inhibition of Aβ42 aggregation eliminated the [*PSI⁺*] induction ability of chimeric protein NM-Aβ42, which supports our hypothesis described above.

2-3-4 Biochemical characterization of N-PrP in yeast

When expressed in the mammalian cytoplasm, N-PrP proteins form aggregates spontaneously and can be precipitated down from cell lysate (Krammer et al., 2008). To test the N-PrP protein in yeast cells, we transformed pMCUP1-N-PrP$_{90-230}$ into strains GT409 [*psi⁻pin⁻*], GT159 [*psi⁻PIN⁺*] and GT81-1C [*PSI⁺PIN⁺*], respectively. After transient overproduction in selective medium (-Ura+100 µM Cu) for 24 hours, the cells were fixed and checked by secondary immunofluorescence straining (see methods section for the detailed description). Visualized by staining, N-PrP formed dot-like aggregates in all 3 strain types having different prion backgrounds (Figure 2-6 A). In a [*psi⁻pin⁻*] strain, 24% of cells contained N-PrP aggregates, the rest of which only showed fluorescent backgrounds. In [*psi⁻PIN⁺*] and [*PSI⁺PIN⁺*] strains, there were 33% and 34% of cells with N-PrP aggregates, respectively. Based on these results, we concluded that N-PrP tends to aggregate in the yeast cell after overproduction. However, the aggregation rate was not affected much by the prion background in the cell.

A

	[*psi⁻pin⁻*]	[*psi⁻ PIN⁺*]	[*PSI⁺PIN⁺*]
N-PrP Aggregates			
% cells with aggregates	24%	33%	34%

B

N-PrP

[*psi⁻ pin⁻*]		[*psi⁻ PIN⁺*]		[*PSI⁺ PIN⁺*]	
Super	Pellet	Super	Pellet	Super	Pellet

C

N-PrP

[*psi⁻pin⁻*]		[*psi⁻PIN⁺*]		[*PSI⁺PIN⁺*]	
Boil: +	-	+	-	+	-
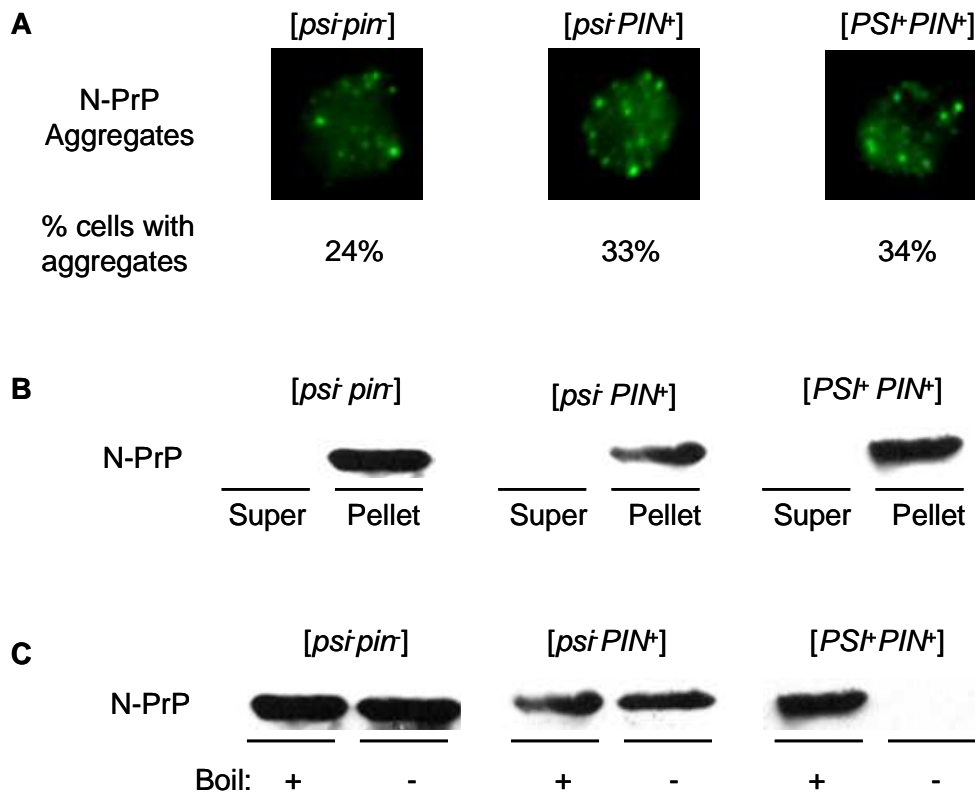
Figure 2-6. Characterization of Sup35N-PrP aggregate in yeast cells of various prion backgrounds. Anti-PrP (6H4) antibody was used for immunofluorescence staining and immunostaining (western blot). **A**-After transient overproduction, N-PrP expressed in [*psi⁻pin⁻*], [*pin⁻PIN⁺*] or [*PSI⁺PIN⁺*] strains were detected by secondary immunofluorescence staining. Aggregation structures (multiple dots) were detected in all cases, with respective frequencies listed in the figure. **B**- Cell lysates were extracted from the respective strains bearing N-PrP. Centrifuged at 16,000g for 30min in 4°C, the supernatants and pellets were collected, boiled, and then analyzed by SDS-PAGE followed with western blot. Most, if not all, of N-PrP is precipitated down from the cell lysates of [*psi⁻pin⁻*],[*pin⁻PIN⁺*] or [*PSI⁺PIN⁺*] strains. **C**-.Cell lysates with 2%SDS was loaded for SDS-PAGE, either with or without boiling. N-PrP did not enter the polyacrylamide gel without boiling from [*PSI⁺PIN⁺*] sample, while N-PrP entered the polyacrylamide gel with or without boiling from [*psi⁻pin⁻*] or [*psi⁻PIN⁺*] samples.

We also performed a centrifugation analysis to test the aggregation state of the N-PrP protein from [*psi⁻pin⁻*], [*psi⁻PIN⁺*] and [*PSI⁺PIN⁺*] strains (Figure 2-6 B). Cell lysates were extracted from the respective strains, followed by centrifugation at 16,000g for 30

minutes in 4°C. The supernatant and pellet were collected separately, boiled and analyzed by SDS-PAGE. The protein gel was analyzed by western blot with a PrP antibody (6H4). The result showed that most, if not all, of the N-PrP is precipitated down into the pellet in all three type of strains with different prion background. Based on this result, all or most of N-PrP aggregates in yeast cells can then be precipitated down. However, only a portion of the aggregates are big enough to be detected by immunofluorescence straining.

The amyloid structure formed by prions is very stable and detergent insoluble. In order to test if N-PrP forms a highly ordered amyloid structure, we performed the gel entry assay. 2% SDS was added to cell lysate from [psi^-pin^-], [psi^-PIN^+] and [PSI^+PIN^+] strains. Then the samples were either boiled for 10 minutes or were not boiled and were then analyzed by SDS-PAGE. If N-PrP forms a SDS-insoluble amyloid, then it can not enter the polyacrylamide gel without boiling. The result showed that N-PrP from the [PSI^+PIN^+] cell lysate is SDS-insoluble and can not enter the polyacrylmide gel without boiling. N-PrP from [psi^-pin^-] or [psi^-PIN^+] cell lysates was SDS-soluble and could enter the polyacrylamide without boiling (Figure 2-6 C).

Based on the results above, we concluded that N-PrP aggregates spontaneously in yeast cells, independently of the presence of endogenous prions. However, a SDS-insoluble complex of N-PrP could only be detected in a [PSI^+] strain. Although PrP can potentially form a prion like structure in yeast, this state may not be properly propagated. The propagation of yeast prions depends on the chaperone Hsp104 whose ortholog has not been identified in mammalian cells. The propagation of PrP^{Sc} may depend on a different

47

system which does not exist in the yeast cell. For this reason, it is possible that PrP can not be assembled into the amyloid, or the assembled complex can only exist transiently. So, there is no SDS-insoluble complex of N-PrP detected in the [*psi*⁻] strain. In the [*PSI*⁺] strain, the Sup35N region of N-PrP is thought to be converted into the prion isoform and forms the amyloid core, which may, in turn, stabilize the PrPSc-like structure. N-PrP may be also associated into the Sup35 prion amyloid, via the Sup35N region. These explain the SDS-insoluble property of N-PrP from the [*PSI*⁺] strain.

2-3-5 Propagation of [*PSI*⁺] state by N-PrP

In order to test the propagation of the [*PSI*⁺] state by N-PrP alone, we designed a plasmid shuffle experiment and checked the maintenance of [*PSI*⁺] by cytoduction. We selected the [*PSI*⁺] strain GT1535, with a genomic SUP35 gene deletion and containing a Sup35 expressing plasmid. Then we performed a plasmid shuffle to replace the original Sup35 plasmid with the plasmids pMCUP1-N-PrP$_{90-230}$ and pRS315-SUP35MC, which express N-PrP and Sup35MC respectively (Figure 2-7 A, panel I-III). Without its prion domain, Sup35MC can not propagate [*PSI*⁺], however, it is needed for cell viability. Then, we performed cytoduction to check whether [*PSI*⁺] was maintained by N-PrP in the strain (Figure 2-7 A, panel III, IV). Cytoduction is the transfer of cytoplasm from one strain of yeast to another, without transferring any nuclear genes (see methods section for detailed procedures). By cytoduction of the test strain with the [*psi*⁻] recipient strain GT953, the cytoplasm material (including the N-PrP complex) was transferred to the recipient, which was obtained using cytoductant selective media. The presence of [*PSI*⁺] in the cytoductants was monitored on selective medium without adenine.
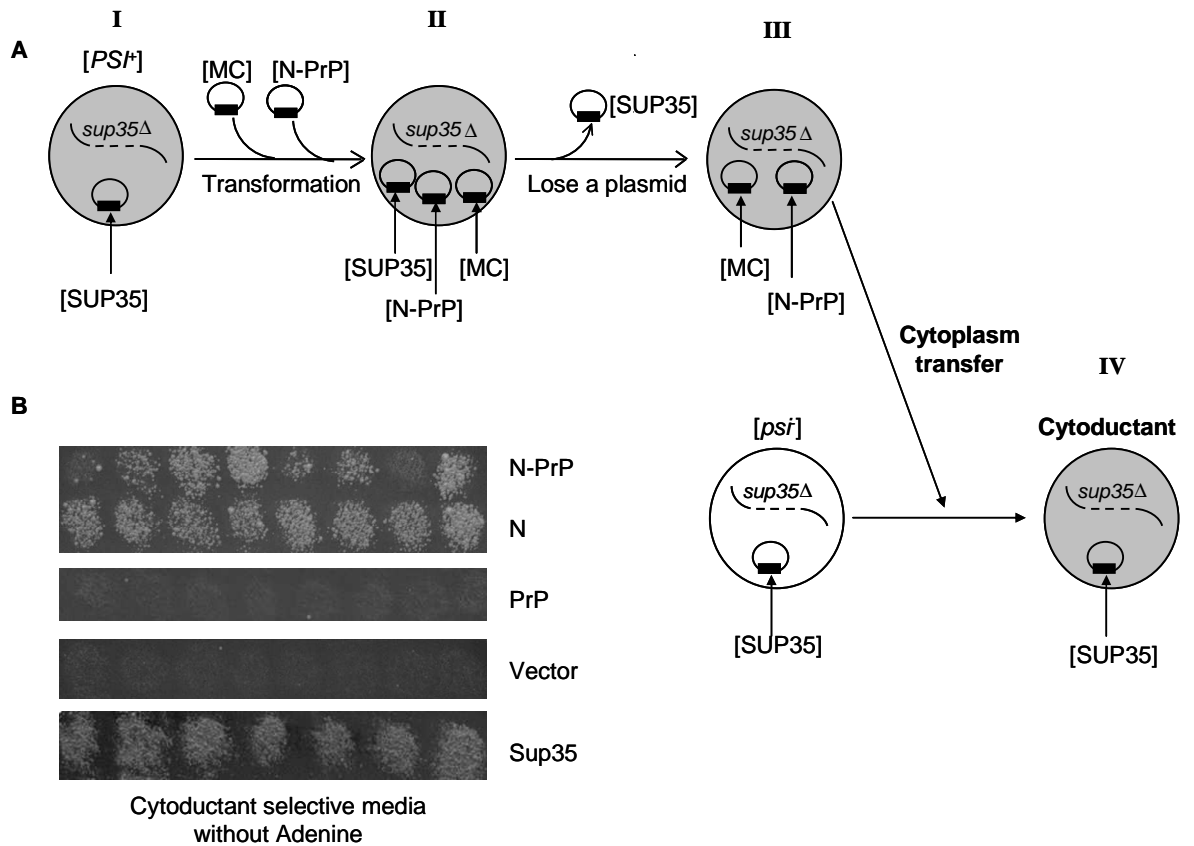
Figure 2-7. Cytoduction test for the [*PSI*⁺] maintenance by Sup35N-PrP.
A- [Sup35],[MC] and [N-PrP] refer to plasmid expressing Sup35, Sup35MC or Sup35N-PrP proteins respectively. Panel I-III: scheme of plasmid shuffle. Panel III-IV: scheme of cytoduction. *sup35Δ* [*PSI*⁺] strain GT1535 containing [Sup35] (stage I) was transformed with [N-PrP] and [MC] together (stage II), and then the original [Sup35] was lost from the strain (stage III). The strain containing [N-PrP] and [MC] was used as cytoduction donor whose cytoplasm was transferred to the *sup35Δ* [*psi*⁻] recipient strain containing [Sup35]. The [*PSI*⁺] state will be transfer to the cytoductant if it is maintained by N-PrP in the donor strain. As controls, Sup35N, PrP$_{90-230}$, empty vector and full length Sup35 were tested in the same way as N-PrP. **B**- The cytoductants from donor strains expressing the respective proteins (listed in the picture) were checked on the selective media without adenine. The existence of [*PSI*⁺] in the cytoductants was judged by the nonsense suppresion. In most cases, N-PrP maintained [*PSI*⁺] and converted Sup35 into [*PSI*⁺] state in the cytoductant. Sup35N or full length Sup35 propagated [*PSI*⁺] state with full efficiency, while PrP$_{90-230}$ alone did not maintain [*PSI*⁺].

The results showed that a majority of [*psi*⁻] recipients became [*PSI*⁺] (Figure 2-7 B) with a [*PSI*⁺] conversion rate of 82% (Table 2-5). This result indicates that N-PrP can maintain [*PSI*⁺] in the absence of full length Sup35, and it can convert native Sup35 back into the [*PSI*⁺] state in the cytoductant strain. For controls, we tested [*PSI*⁺] propagation using either Sup35N, PrP$_{90-230}$, full length SUP35 or an empty vector, in the same manner as for N-PrP. The following corresponding plasmids were used: pMCUP1-SUP35N, pMCUP1-PrP$_{90-230}$, pCUP-SUP35, and pMCUP1. The results showed that either Sup35N or full length Sup35 can propagate [*PSI*⁺] with full efficiency, while PrP$_{90-230}$ alone can not maintain [*PSI*⁺] (Figure 2-7 B; Table 2-5).

Table 2-5. Cytoduction test for [*PSI*⁺] maintenance

Donor	Recipient	Cytoductants		% of [*PSI*⁺] Cytoductants
		Total	[*PSI*⁺]	
GT1535 [N-PrP]	GT953 ([*psi*⁻])	45	37	82
GT1535 [N]	GT953 ([*psi*⁻])	48	46	96
GT1535 [PrP]	GT953 ([*psi*⁻])	48	0	0
GT1535 [vector]	GT953 ([*psi*⁻])	44	0	0
GT1535 [Sup35]	GT953 ([*psi*⁻])	25	25	100

The molecular chaperone Hsp104 is crucial for [*PSI*⁺] propagation; however, excess Hsp104 will eliminate [*PSI*⁺] from the yeast cell. In order to check how Hsp104 affects the [*PSI*⁺] state maintained by N-PrP, plasmid pZTD104, a Hsp104 overproducing plasmid, was transformed into a strain bearing the prion state of N-PrP. After transient

overproduction of Hsp104, pZTD104 was then lost from the strain. The prion state of N-PrP was then checked with cytoduction again with the [*psi*⁻] recipient strain GT953 (Table 2-6). Based on this result, the prion state of N-PrP was lost in 15 colonies out of the16 individual colonies checked, for a prion state loss at a rate of 94%. In contrast, for the strain without Hsp104 overproduction, the prion state of N-PrP was lost at a rate of 25%. Although not 100% efficient, transient overproduction of Hsp104 did cure the [*PSI*⁺] state maintained by N-PrP at a high rate.

Table 2-6. Cytoduction test for the prion curing effect of excess Hsp104

Donor	Recipient	Cytoductants		% of [*psi*] Cytoductants
		Total	[*psi*]	
GT1535 [N-PrP]	GT953 ([*psi*])	8	2	25%
GT1535 [N-PrP] Hsp104↑	GT953 ([*psi*-])	16	15	94%
GT1535 [Sup35]	GT953 ([*psi*])	6	0	0
GT1535 [Sup35] Hsp104↑	GT953 ([*psi*-])	8	8	100%
GT1535 [N]	GT953 ([*psi*])	8	0	0
GT1535 [N] Hsp104↑	GT953 ([*psi*-])	8	0	0

For the control, the [*PSI*⁺] state maintained by either Sup35N or full length Sup35 was also tested in the same manner. The results showed that [*PSI*⁺] can be stably maintained by Sup35 or Sup35N at a normal Hsp104 expression level; however, overproduction of Hsp104 can fully cure the Sup35 maintained prion but can not cure the Sup35N maintained prion (Table 2-6). Some recent studies indicated that Sup35 M region can affect [*PSI*⁺] propagation, presumably by mediating the interaction between Hsp104 and

Sup35 prion aggregate (Liu et al., 2002; Chen et al., 2007). Without a proper binding site in the Sup35N prion, it is likely that overproduced Hsp104 can not efficiently interact with the Sup35N prion and eliminate it. Thus, the PrP region may facilitate an interaction between Hsp104 and the prion state of N-PrP, which accounts for its high curing rate by excess Hsp104.

2-3-6 Prion-like state of N-PrP facilitates the [*PSI*$^+$] *de novo* formation

Since excess Hsp104 can cure [*PSI*$^+$] without affecting other prions, we wanted to eliminate the [*PSI*$^+$] prion induced by N-PrP by transient Hsp104 overproduction, and then check whether the PrP^{Sc}-like state remained to facilitate [*PSI*$^+$] *de novo* induction again. To check this, we randomly picked 30 individual [*PSI*$^+$] colonies induced by N-PrP overproduction (described in section 2-3-1). In order to eliminate the [*PSI*$^+$] prion, the Hsp104 overproducing plasmid pZTD104 was transformed into the strain and was then lost from the strain. With transient overproduction of Hsp104, [*PSI*$^+$] was eliminated in all colonies, as shown by the nonsense suppression assay. Then pLA1-SUP35, a plasmid expressing the Sup35 protein under the *GAL* promoter, was transformed into these colonies. By transient overproduction of Sup35 protein on galactose medium, the *de novo* formation of [*PSI*$^+$] was monitored by nonsense suppression. The results showed that one colony out of 30 had *de novo* [*PSI*$^+$] formation, and it was labeled as a N-PrP reinducible strain (Figure 2-8 A).
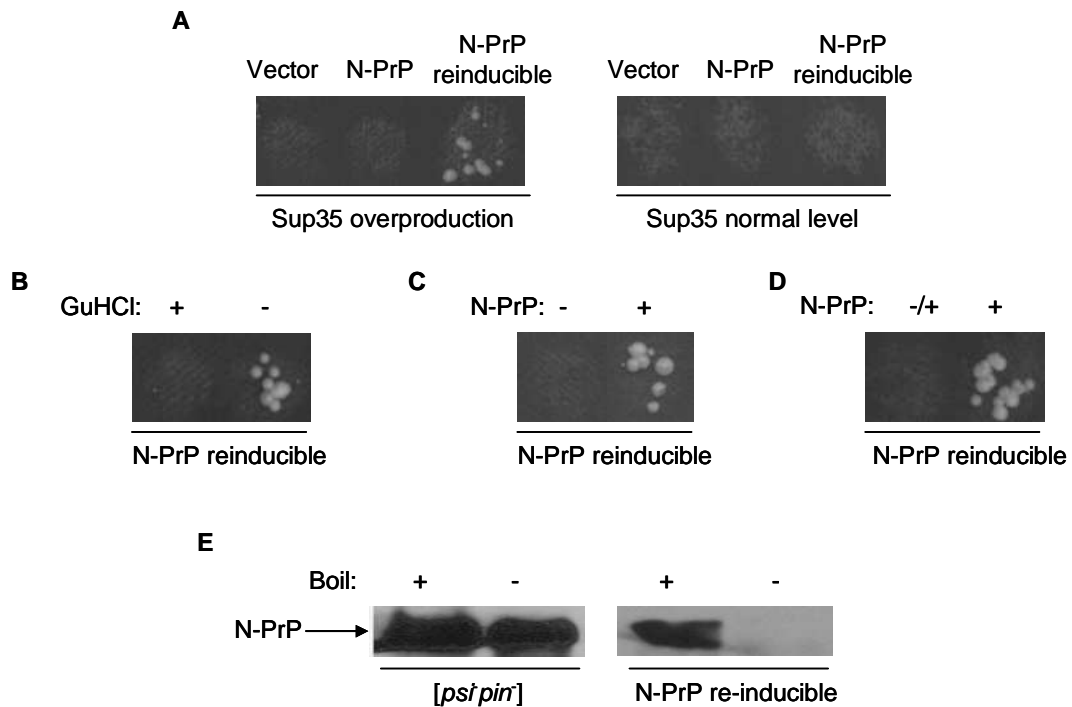
Figure 2-8. Prion-like state of N-PrP facilitated the *de novo* [*PSI*⁺] formation.
Nonsense suppression was checked on –Ade medium. **A**- The [*PSI*⁺] prion induced by N-PrP was cured with excess Hsp104, then Sup35 was overproduced in the strain and *de novo* formation of [*PSI*⁺] was monitored by nonsense suppression. Of all the 30 individual colonies checked, one colony had *de novo* [*PSI*⁺] formation after Hsp104 curing (named as N-PrP reinducible). No [*PSI*⁺] was induced if Sup35 was produced on a normal level. As controls, empty vector or N-PrP plasmid was transformed into [*psi⁻ pin⁻*] strain. With overproduction of Sup35, no [*PSI*⁺] was induced in the control strains. **B**- N-PrP reinducible strain was treated with GuHCl, and then no [*PSI*⁺] could be induced again after Sup35 overproduction. **C**- N-PrP expressing plasmid was lost from the N-PrP reinducible strain, then no [*PSI*⁺] could be induced again by Sup35 overproduction. Then the N-PrP expressing plasmid was transformed back to the strain (N-PrP -/+) (**D**), no [*PSI*⁺] was induced after Sup35 overproduction. **E**- N-PrP from reinducible strain or [*psi⁻ pin⁻*] strain was tested by gel entry assay. Cell lysate with 2% SDS (boiled or not boiled) was loaded for SDS-PAGE and then checked by western blot with Anti-PrP (6H4). N-PrP from the reinducible strain is SDS-insoluble and can not enter polyacrylamide gel without boiling. In contrast, N-PrP from [*psi⁻ pin⁻*] strain is SDS-soluble and can enter polyacrylamide gel without boiling.

Notably, after treating the reinducible strain with GuHCl, [*PSI*⁺] could not be induced again by Sup35 overproduction (Figure 2-8 B). Since GuHCl is a prion eliminating agent,

there should be some prion or prion-like complex responsible for the *de novo* [*PSI*$^+$]

induction in the reinducible strain. We further tested the reinducible strain by eliminating

the N-PrP expressing plasmid from it, and then, no [*PSI*$^+$] could be induced again by

Sup35 overproduction (Figure 2-8 C). This result indicated that no [*PIN*$^+$] or other yeast

prions existed in the reinducible strain; and N-PrP protein is required for the [*PSI*$^+$] re-

induction. Next, the N-PrP expressing plasmid was transformed back into the reinducible

strain, but [*PSI*$^+$] still could not be induced by Sup35 overproduction (Figure 2-8 D).

Based on these results, we concluded that the prion-like complex formed by N-PrP is

GuHCl curable and is responsible for the *de novo* [*PSI*$^+$] re-induction; without the prion-

like structure, N-PrP can not facilitate [*PSI*$^+$] induction.

Finally, we biochemically tested the N-PrP protein by the gel entry assay (Figure 2-8 E).

The cell lysate was extracted from an N-PrP reinducible strain, 2%SDS was added and

the samples (either boiled for 10 minutes or not boiled) were analyzed using SDS-PAGE.

The result showed that N-PrP was SDS-insoluble; it could not enter tha polyacrylamide

gel without boiling. In contrast, N-PrP extracted from a [*psi*$^-$*pin*$^-$] strain was soluble and

did enter into the polyacrylamide gel without boiling. This result further supports the

hypothesis that N-PrP forms a prion-like complex in a reinducible strain.

2-3-7 The effects of PrP and Aβ on the [*PSI*$^+$] associated cell toxicity

Although the presence of the [*PSI*$^+$] prion by itself is not detrimental to yeast cells,

overproduction of SUP35 or Sup35NM in [*PSI*$^+$] cells leads to growth inhibition

(Dagkesamanskaya et al., 1991; Derkatch et al., 1996). The source of this lethality has

been attributed to either the accumulation of Sup35p isoforms that might be toxic to the cell, or the depletion of essential factors (Derkatch et al., 1996; Derkatch et al., 1998).

In order to check how PrP or Aβ chimeric proteins affect the [PSI^+] associated cell toxicity, the respective proteins were overproduced in a [PSI^+] strain and the cells viabilities were monitored (Figure 2-9).

To test the PrP chimeric proteins, plasmids pMCUP1-SUP35N, pMCUP1-N-PrP$_{90-230}$, pMCUP1-N-PrPΔ90-119, pMCUP1-N-PrPΔ160-230, and pMCUP1-N-PrPΔ172-230 were transformed into the [PSI^+PIN^+] strain GT81-1C. Beginning from a uniform cell density (10^6 cells/ml), strains with different plasmids were incubated in overproduction inducing media (-Ura+100 µM CuSO4, liquid). After either 0 hour or 48 hours of incubation, cell viabilities were monitored by serial dilutions of the cell cultures followed by spotting onto selective media (-Ura).

Without protein overproduction, the [PSI^+] strain grew at the same level with no cell toxicity effect. However, after protein overproduction, the [PSI^+] strain with Sup35N showed a severe growth defect. Interestingly, N-PrP or N-PrPΔ90-119 ameliorated the cell toxicity; PrPΔ90-119 almost restored the cell viability to its normal level, as compared to the strain harboring an empty vector. In contrast, strains with N-PrPΔ160-230 or N-PrPΔ172-230 exhibited cell toxicities of the same level as that of Sup35N.
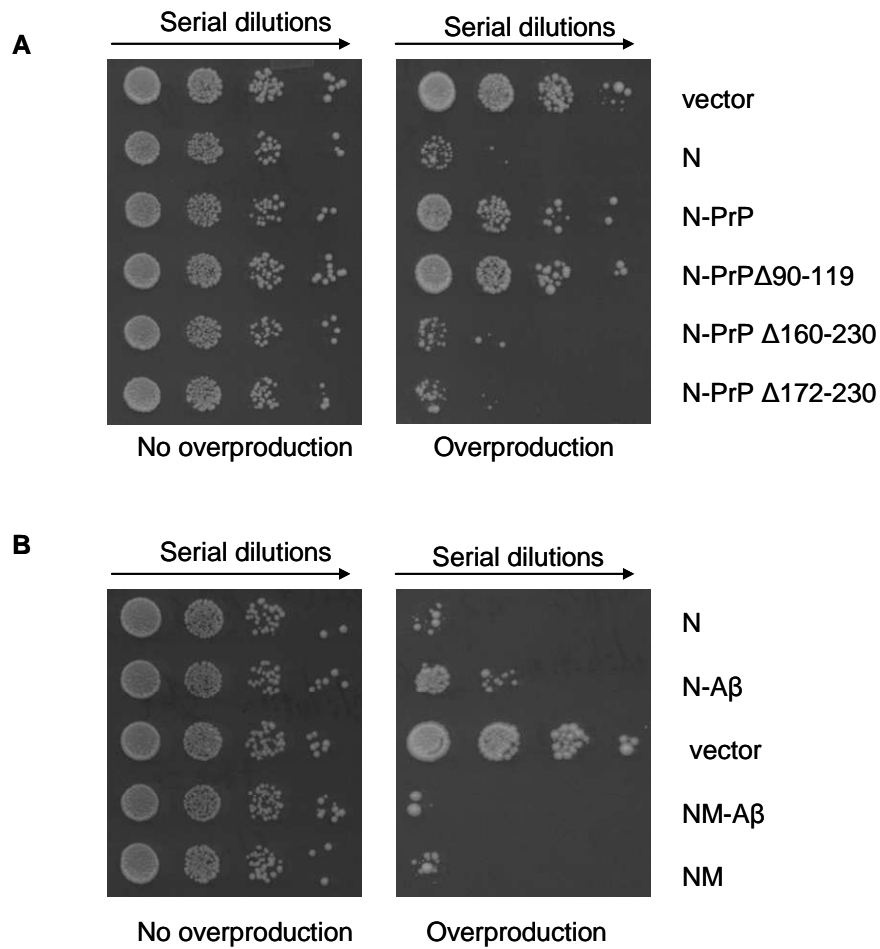
Figure 2-9. The effects of PrP and Aβ on the [*PSI*⁺] associated cell toxicity. "vector" refers to empty vector expressing no proteins in the cell. With or without incubating in the overproduction-inducing media (-Ura+100 μM CuSO4), [*PSI*⁺] cell cultures bearing the respective proteins were serial diluted and spotted onto synthetic media selective for the plasmids (-Ura). The [*PSI*⁺] associated toxicity was monitored by the growth on the synthetic media.

More evidence supported the hypothesis that [*PSI*⁺] associated cell toxicity is attributed to the depletion of certain essential factors. Specifically, overproduction of Sup35 in a [*PSI*⁺] strain was shown to sequester Sup45 (eRF1), another translation termination factor which is required for cell viability. Overproduction of Sup35NM in a [*PSI*⁺] strain was

shown to sequester Sup35, and the depletion of functional Sup35 caused cell death (Vishveshwara et al., 2009).

For this result, overproduction of Sup35N in a [*PSI*⁺] strain was presumed to sequester functional Sup35 (Sup45 may be sequestered too) and cause cell death. Notably, N-PrPΔ90-119, which induced no *de novo* [*PSI*⁺] formation, had the least cell toxicity effect; N-PrP which moderately induced [*PSI*⁺] formation, had a slight cell toxicity effect; N-PrPΔ160-230 or N-PrPΔ172-230, which promoted a much stronger [*PSI*⁺] induction, had severe cell toxicity. Since the formation of a PrP^Sc-like structure is attributed to the *de novo* [*PSI*⁺] induction, the cell toxicity effect may also be linked to the conformation of the PrP region in the chimeric proteins. Based on this result, native structured PrPΔ90-119 may prevent Sup35N from interacting and sequestering Sup35. Following the formation of a PrP^Sc-like structure, Sup35N more easily sequesters Sup35, causing cell death. Also, the PrP^Sc-like structure may have toxic effect, in of itself.

.

The Aβ42 chimeric proteins were also tested in the same manner. Plasmids pMCUP1-N-Aβ42, pMCUP1-NM-Aβ42, pMCUP1-NM-HA, pMCUP1-SUP35N and pMCUP1 were transformed into the [*PSI*⁺*PIN*⁺] strain GT81-1C. After overproduction, N-Aβ42 moderately ameliorated the cell toxicity effect as compared to the toxic effect caused by Sup35N.   The cell toxicities caused by excess NM-Aβ42 and NM-HA were of a similar level, and they both caused a severe growth defect. The fusion of Aβ42 may prevent Sup35N from interacting with and sequestering functional Sup35, which would decrease the cell toxicity to some extent. It is reported that aggregation of Aβ42 has neurotoxic

effects in a mammalian model (LaFerla et al., 2005; Hardy et al., 2002). The aggregation of Aβ42 in the chimeric proteins may also be partially responsible for the cell toxicity.

2-4 Discussion:

We have developed a novel yeast model system which employs the *de novo* prion induction assay for studying properties of a mammalian prion protein.

Overproduction of Sup35 or Sup35N can promote *de novo* [*PSI*$^+$] formation only in the presence of other yeast prions such as [*PIN*$^+$]. In our system, by fusing Sup35N with mouse PrP$_{90\text{-}230}$, the overproduced chimeric protein can promote *de novo* formation of [*PSI*$^+$] even in the absence of other pre-existing prions. Previous studies showed that mammalian PrP can aggregate and form a PrP^{Sc}-like conformation in yeast cells, while the N-terminal region is required for PrP^{Sc} formation both in mammalian cells and yeast. Notably, our result showed that a deletion of N-terminal residues 90-119 from PrP eliminates the [*PSI*$^+$] induction ability of N-PrP, indicating that the prion-like state formed by PrP was important for the [*PSI*$^+$] induction ability of N-PrP. Interestingly, deletions of PrP C-terminal residues 160-230 or 172-230 promote the [*PSI*$^+$] *de novo* induction by N-PrP. Clinical evidence showed that several cases of human prion diseases were linked with nonsense mutations in the C –terminal region of the PrP coding gene. Especially, one case of human GSS disease was linked with a nonsense mutation at residue 160 in PrP, which agreed with our result.

When overexpressed in [*psī⁻pin⁻*], [*psī⁻PIN*$^+$] or [*PSI*$^+$*PIN*$^+$] strains, N-PrP can always be precipitated from yeast extracts at 16,000 g, indicating that it is aggregated.

58

Immunofluorescence analysis detected multiple N-PrP aggregates (similar to those formed by yeast prions) in a significant fraction of the yeast cells. This is in agreement with both our prion induction results and previous observations by I. Vorberg (Krammer et al., 2008), who detected multiple N-PrP aggregates in mammalian cells. Therefore, patterns of N-PrP aggregation are conserved between yeast and mammals.

Detergent resistance is a common feature shared by prion amyloids. With overproduction, the SDS-insoluble complex of N-PrP can be detected in the [PSI^+] strain but not in the [psi^-] strain. The amyloid-like structure formed by PrP (part of N-PrP) may be unstable and could be stabilized by the Sup35N (part of N-PrP) prion amyloid in a [PSI^+] strain. In an exceptional case, from a [PSI^+] colony induced by N-PrP, a detergent-insoluble N-PrP complex was identified after eliminating the [PSI^+] prion by excess Hsp104. The prion-like structure of N-PrP (without overproduction in the strain) was shown to facilitate the [PSI^+] *de novo* formation upon Sup35 overproduction.

We further investigated [PSI^+] propagation by N-PrP. It was shown that N-PrP can maintain the [PSI^+] sate even in the absence of full length Sup35, and the [PSI^+] state can be transfered back to native Sup35. The Sup35N region from N-PrP is expected to maintain the [PSI^+] conformation by itself, and by interacting with the N domain of native Sup35, it converts Sup35 into the prion state. Notably, Hsp104 overproduction can not cure the [PSI^+] state maintained by Sup35N. However, excess Hsp104 cures [PSI^+] maintained by N-PrP quite efficiently.

Based on the evidence above, we propose a model for the PrP induced [*PSI*+] *de novo*

formation (Figure 2-10). With overproduction of N-PrP, the chimeric proteins aggregate

together via PrP regions. Then, a transient prion-like structure is formed by PrP, which

increases the initial nucleation of the attached Sup35N and promotes its prion formation.

The resulting prion would incorporate full-length Sup35 and convert it into a prion state.

Therefore, the initial PrP^Sc-like formation would be fixed in the form of a stably inherited

phenotype, detectable by the nonsense suppression assay.
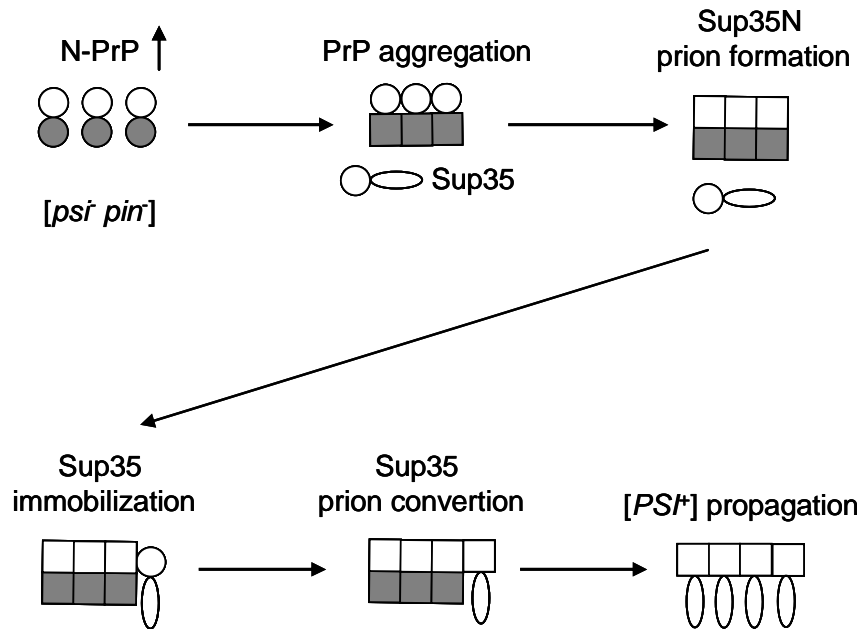
Figure 2-10. Model for PrP mediated [*PSI*+] induction. PrP is shown in dark filling
and Sup35N is in blank filling. Circles and squares correspond to non-prion and prion
isoforms, respectively. Oval corresponds to Sup35MC region.

Interestingly, a physical link between Sup35N and PrP is important for the prion

induction, as overproduction of PrP alone does not promote [*PSI*+] induction. In contrast,

the [*PIN*+] prion promotes [*PSI*+] *de novo* formation without any physical linkage

between Rnq1 and Sup35. The seeding model suggests that the [*PIN*+] prion promote [*PSI*+] formation by providing a nucleus to facilitate the initial prion formation (Derkatch et al., 2001). Yeast prions always contain Q/N-rich prion domains; one yeast prion may nucleate other yeast prion via heterologous prion domains. However, mammalian PrP is nonhomologous to any of the yeast prion proteins, and it does not have a Gln/Asn-rich prion domain. So presumably, the cross-seeding between mammalian PrP and a yeast prion can not occur spontaneously unless a physical link existed. Data showed that [*PSI*+] can also promote [*PIN*+] formation, while another yeast prion [URE3] can promote both [*PIN*+] and [*PSI*+] formation (Derkatch et al., 2000; Derkatch et al., 2001). Moreover, it was also shown that mixing of the PrP prion with Aβ42 amyloid in an Alzheimer's transgenic mouse model dramatically accelerated both pathologies (Morales et al., 2010). Heterozygous prions cross-seeding may be a widespread phenomenon which needs to be further studied.

The *de novo* prion induction assay can also be employed to study other mammalian amyloidogenic proteins which cause diseases. Fused with Sup35N or Sup35NM, Aβ42 also induced [*PSI*+] *de novo* formation in the absence of other yeast prions. Inhibiting the aggregation of Aβ42 by triple mutations eliminated the [*PSI*+] induction ability of NM-Aβ42. Other amyloid related properties of Aβ42 are ready to be studied in this model, which may shed light on the mechanism of Alzheimer's disease.

Yeast cytoplasm is an environment that is very different from one where PrP^{Sc} or Aβ usually exist. However, these differences are more likely to influence prion propagation

rather than initial prion formation targeted in our work. Aggregation and prion formation by PrP are detected even *in vitro* (Castilla et al., 2005; Kocisko et al., 2006), and yeast prions can be formed in bacterial (Garrity et al., 2010) or mammalian (Krammer et al., 2009) cells. Thus, major parameters of the initial prion formation are largely independent of the environment.

The initial origin of the prion conformation is largely unclear. Prion diseases occur more sporadically, and some heritable prion diseases are linked with disease-promoting mutations in PrP (van der Kamp et al., 2009; Solomon et al., 2009). Systematic studies of mutations preventing PrP from forming a prion have been difficult due to both laborious monitoring techniques in animal models and the multi-step nature of the prion disease, itself, making it hard to determine which step is influenced by a mutation. In most cases, it was impossible to conclude whether these mutations affect prion formation or only propagation of the pre-existing prion state. Directly linked with the initial prion formation of PrP, our assay provides a unique opportunity for the simple and very fast large-scale screening of the effects of PrP mutations, as well as chemicals and peptides on prion-inducing properties of PrP. This may help to develop new anti-prion and prophylactic treatments, as well as to better understand the general mechanisms of prion formation.

2-5 Conclusions:

- Fusion to PrP or Aβ42 enabled the sup35 prion domain to induce *de novo* formation of [*PSI*⁺] in the absence of other prions.

- PrP deletions strongly affected the [*PSI*⁺] inducing ability of N-PrP.

- Sup35N-PrP aggregated in the yeast cells and acquired the SDS-insoluble state only in the presence of the Sup35 prion.

- The prion state can be maintained by N-PrP in the absence of full-length Sup35, partially cured by excess of the Hsp104 chaperone.

- The prion-like state of Sup35N-PrP facilitated the [*PSI*⁺] *de novo* induction in the absence of other prions.

- Fusion of PrP or Aβ42 to Sup35N affected the [*PSI*⁺] associated cell toxicity.

CHAPTER 3

DEVELOPMENT OF EXPRESS-ASSAYS FOR PRION DETECTION

3-1 Introduction

Prion is a widespread phenomenon

All proven yeast prions contain a Q/N-rich prion domain (PrD) which is essential for prion formation and propagation. 1-4% of eukaryotic proteins contain a QN-rich domain similar to known yeast PrDs based on amino acid composition (Harrison and Gerstein, 2003). A genome-wide screening in *S. cerevisiae* yeast was conducted to search for prion candidates (Alberti et al, 2009). About 100 proteins were identified having a PrD-like sequence, and 19 of them can potentially form a prion-like structure. One protein (Mot3) was confirmed to form a prion with a phenotype that is likely to be advantageous under certain environmental conditions. The prion-forming ability may be widespread among yeast proteins or proteins from other species. Moreover, non-QN rich prion proteins are found in other organisms, *e.g.* Het-s in the fungus Podospora (Malato et al., 2007) and PrP in mammals. Thus, the prion phenomenon may be widespread in many species, and there are many more prion-forming proteins yet to be identified and studied.

.

Biological roles of yeast and fungal prions

Prion formation of the mammalian prion protein is strongly linked to a series of neurodegenerative diseases in humans and animals. However, yeast prions generally do not appear to bestow detrimental effects on the cells, and the prions may even convey

protective functions in some adverse environments. For example, yeast cells having the [*SWI*[+]] prion were shown to be resistant to the microtubule disruptor, benomyl. Another yeast prion [*MOT3*^{+}] was shown to increase cellular resistance to certain cell wall stressors. The [*OCT*+] prion induces flocculation, a growth form that has been shown to protect cells from various stresses (Du et al., 2008; Patel et al., 2009). The [*PSI*[+]] prion is only detected in laboratory strains; however, it was shown that the prion-forming ability of the Sup35 prion domain is maintained throughout yeast evolution despite divergence of the specific amino acids (aa) sequences (Chen et al, 2007, Chernoff et al, 2000). In fact, it was shown that the Sup35 prion provides resistance to some toxic agents or unfavorable conditions in certain laboratory strains (True and Lindquist, 2000). It was, thus, proposed that a decrease in the translation termination function of Sup35 increases phenotypic variability by allowing readthrough of stop codons, thus producing proteins of extended lengths.

Methods of prion detection

Prion is a widespread phenomenon in yeast; however, our understanding of the distribution and biological roles of yeast prions in natural conditions remains at rudimentary levels, partially due to the lack of sequence- and phenotype-independent approaches for prion detection and monitoring. Approaches to phenotypic detection of yeast prions are based on functions of individual prion proteins (Chernoff et al, 2002). Prion formation usually causes a partial loss of the protein's normal function, such as for the Sup35 prion [*PSI*[+]] or for the Ure2 prion [URE3]. Specially designed strains are needed to detect the phenotypes caused by each respective prion. Thus, phenotypic

detection is restricted to a specific prion in each case. Alternatively, candidate prion domains can be tested in phenotypic assays by fusing them to the proteins with known function, e.g. Sup35MC. However, not all fusions remain functional and, therefore, not all prion domains can be detected in this way.

Biochemical approaches for prion detection *in vivo* are based on the properties of amyloid aggregates, such as protease resistance and high sedimentation rate (Chernoff et al, 2002). However, these approaches can only be applied to detect prions formed by known proteins, since a specific antibody or tag is needed to visualize the target protein. None of these approaches is selective enough for separating a previously unknown prion from the cell lysate, as many non-prion proteins or protein complexes are also characterized by high proteinase resistance or high sedimentation rate. Amyloids assembled *in vitro* can be detected by electron or atomic force microscopy, a thioflavin T (ThT) or Congo Red binging test, a detergent insolubility test or a light-scattering test (for review see Chernoff et al, 2002). These techniques work well for detecting purified proteins; however, they are not easily applicable to living cells or cell extracts. It was reported that [*PIN*[+]] containing structures have been stained and visualized by ThT (Douglas et al, 2008); however, the specificity and sensitivity of this staining remains questionable. Amyloid fibers have been detected in [URE3] cells with electron microscopy, but only when Ure2 is overproduced at a high level (Speransky et al, 2001).

The "gel-entry" assay can efficiently identify prions formed by known proteins (Kushnirov et al., 2006). Yeast prions or other amyloids of different fiber types are detergent-insoluble; they cannot enter polyacrylamide gel without boiling. So by comparing boiled and unboiled samples of the same protein, prion-forming proteins can be distinguished from non-prion proteins. The gel-entry assay cannot identify unknown prions, and it would be too laborious to use this method for a large-scale analysis. SDD-AGE (semi-denaturing detergent-agarose gel electrophoresis) is also used to analyze prion polymers (Kryndushkin et al, 2003). Different sized prion polymers in 2% SDS can be separated by electrophoresis in a semi-denaturing agarose gel. This technique has been used extensively for confirming prion properties of individual proteins and for characterizing polymer size *in vivo*. However, this approach is not useful for prion screening, and it cannot identify unknown prions. To date, no effective biochemical tool exists that can identify previously unknown prions in cell extracts based solely on their physical patterns.

The ability to form transmissible amyloids (prions) is widespread among yeast proteins and is likely an intrinsic property of proteins from other organisms. However, the distribution of yeast prions in natural conditions is not yet clear, thus preventing us from understanding the relationship between prions and their adaptive roles in various environmental conditions.

Objectives

The main goal in this work is to develop and optimize the sequence-independent biochemical approaches for known and unknown prion detection in yeast. Large scale prion-profilling can be perfomed with the new approches, which can shed light on the relationship between prions and their adaptation to various environmental conditions in the yeast model.

3-2 Materials and methods

<u>Yeast strains</u>

See appendix for a description of yeast strains used in this study.

<u>Gel preparation</u>

10% acrylamide gel: 2.64 ml DI water, 3.33 ml 30% Acrylamide, 1.33 ml 2% Bis, 2.5 ml 1.5 M Tris PH 8.8, 0.1 ml 10% SDS, 0.1 ml 10% APS, 4 µl TEMD (for 10 ml gel)

5% acrylamide gel (Stacking gel): 2.475 ml DI water, 0.833 ml 30% Acrylamide, 0.332 ml 2% Bis, 1.26 ml 0.5 M Tris PH 6.8, 0.05 ml 10% SDS, 0.05 ml 10% APS, 7 µl TEMD (for 5 ml gel)

1.8% Agarose gel: 0.18 g agarose, 9.9 ml TAE buffer PH 8.0, 0.1ml 10% SDS (for 10ml gel)

<u>Flamingo staining</u>

Flamingo staining was performed using a Flamingo Fluorescent Gel Stain kit from Bio-rad, which provided a 0.5 ng sensitivity for protein visualization. The gel was fixed for 2 hours in fixing solution (40% (v/v) ethanol and 10% (v/v) acetic acid), and then strained in 1X Flamingo fluorescent gel stain solution for at least 3 hours. The gel was then washed with water and scanned using a Typhoon gel and blot imager from GE. Protein signals were visualized with a 532 nm Green laser.

3-3 Results

3-3-1 Adjustment of the "Gel-boiling" assay for prion profiling

Amyloids formed by prions are detergent insoluble and cannot enter into polyacrylamide gel without boiling (Figure 3-1). This feature is used to distinguish prion amyloids from other cellular proteins or from non-prion aggregates.
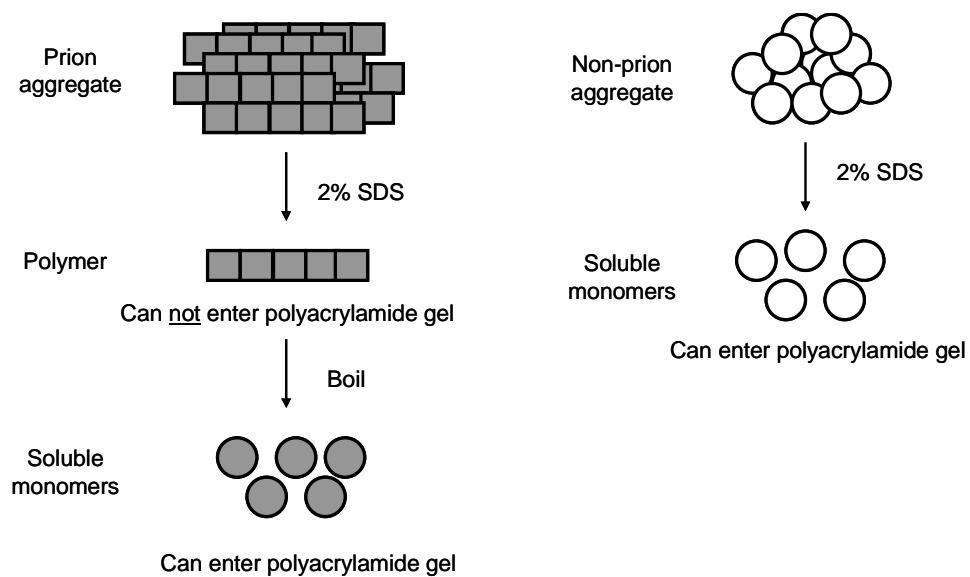
Figure 3-1. Yeast prion polymers are SDS stable. SDS can disrupt the prion aggregate into stable polymers; the polymers are too big to enter polyacrylamide gel. Boiling of the prion polymers can destruct them into soluble monomers which can enter the polyacrylamide gel. In contrast, SDS can dissolve non-prion aggregate into soluble monomers which can enter the polyarylamide gel without boiling.

The "gel-boiling" assay for prion detection (Kushnirov et al., 2006), modified by us and based on this principle, was used to detect and analyze amyloid-based prions in yeast strains. This experiment was performed using a standard SDS–PAGE; however, the gel uniformly consisted of a 10% acrylamide gel without the addition of a stacking gel. The cell lysate was extracted using a standard protocol, mixed with 4X sample buffer (0.25M Tris–HCl, pH 6.8, 8% w/v SDS, 8% 2-mercaptoethanol, 20% glycerol, 0.2% w/v bromophenol blue), incubated for 5 min at room temperature, and then loaded on a SDS-PAGE gel without boiling. Only soluble proteins could enter the gel, while prion polymers remained trapped in the bottom of the wells. After the gel was run for a period of time, depending on the size of the target protein (for Sup35 it takes 45 ~ 60min until the bromophenol blue reaches the middle of the gel), electrophoresis was interrupted, and a new portion of polyacrylamide was added to the wells and allowed to solidify. This was followed by boiling the whole gel (gel was sealed in a plastic bag and submerged vertically in boiling water) for 10 min, cooling it down and running it again. Due to the destruction of polymers by boiling, prion proteins previously trapped in the wells could now enter the gel in the second run. Western blot, followed by reaction with the appropriate antibody, allowed detection of the prion isoform which was visible as the upper band. The non-prion isoform (that entered the gel without boiling) was visualized as the bottom band. The "gel-boiling" assay reproducibly distinguished prion isoforms of Sup35 and Rnq1 from the cell extracts (Figure 3-2 A, B). When compared to the "gel-

entry" assay (cell extracts with 2% SDS were loaded for SDS-PAGE, with or without

boiling; prion protein was identified through its ability to enter the gel), the "gel- boiling"

assay distinguished prion isoforms from a single sample, and it also showed the

proportion of protein found in the polymeric and the monomeric fraction. For the [URE3]

prion amyloid, although boiling in 2% SDS was not sufficient to disaggregate the prion,

boiling in a 8M urea solution could disaggregate it into monomers, and the Ure2 protein

was found to enter the SDS-PAGE gel (Data not shown).
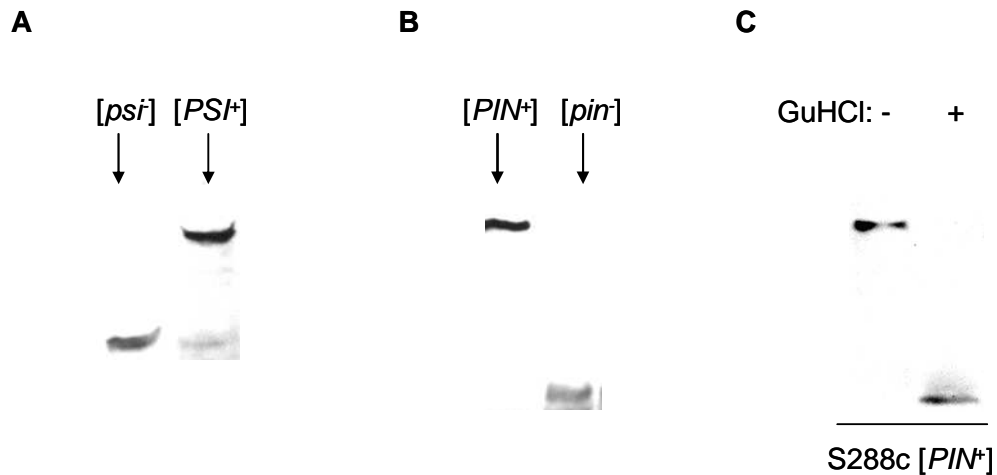
Figure 3-2. "Gel boiling" assay identifies the prion forms of Sup35 and Rnq1 proteins. Sup35 and Rnq1 anti-bodies were used to detect [PSI^+] or [PIN^+] respectively. The upper protein bands came from denatured amyloids, while the bottom bands came from protein monomers. **A,B**- In [psi^-] or [pin^-] strains, Sup35 and Rnq1 are in monomer forms with 2%SDS, and can enter polyacrylamide gel without boiling. In [PSI^+] or [PIN^+] strains, Sup35 and Rnq1 are in amyloid form with 2% SDS, which can only enter polyacrylamide gel after boiling, appearing on the top of the gel. **C**- One example of prion profiling result. [PIN^+] prion was identified from *S. cerevisiae* strain S288c. After GuHCl curing, there was only SDS-soluble Rnq1 protein detected in the strain.

3-3-2 Prion detection in yeast strains of various origins.

Previous screens for yeast prions have been performed for some randomly chosen strains with uncertain evolutionary relationships (Chernoff et al., 2000; Nakayashiki et al., 2005). Using the "gel-boiling" assay, we searched for prions within certain *S. cerevisiae* and *S. paradoxus* strains of known origin, having completely sequenced genomes and well-defined phylogenetic relationships. These were provided by Drs. G. Liti and E. Louis (Liti et al., 2009). We have also checked 11 other *S. cerevisiae* strains having partially known phylogenetic relationships, provided by J. Fay (Fay and Benavides, 2005). In addition, we have checked two representative strains of the Petershoff Genetic Lines (PGL), the *S. cerevisiae* laboratory strain collection of St. Petersburg University, Russia, that is independent from the US laboratory strains, one commercial *S. cerevisiae* strain purchased from Mr. Beer, and Saccharomyces strains of different species used in our previous papers (Chernoff et al., 2000; Chen et al., 2007). (See appendix for the description of the yeast strains checked in this study)
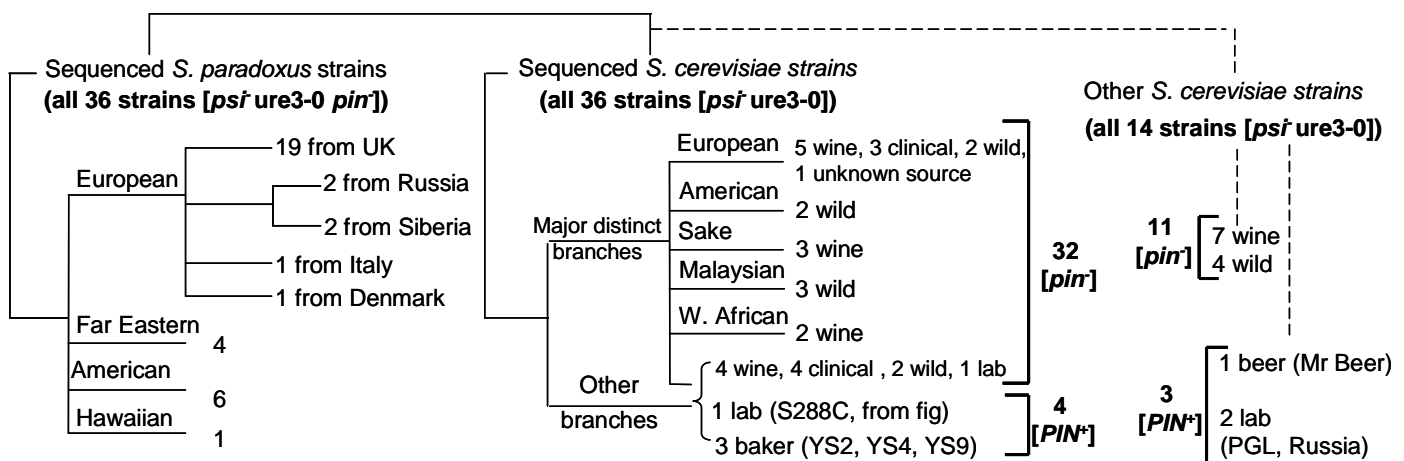
Figure 3-3. Prion distribution among the yeast strains of various origins. Phylogenetic relationships of yeast strains are based on ref. Liti et al. 2009 and presented in a simplified way. "Wine" strains include grape, berry, sake and palm

wine strains. Sake group is mostly of Asian origin but also includes some palm wine strains from African sources.

Although the [PSI^+] prion is frequently found in laboratory strains originating from S288C or PGL strains, no prion form of Sup35 or Ure2 proteins are detected in *Saccharomyces* strains checked in this study. The "Gel-boiling" assay detected the [PIN^+] prion in 4 out of 36 natural and industrial strains of *S. cerevisiae* received from the Liti lab (Figure 3-2 C), as well as in two PGL laboratory strains and in the commercial strain obtained from Mr. Beer. In each strain containing [PIN^+], after treatmentwith the prion-eliminating agent GuHCl, Rnq1 was present in the monomeric form within the strain. No [PIN^+] prion was detected in the remainder of the *S. cerevisiae* strains or in any strains from species other than *S. cerevisiae* (Figure 3-3).

Our results agreed with previous data obtained by other groups, and we also found that all [PIN^+]-containing strains originate from either laboratory, brewery or bakery strains, while none of the 21 wine strains tested (including grape, palm and sake wine) or 13 wild strains tested contain the [PIN^+] prion. The 3 [PIN^+]-containing bakery strains are closely related to each other, while S288C that originates from rotting figs is diverged both from them and from other major distinct phylogenetic branches. Among non-sequenced strains, the [PIN^+]-containing PGL laboratory strains are known to originate from bakery strains. Notably, by analyzing previous prion screening data (Nakayashiki et al, 2005), it was also found that all [PIN^+]-containing isolates having known origins originated from either the lab, brewery, bakery or clinic,

but never from the winery or from the wild. Taken together, these results suggest that the [*PIN*⁺] prion is underrepresented among the wine strains which are involved in an intense fermentation process resulting in accumulation of high concentrations of ethanol.

3-3-3 Development of the "Agarose trapping" assay for prion profiling.

In order to indentify unknown prions from a yeast strain, it is necessary to   isolate potential amyloids in the amount sufficient for visual or mass-spectroscopic detection. For this purpose, we developed an "agarose trapping" assay (Figure 3-4) that is based on the observation that detergent-insoluble prion polymers cannot enter into polyacrylamide gel but can move into the agarose gel (Kryndushkin et al., 2003).

The experiment was performed on a SDS–PAGE base; however, a combined gel was used having a 1.8% agarose gel on the top and a 10% polyacrylamide gel on the bottom. Cell extracts were then mixed with 4X sample buffer (with 2% SDS in the final mixture) and were incubated for 30 min at room temperature. Samples were then loaded on the combined gel without boiling. With electrophoresis, the soluble proteins ran into the polyacrylamide gel, while the SDS-insoluble prion polymers were trapped on the bottom of the agarose gel. The electrophoresis was run for an extended length of time (3 hours or more) to make sure that all soluble proteins were run out of the agarose gel. The bottom portion of the agarose gel was cut out, boiled and then loaded onto a normal SDS-PAGE gel (for the purpose of loading, we used a low melting point agarose). After separation by electrophoresis, the trapped proteins were visualized by western blotting (in the case of

74

known prions) and by Flamingo staining (Berkelman et al., 2009) for any proteins present

in sufficient amounts. For unknown prion identification, protein trapped in agarose were

extracted and analyzed by mass spectrometry (MS).
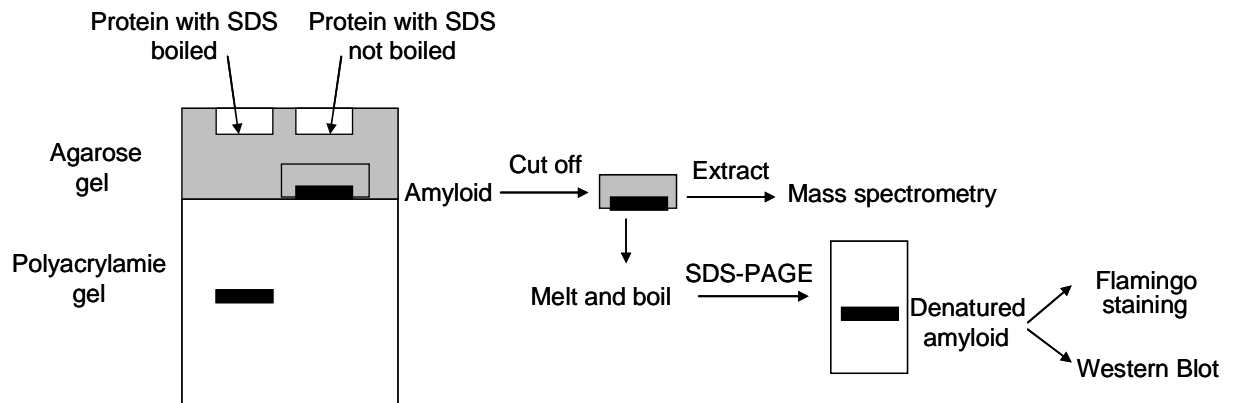
Figure 3-4. A model of the agarose trapping assay for prion identification. Without boiling, prion polymers are SDS stable and can be trapped in agarose. The trapped polymers can be either extracted and analyzed by mass-spectroscopy or denatured by boiling and run on a SDS-PAGE gel to visualize individual proteins. If a sample is pre-boiled, polymers are solubilized and cannot be trapped in agarose.

Our results showed that the prion isoforms of Sup35, Rnq1 and Ure2 can be trapped in

the agarose from their respective prion-containing cell extracts. The trapped proteins

were visualized by western blot with respective antibodies (Figure 3-5 A-C). In contrast,

there were no prion proteins trapped from the pre-boiled samples of prion-containing

extracts or from non-prion containing extracts. As an additional control, the non-prion

protein Ade2 was tested and not found to be trapped in the agarose (Figure 3-5 D).
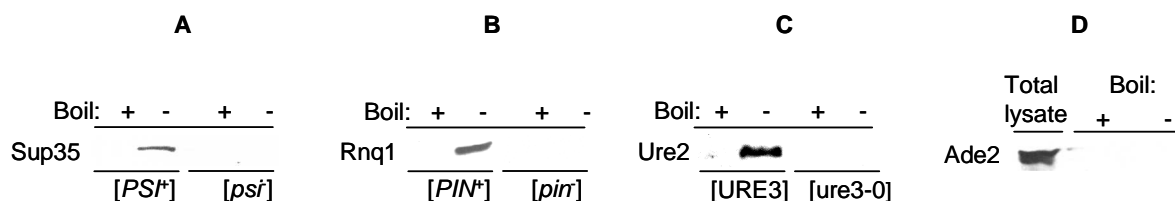
Figure 3-5. Identification of prion proteins by the agarose trapping assay An analysis was performed as shown in Fig. 3-4. The prion forms of the proteins Sup35 (**A**), Rnq1 (**B**) and Ure2 (**C**) were detected by immunostaining with respective antibodies in the agarose traps of the respective prion-containing strains. However, they were not detected in the traps of non-prion strains or in cases when samples were boiled before trapping. (**D**) Ade2 protein, used as a control, was present in the total lysate but was not trapped in agarose for samples that were either boiled or not boiled.

The protein samples from the agarose trap were also analyzed by MS, performed by E. Dammer and J. Peng (Emory University). Initially there were significant amounts of unspecific proteins detected in the samples, including high molecular weight (MW) complexes (*e. g.* ribosomes) and chaperons (*e. g.* Hsp70). To minimize contamination, we subjected the samples to additional treatments before loading. Cell extracts with 10%SDS were incubated at a higher temperature (37^0C) to removes most of the aggregate-associated chaperones. Then the samples were centrifuged at high speed (200,000g, 30mins) to remove most of the ribosomes and other complexes. This kept most of the prion polymers in solution. After these steps, the samples were run through the agarose trap, and the trapped proteins were analyzed by MS again. It was found that Sup35 wasthe most abundant protein, and Rnq1 was the second most abundant protein from the cell extract containing both proteins in the prion isoforms ($[PSI^+\ PIN^+]$). In the $[psi^-\ PIN^+]$ sample, it was found that Rnq1 was the most abundant protein, while in the $[psi^-\ pin^-]$ sample, none of these proteins was detected (Table 3-1). Ultimately, the "agarose

trapping" assay can potentially identify any prion-like complex that can move into the agarose gel but cannot enter into the polyacrylamide gel.

Table 3-1. Proteins that are overabundant in the agarose traps of prion-contaig strains

Protein	Description	Size, (kD)	Abundance in the agarose traps		
			[*PSI*⁺ *PIN*⁺]	[*psi*⁻ *PIN*⁺]	[*psi*⁻ *pin*⁻]
Sup35	Prion (translation termination factor)	79	Highest	None	None
Rnq1	Prion (unknown function)	43	2nd highest	High	None
Pyk1	Pyruvate kinase	55	High	Moderate	Low
Tdh1/2/3	Trioso-phosphate dehydrogenase	37	High	Moderate	Moderate
Eno1/2	Enolase	47	Moderate	Moderate	None

In addition to Sup35 or Rnq1, several more proteins were identified by MS which are exclusively or preferably abundant in [PSI^+ PIN^+] or in [psi^- PIN^+] extracts, when compared with non-prion extracts. Interestingly, all of these proteins turned out to be yeast glycolytic enzymes, including pyruvate kinase (Pyk1), triose-phosphate dehydrogenase (Tdh1, 2 and 3), and enolase (Eno1 and 2). The appearance of these glycolytic enzymes in the agarose trap does not appear to be accidental. Previous results showed that Eno2 interacted with the Sup35 prion domain (Bailleul et al., 1999); Tdh and Eno2 were found to co-immunoprecipate with polyQ aggregates produced in the prion-containing strain (Wang et al., 2007). These results point to the possibility that prion formation may influence glycolysis, which represents one of the major driving forces of yeast adaptation and evolution.

Several more proteins were identified in agarose traps from both prion-containing and non-prion-containing cell extracts (Table 3-2). These include: (1) High MW (200 kD or higher) proteins, including the glycoprotein Ygp1; (2) membrane-associated proteins Pma1/2; (3) the cell wall protein Bgl2; (4) actin which is the major component of polymeric cytoskeletal structuresand (5) and ubiquitin (Ub) which is attached to many misfolded or aggregated proteins and can form long poly-Ub chains. Some ribosomal proteins and ribosome-associated translational factors (Ef-1α or EF-2) were also detected in the agarose traps with variable abundance. All of these proteins were significantly less abundant than known prions. The contaminations do not prevent identification of proteins having the prion isoform. Prion polymers can be removed from the sample by pre-boiling, and prion containing strains can simply be cured by GuHCl; these enable us to distinguish prion proteins from the contaminants. Interestingly, Bgl2 is shown to possess amyloid properties (Kalebina et al., 2008), while Pma1 is suspected to be involved in a prion-like phenomenon related to glucosamine resistance (Brown and Lindquist, 2009), indicating that the presence of these proteins in our samples could not be due to simple contamination.

Table 3-2 . Background and contaminant proteins detected in agarose traps

Protein	Description	Size, kD
Mdn1	Midasin, involved in ribosome assembly and export	559
Gcn1	Positive regulator of Gcn2 kinase	297
Acc1	Acetyl-CoA-carboxylase, involved in fatty acid biosynthesis	250
Fas2	Fatty acid synthetase	207
Ygp1	Cell wall glycoprotein	37 (>200 when glycosylated)
Pma1/2	Plasma membrane ATPase	100/102
Act1	Actin, major component of cytoskeleton	42
Bgl2	β-glucanase, cell wall protein with known amyloid properties	34
Some translation factors	Associated with ribosomes	50-93
Some ribosomal proteins	Components of ribosomes	15-25
Ubiquitin	Covalently attached to misfolded and aggregated proteins	Fusions and polymers of variable sizes

3-3-4 Detection of new prion candidates with the "agarose trapping" assay

We employed the "agarose trapping" assay to identify new prion candidates within the set of yeast strains tested in section 3-3-2. The agarose trapped samples were analyzed by loading and running on a SDS-PAGE gel, followed by Flamingo staining. The protein bands shown in the gel were cut out, extracted and sent for MS analysis. With this procedure, Sup35 and/or Rnq1 proteins were confirmed corresponding to the respective protein bands from [*PSI*$^+$ *PIN*$^+$] or from [*psi*$^-$ *PIN*$^+$] samples (Figure 3-6). By analyzing several strains of various origins (Liti et al., 2009), Rnq1 was confirmed in the agarose trap from the extract of the bakery strain YS2 that was previously shown to contain the [*PIN*$^+$] prion. In addition, several more bands were detected in the extract of this strain (Figure 3-8), and at least some of them (as well as Rnq1) disappeared if samples were pre-boiled before agarose trapping (data not shown). One of the bands corresponding to

55kD in size (also seen in laboratory [*PSI*⁺ *PIN*⁺] strain) was confirmed to be Pyk1 by MS analysis. As a pyruvate kinase functioning in the glycolysis process, Pyk1 was isolated in prion-containing strains by agarose trapping, indicating its amyloid-like character. Our results suggest that Pyk1 can potentially form a prion-like structure in a [*PSI*⁺] or [*PIN*⁺] strain.
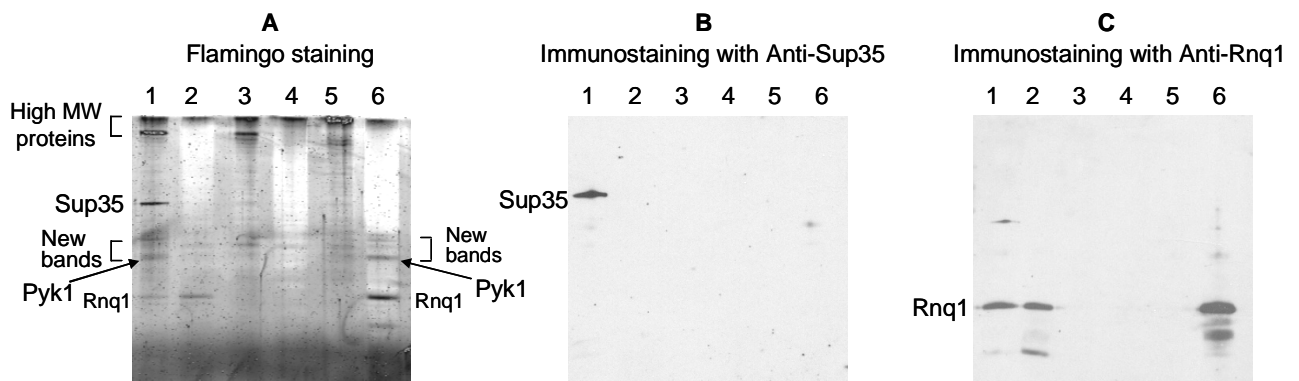
Figure 3-6. Detection of new prion aggregates by agarose trapping. 1, 2 and 3 – isogenic lab strains ([*PSI*⁺ *PIN*⁺], [*psi*⁻ *PIN*⁺] and [*psi*⁻ *pin*⁻], respectively); 4 and 5 – natural strains, 6 – bakery strain YS2.

3-4 Discussion

In this work, we modified the "gel-boiling" assay and employed it to screen known prions in a set of yeast strains of various origins. To indentify unknown prions, we developed the "agarose trapping" assay. Some prion candidates were identified by this assay.

With the "gel-boiling" assay, some known yeast prions were screened in a set of *S. cerevisiae* and *S. paradoxus* strains having known origins, completely sequenced

genomes and well-defined phylogenetic relationships (Liti et al., 2009). Combined with our results and previous data, it was shown that the prion forms of Sup35 or Ure2 were not found in any of the natural and industrial strains. The [PIN^+] prion was found in laboratory, brewery or bakery strains of *S. cerevisiae*, but not in wild or winemaking strains. [PIN^+]-containing isolates originated from different sources and were mixed in the past with different phylogenetically separated branches (Figure 3-3); thus, it is clear that not all prion-containing strains have a common origin. It is possible that strains of different origins acquire different prions that are not compatible with each other. Alternatively but not exclusively, certain environmental conditions or genetic changes may influence the *de novo* formation and/or maintenance of certain prions.

With the "agarose -trapping" assay, Sup35 and/or Rnq1 proteins were identified in their respective prion-containing strains. Additionally, several glycolytic enzymes were identified which are more abundant in prion-containing extracts when compared with non-prion extracts. Visualized by flamingo staining, a 55kD protein band was present in the [PSI^+] and/or [PIN^+] containing samples; MS results confirmed the protein to be the pyruvate kinase Pyk1. A mammalian homolog of pyruvate kinase was shown to form aggregates *in vitro* upon denaturing. It was noted that the aggregates were not completely solubilized after the denaturing agent was removed (Pierce and Stevens, 1983). It was also found that a dysfunction of glucose metabolism was associated with Alzheimer's disease, featuring amyloid formation of Aβ42 (Hunt et al., 2007). Thus, Pyk1 may potentially form an amyloid-like structure that is promoted by other prions such as [PSI^+] or [PIN^+]. Alternatively, the glycolytic enzymes (including Pyk1) trapped from prion-

containing cell extracts may not be prion, *per se*. They may interact tightly with prion or be included in the prion amyloid. Those proteins will still be of great interest, since they may help us to understand the biological effect of the prions. The specific presence of the glycolytic enzymes in the agarose traps from prion-containing strains may point to the role of prions in modulating the parameters of glycolytic and respiratory pathways.

A comprehensive prion profiling for known and unknown prions will help our understanding of the biological and evolutional role of prions. Our established assays were proven to detect prions effectively and can be employed for the task of large-scale prion profiling. For profiling known prions, the "gel boiling" assay will be more applicable. By using a larger gel with more wells, more samples can be analyzed in the same amount of time. For further high-throughput analysis, a specially designed device can be constructed usingthe same principle employed for gel boiling. This device contains multiple holes (e.g. 96 holes), and each hole is filled with 10% polyacrylamide gel. By loading cell extracts with 2%SDS into each hole and performing electrophoresis, the non-prion protein will run out of the gel, while the prion polymers are trapped on the top. Then, the electrophoresis is interrupted, polyacrylamide is added to each hole and allowed to solidify, and the whole plate is then boiled. After a short electrophoresis run, the denatured prion polymers enter the gel and will be transferred to a nitrocellulose filter by western blotting and are reacted to the appropriate antibody. To screen unknown prions on a large scale, the "agarose-trapping" assay could be simplified to decrease the work amount. To do this, the samples are loaded on the agarose trap, and electrophoresis is run for an extended duration. After the first run, all of the non-prion proteins enter the

polyacrylamide gel and eventually run out of it. The agarose gel containing trapped prion polymers is not cut out and is further tested in a new SDS-PAGE. The whole gel is boiled, cooled down, and electrophoresis is run again, followed by flamingo staining. The prion polymers are denatured with boiling and will enter polyarylamide gel, and the prion proteins will be visualized with flamingo staining.

In summary, we developed and optimized new unbiased biochemical approaches for prion detection in yeast, which are potentially amenable to high-throughput analysis for large scale prion profiling. The prion detection approaches are applicable to other organisms such as humans or animals, which will provide easy detection tools for PrP^{Sc} prion or other disease-associated amyloids. .

3-5 Conclusions:

- The "Gel-boiling" assay can effectively identify previously known prions from yeast strains of various origins.

- The [PSI^+] or [URE3] prions are not present in the 86 yeast strains of various origins, while the [PIN^+] prion is underrepresented among the wine strains involved in an intense fermentation processes.

- The newly developed "Agarose-trapping" assay can identify known prions as well as proteins with prion-like properties.

CHAPTER 4

CHARACTERIZATION OF A NEW PRION-LIKE PHENOMENON [*MCS*[+]]

4-1 Introduction

In contrast to all other known infectious agents, a prion is an infectious agent composed of protein in a misfolded form. Apart from the nucleic acid element, prion itself acts as a heritable protein-based element which shows non-Mendelian patterns of inheritance during meiosis. By studying yeast prions, three unusual genetic traits were proposed to distinguish prion from other nucleic acid-based replicons (Wickner et al., 1994). (1) The first is reversible curability. If a prion is cured, it should still be possible to arise again because the responsible protein is still produced in the cells. In contrast, curing of other nucleic acid-based replicons is irreversible unless they are re-introduced into the cell again. (2) Secondly, overproducing the prion protein increases the frequency of the prion formation. Since protein is the only agent responsible for prion formation, excess protein will increase the chance of prion formation. In contrast, overproducing a chromosomal protein is not likely to promote the formation of other nucleic acid-based replicons. (3) Lastly, a mutant phenotype may resemble the prion phenotype. If prion formation causes an inactivation of the normal form of the protein (such as for Sup35 or Ure2 prions), then the prion phenotype should be the same or similar to that produced by a mutation in the coding gene of the protein. This is the opposite of the relationship between nucleic acid-based replicons and the corresponding genes.

Different from the classical yeast prions described before, we found a new prion-like state called [MCS^+] which exists only in yeast strains expressing Sup35 without the Sup35 prion domain. [MCS^+] caused a nonsense suppression phenotype which was cured by the prion eliminating agent, GuHCl. However, the prion-like [MCS^+] state followed a Mendelian pattern inheritance, suggesting the involvement of a nuclear element.

Objectives

The main goal of this work is to study the new prion like state [MCS^+], which will help us understand the prion-related phenomena, as well as nonsense suppression epigenetic control.

4-2 Materials and methods:

4-2-1 Materials

Plasmids

Plasmids used in this study are listed in table 4-1

Table 4-1: Plasmids used in this study

Plasmid name	Protein	Yeast marker	Promoter	Source
pmCUP1MCSc	Sup35MC	URA3	*CUP1*	
pRS315-SUP35MC	Sup35MC	LEU2	P_{SUP35}	
pASB2	Sup35	LEU2	P_{SUP35}	
pRS315-SUP35 del3ATG	Sup35C	LEU2	P_{SUP35}	
pRS315	empty vector	LEU2		
pCUP-SUP35	Sup35	URA3	*CUP1*	Chernoff lab
pYS-L5	LEU2 disrupted Hsp104	LEU2		Lindquist lab

Strains

The yeast strains used in this study are listed in table 4-2.

Table 4-2: Yeast strains used in this study

Strain name	Prion background	Genotype
GT17	[*psi⁻pin⁻*]	MAT a ade1-14 his3-Δ200 leu2-3, 112 trp1-289 ura3-52
GT671	[*psi⁻pin⁻*]	MATa ade1-14 his3Δ (or 11,15) lys2 ura3-52 leu2-3,112 trp1 sup35::HIS3 [CEN LEU2 SUP35]
GT1120		MATa ade1-14 his3Δ (or 11,15) lys2 ura3-52, leu2-3, 112 trp1 sup35::HIS3 hsp104::LEU2 [URA3, SUP35MC]
GT1123	[*psi⁻PIN⁺*]	MATa ade1-14 his3Δ leu2-3,112 trp1-289 ura3 kar1 cyh^R rho⁻ sup35::HIS3 [SUP35MC LEU2]
GT1124	[*psi⁻PIN⁺*]	MATa ade1-14 his3Δ leu2-3,112 trp1-289 ura3 kar1 cyh^R rho⁻ sup35::HIS3 [SUP35C LEU2]
OT372		MAT α can1D::STE2pr-Sp_his5 lypD; his3D1 leu2D0 ura3D0 met1 5D0LYS2+
GT1292		MAT α sup35Δ::natR can1Δ::STE2pr-Sp_his5 lypΔ his3Δ leu2Δ ura3Δ met15Δ LYS2+ [SUP35MC URA3]
GT1293		MAT α sup35Δ::nat, [CUP1-SUP35 URA3], can1Δ::STE2pr-Sp_his5 lypΔ; his3Δ1 leu2Δ0 ura3Δ0 met1 5Δ0LYS2+

GT1120 was constructed by disrupting the genomic *HSP104* gene in a [*MCS*$^+$] bearing strain. A 4 kb DNA fragment was amplified by PCR from plasmid pYS-L5, containing the *LEU2* gene marker with a flanking sequence homologous to the *HSP104* gene. The primers used for the PCR were: GCCGCGATTTTTTGTTCA and GCACCATCCTTTACAAT. By transforming the PCR-amplified fragment into a [*MCS*$^+$] bearing strain, it replaced the 1kb *HSP104* gene portion by homologous recombination, thus disrupting the genomic *HSP104* gene in the strain. The resulting cells were grown on media selective for the *LEU2* marker. The gene disruption was confirmed by PCR.

4-2-2 Methods

Yeast extract transfection

To transfect [*MCS*$^+$] cell extract into an isogenic strain bearing no [*MCS*$^+$] factor, we used the transfection protocol described in Tanaka et al., 2004, with some modifications. Yeast strains to be transfected were grown in 50ml YPD media to an optical density of 0.5 at 600 nm and were successively washed with sterile water and 1M sorbitol, and resuspended in 20ml SCE buffer (1M sorbitol, 10mM EDTA, 10mM dithiothreitol, 100mM citrate, pH 5.8). Cells were spheroplasted with lyticase (250 mg) and DTT (200µM) in SCE buffer at 30 $^\circ$C for 30 min. Spheroplasts were washed with 1M sorbitol and STC buffer (1M sorbitol, 10mM CaCl2, 10mM Tris, pH 7.5). Pelleted cells were resuspended in 2ml STC buffer, and 100µl of the protoplast suspension was mixed with up to 10µl of [*MCS*$^+$] cell extract, 2 µg of the *LEU2-based* plasmid (pRS315) and 10µg of salmon sperm DNA (100 mg/ml). Fusion was induced by the addition of 9 volumes of

PEG buffer (40% (w/v) PEG 4000, 10mM CaCl2, 10mM Tris, pH 7.5) for 30min. Cells were centrifuged, resuspended in SOS buffer (1M sorbitol, 7mM CaCl2, 0.25% yeast extract, 0.5% bacto-peptone), incubated at 30°C for 30 min and plated on synthetic media lacking leucine (selective for cells absorbing the transfection-mix) and were overlaid with top agar (2.5% agar). To check the transfection result, the transfectants were picked up, and nonsense suppression was checked on –Ade media.

SGA screening

The synthetic genetic array (SGA) analysis (Tong et al., 2001) was performed in Dr Boone's lab at the University of Toronto. The starting strain GT1292 was constructed by us and was based on the OT372 strain from Dr Boone's lab. Plasmid pmCUP1MCSc was transformed into the OT372 strain first. Then, the whole *SUP35* gene in the genome of the host strain was replaced by a natNT cassette with a PCR-mediated gene deletion method (Tong et al., 2006). This starting strain contained all of the genetic and antibiotic markers for a SGA screening and only expressed Sup35 without the prion domain. Another starting strain, GT1293, was constructed as a control. Plasmid pmCUP1MCSc from GT1292 was replaced with plasmid pCUP-SUP35. The resulting strain expressed only full-length Sup35. A small scale SGA screening was manually performed by us following the SGA protocol described in Tong et al., 2006.

4-3 Results

4-3-1 A [*MCS*$^{+}$] prion-like state was identified in the yeast strain lacking the Sup35 prion domain

Initially, a yeast strain expressing only the Sup35 protein without the prion domain was constructed by a plasmid shuffle procedure (Figure 4-1 A). A Sup35MC-expressing plasmid (pmCUP1MCSc, with the URA3 marker) was transformed into the [*psi⁻ pin⁻*] strain GT671 with the genomic *SUP35* gene deleted, bearing a Sup35-expressing plasmid (pASB2, with the *LEU2* marker). Then, the original Sup35-expressing plasmid was lost from the strain by counterselecting on –Ura and –Leu media. Next, 20 individual colonies bearing only the Sup35MC plasmid were checked on –Ade media for nonsense suppression. Interestingly, after these colonies were patched on a –Ade plate and were incubated for more than 10 days, some Ade+ papillae appeared on one exceptional patch (Figure 4-1 A). The *de novo*-formed Ade+ papillae were individually picked and were treated with the prion eliminating agent GuHCl (5mM). Strikingly, one of the Ade+ colonies was cured, indicating a prion-like factor involved in it. The GuHCl-curable nonsense suppression state was named [*MCS⁺*]. This nonsense-suppression state was found to be stably maintained. After 3 passages of growth on YPD, all of the daughter cells were still Ade+ and showed a white color on YPD (Figure 4-1 B).

A Plasmid shuffle

Most colonies:
No suppression

[*psi⁻ pin⁻*]

[*SUP35MC*]

[*SUP35*]

sup35 Δ

sup35 Δ

sup35 Δ

-Ade

Transformation

Lose a plasmid

One exceptional
colony

[*SUP35*]

[*SUP35*]

[*SUP35MC*]

[*SUP35MC*]

-Ade

B

[*MCS⁺*], 3 passages
on YPD

GuHCl Cured
(Curing rate: 72%)

YPD
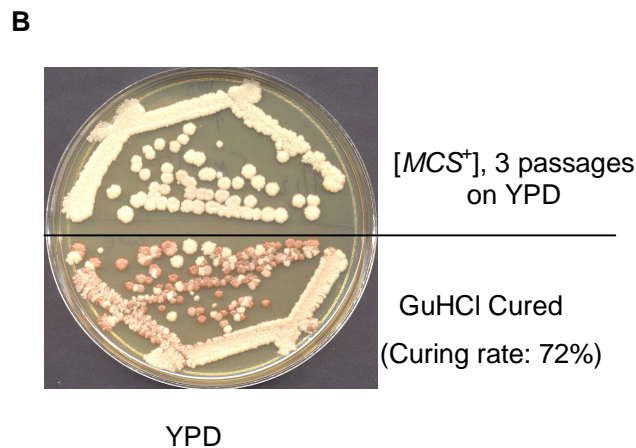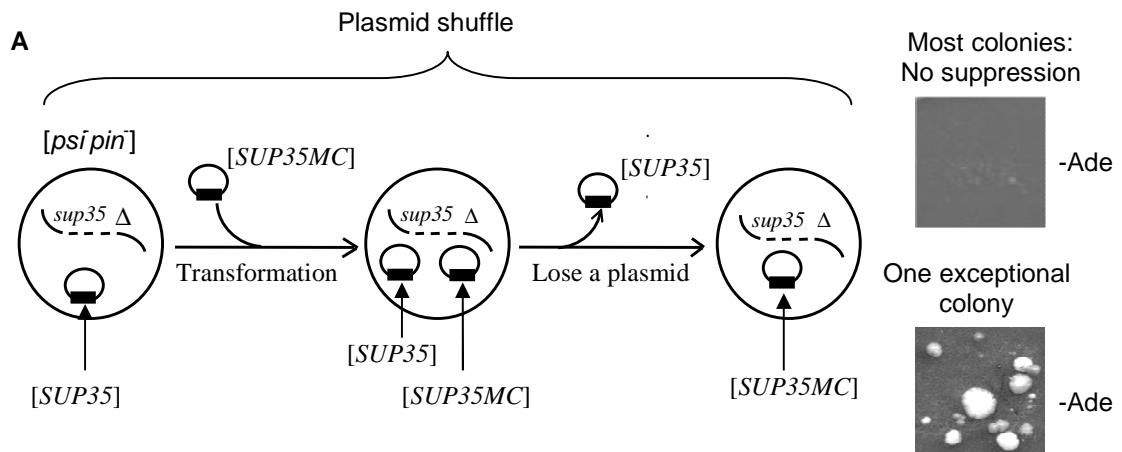
Figure 4-1. A prion like phenomenon [*MCS⁺*] is detected in a yeast strain lacking the Sup35 prion domain.
A- The plasmid shuffle procedure is shown in the scheme. A [*psi⁻ pin⁻*] *sup35Δ* strain with the *SUP35* gene on a *CEN* plasmid was transformed with a *CEN* plasmid expressing Sup35MC. Then, the original Sup35-expressing plasmid was lost from the strain, and only the SUP35MC plasmid was left. After the plasmid shuffle, one exceptional colony showed nonsense suppression. Colony purification of the Ade⁺ papillae and one isolate was shown to be GuHCl-curable. The GuHCl-curable nonsense suppression state was termed [*MCS⁺*]. **B**-The [*MCS⁺*] colony was white in color on YPD media and turned a red color when the nonsense suppression state was eliminated by GuHCl. The [*MCS⁺*] state was stably propagated.

4-3-2 Suppression in a [*MCS⁺*] strain is not due to prion formation by Sup35MC

Since prion formation of Sup35 is known to cause nonsense suppression, one explanation for [*MCS⁺*] was due to prion formation by Sup35MC, even without the prion domain. To check this, a centrifugation analysis was performed. Cell extracts of the [*MCS⁺*] strain and the GuHCl-cured strain (named [*mcs⁻*]) were centrifuged at 8,000 g for 30 minutes at

90

4 °C. Then, the supernatant and pellet were collected, boiled and checked by SDS-PAGE and western blot. The distribution of Sup35MC protein in the supernatant and pellet was the same from the [MCS^+] strain and from the [mcs^-] strains (Figure 4-2). In contrast, most Sup35 was precipitated to the pellet from the [PSI^+] strain, while most of the Sup35 was retained in the supernatant for the [psi^-] strain. Thus, Sup35MC did not aggregate in the [MCS^+] strain, so the nonsense suppression was not due to prion formation of Sup35MC.
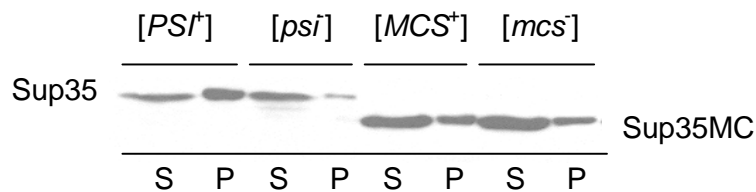
Figure 4-2. Centrifugation analysis of Sup35MC from [MCS^+] strain. The speed of centrifugation was 8,000 g. "S" and "P" refer to supernatant and pellet, respectively. The Sup35 antibody was used for the immunostaining detection.

4-3-3 Different regions of Sup35 affect the appearance of the [MCS+] phenotype

Since [MCS^+] was found in the strain expressing only the Sup35MC protein but never in strains expressing full-length Sup35, the Sup35N domain may inhibit the existence of [MCS^+]. Alternatively, [MCS^+] has the same phenotype as [PSI^+], so it may be ignored in normal strains producing full-length Sup35. In this case, the existence of [MCS^+] may be irrelevant to the Sup35 protein.

First, to eliminate the possibility that the [MCS^+] phenomenon is plasmid-specific, we performed a plasmid shuffle to replace the Sup35MC-expressing plasmid

91

(pmCUP1MCSc) with a different plasmid bearing *SUP35*MC (pRS315-SUP35MC). The result showed that the [*MCS*$^+$] phenotype was not changed with a different plasmid (Figure 4-3).

To test if [*MCS*$^+$] can co-exist with Sup35C alone, plasmid pRS315-SUP35 del3ATG (expressing Sup35C) was transformed into a [*MCS*$^+$] strain, and the Sup35MC plasmid was then lost. The result showed that nonsense suppression was not altered in the strain expressing only Sup35C (Figure 4-3), suggesting little or no effect of the Sup35M region on [*MCS*$^+$].

.

In order to check if Sup35N affects the existence of [*MCS*$^+$], plasmid pASB2 (expressing the Sup35 full length protein) was transformed into the [*MCS*$^+$] strain, and the Sup35MC plasmid was then lost. With the existence of the Sup35 protein, the nonsense suppression phenotype of [*MCS*$^+$] disappeared. Then a reverese shuffle was performed by transforming in the Sup35MC plasmid followed by loss of the full-length Sup35-producing plasmid. The nonsense suppression was partially restored in the strain expressing only the Sup35MC again (Figure 4-3). Taken together, [*MCS*$^+$] did not cause nonsense suppression in the presence of Sup35N; however, the propagation of [*MCS*$^+$] was partially maintained, and the nonsense suppression could be restored when Sup35N was eliminated from the cell.
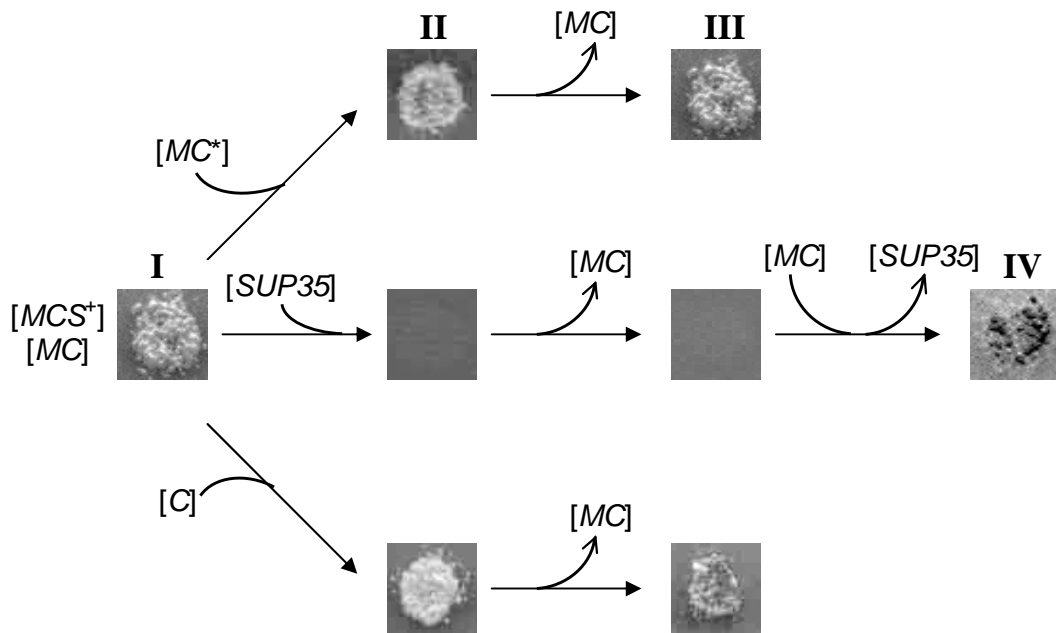
Figure 4-3. Manifestation of [*MCS*⁺] is affected by different regions of Sup35. [*MC*], [*C*] and [*SUP35*] refer to *CEN* plasmids expressing Sup35MC, Sup35C or full-length Sup35 protein, respectively. [*MC**] refers to a heterogeneic plasmid of [*MC*] which also expresses Sup35MC. Nonsense suppression was checked on –Ade media. A [*MCS*⁺] strain with [*MC*] (Stage I) was transformed individually with [*MC**], [*SUP35*] or [*C*] containing *LEU2* markers (Stage II), and nonsense suppression was judged by the growth on –Ade media selective for both plasmids. After elimination of the original [*MC*] plasmid (stage III), there was only Sup35MC, full length Sup35 or Sup35C protein expressed in the strain respectively. Judged by the growth on –Ade media, the nonsense suppression state was maintained in [MC] and [C] containing strains but not in the [*SUP35*] containing strain. For the [*SUP35*] containing strain (stage III), [*MC*] was transformed in again, and [*SUP35*] was lost (stage IV), yet the nonsense suppression was partially restored, as seen by the growth (weaker) on –Ade media.

4-3-4 [*MCS*⁺] is infectious

Prion is an infectious agent which can convert the non-prion form of the same protein into the prion form. In order to test whether the [*MCS*⁺] state is infectious, the yeast extract transfection assay was performed. Cell lysate from the [*MCS*⁺] strain was extracted using the protocol described in the Chapter 2 methods section. Then, the

[MCS^+] cell extract was transfected into an isogenic [mcs^-] strain. 1% [mcs^-] cells became Ade+ after transfection and were also GuHCl curable. In contrast, no [mcs^-] cells became Ade+ if transfected with water instead of [MCS^+] extract. Notably, the transfection rate of [MCS^+] was much less than that of [PSI^+], indicating a weaker infectivity.

Table 4-3. [MCS^+] cell extract transfection result

Transfection Donor	Recipient	Transfectants		% Transfection rate
		Total #	Ade+	
[MCS^+]	[mcs^-]	700	7	1%
H_2O	[mcs^-]	260	0	0
GT81-1C	GT17	80	6	7.5%
H_2O	GT17	180	0	0

(GT81-1C: [PSI^+PIN^+], GT17: [psi^-pin^-])

4-3-5 Effects of the Hsp104 chaperone on [MCS^+]

As mentioned above, the Hsp104 chaperone is required for yeast prion propagation. Transient overproduction of Hsp104 cures the [PSI^+] prion but not [PIN^+] or [URE3]. In this study, we also tested the effects of Hsp104 on [MCS^+]. In order to test if Hsp104 is required for [MCS^+] propagation, we disrupted the *HSP104* coding gene in the [MCS^+] strain (described in the methods section), so that no functional Hsp104 was produced. Strikingly, the nonsense suppression phenotype still existed in the *HSP104*-disrupted strain (Figure 4-4 A). The nonsense suppression could still be cured by GuHCl; however, the curing efficiency was decreased dramatically when compared with that of the

HSP104 wildtype strain. It was suggested that GuHCl cures yeast prions by inactivating Hsp104 activity, which would eliminate prion propagation (Glover et al., 2009). However, [*MCS*[+]] was GuHCl curable, but not Hsp104 dependent, indicating a potentially different, but not a necessarily exclusive system for propagation. GuHCl can still cure HSP104 disrupted strain with less efficiency, indicating that GuHCl can possibly inactive other propagating factors, but not as efficiently as Hsp104.

Additionally, Hsp104 was transiently overproduced in a [*MCS*[+]] strain by transforming in the Hsp104-overproducing plasmid pLH105 and by then eliminating this plasmid from the strain. Notably, the nonsense suppression phenotype of [*MCS*[+]] was cured following Hsp104 overproduction (Figure 4-4 B). This result is interesting becausepropagation of [*MCS*[+]] was not Hsp104-dependent, but excess Hsp104 did eliminate [*MCS*[+]] from the strain. This result indicates that Hsp104 still interacts with the prion factor of [*MCS*[+]] and functions to disaggregate this prion.
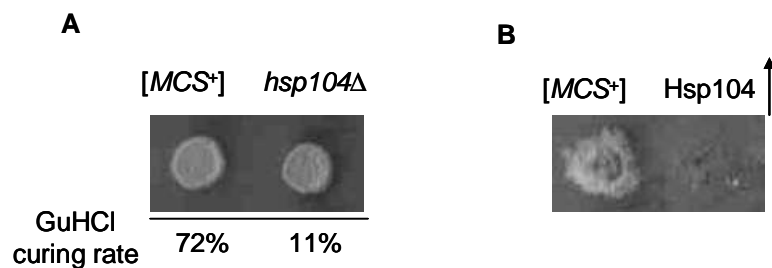
Figure 4-4. Effects of the Hsp104 chaperone on [*MCS*[+]]. *hsp104Δ* refers to the [*MCS*[+]] strain having the genomic *HSP104* gene disrupted. Nonsense suppression was tested on –Ade media. **A**- Nonsense suppression was not eliminated in the [*MCS*[+]] strain with the genomic *HSP104* gene disrupted. The suppression was eliminated from the *hsp104Δ* strain by GuHCl, while the curing rate was decreased when compared with that of the wild type strain. **B**- Transient overproduction of Hsp104 eliminated the nonsense suppression of [*MCS*[+]].

4-3-6 Analysis of the [*MCS*$^+$] prion factorby "agarose trapping"

As described in chapter 3, amyloid formed by prion can be isolated by the "agarose trapping" assay and can then be identified by MS. We analyzed the cell lysate extracted from a [*MCS*$^+$] strain using the "agarose trapping" assay. The sample trapped in agarose gel was both tested by flamingo staining and was then analyzed by MS. There were no apparent protein bands visualized by the flamingo strain, indicating less abundance of the proteins trapped. MS analysis confirmed that no proteins trapped were abundant. The detected proteins are listed in table 4-4. Ygp1, Tdh1/2/3 and Pma1 were also detected as backgrounds or contaminations from other non-[*MCS*$^+$] samples (Table 3-1, 3-2). There are 2 proteins found to be specific to the [*MCS*$^+$] sample as compared with the pre-boiled sample of [*MCS*$^+$] or the sample from the GuHCl-cured strain. However, the abundances of these were too low to be confirmed as being "trapped".

Table 4-4. Proteins detected in agarose trap from [*MCS*$^+$] sample

Protein	Description	Size, kD
Ygp1	Cell wall-related secretory glycoprotein	37 (>200 when glycosylated)
Tdh1/2/3	Trioso-phosphate dehydrogenase	37
Ecm33	GPI-anchored protein of unknown function	44
Pma1	Plasma membrane H+-ATPase	100
([*MCS*$^+$] specific, less abundant)		
Fks1	Glucan synthase, cell wall synthesis and maintenance	215
Cox15	Mitochondrial inner membrane protein	55

4-3-7 A nuclear element is involved in [*MCS*$^+$]

[MCS⁺] is not cytoducible

Unlike chromosomal elements, yeast prions are cytoplasmic elements that can be transmitted to other cells via cytoplasmic transfer (cytoduction). We tested the cytoduction effect of [*MCS*⁺] by mating a [*MCS*⁺] strain with the cytoduction recipient strain GT1123 which is [*mcs*⁻] and expresses only Sup35MC. Mixed with the cytoplasmic materials from the [*MCS*⁺] strain, the cytoductants were tested on –Ade media for nonsense suppression. The result showed that none of the 226 cytoductants acquired the nonsense suppression phenotype from [*MCS*⁺]. This indicates that [*MCS*⁺] may not simply be caused by a cytoplasmic prion factor as is the case for other known yeast prions.

[MCS⁺] is dominant and follows a pattern of Mendelian inheritance

Prions display patterns of non-Mendelian inheritance during meiosis. We checked the inheritance of [*MCS*⁺] by mating a [*MCS*⁺] strain with a [*mcs*⁻] strain (expressing only Sup35MC) having an opposite mating type. The diploid strain was induced to sporulate, and the 4 spores within a single tetrad were dissected and analyzed phenotypically. For a given trait, the typical Mendelian inheritance will present as a 2:2 segregation rate. In contrast, prions follow a non-Mendelian type of inheritance; instead, all progeny inherit the prion state, showing a 4:0 segregation rate. By mating a [*MCS*⁺] strain with a [*mcs*⁻] strain, the diploid strain showed a nonsense suppression phenotype (data not shown), indicating that [*MCS*⁺] is dominant. Then, a tetrad analysis was performed for the diploid

strain. Strikingly, the [*MCS*$^+$] strain showed a 2:2 segregation rate (Table 4-5), different from classical prion-inheritance. Overall, the Mendelian inheritance of [*MCS*$^+$] indicated the existence of a nuclear element. This is particularly interesting since the [*MCS*$^+$] prion-like state is not simply due to a conformational change of a specific protein; it is also controlled by a nuclear element. Since Sup45 is another translation termination factor working together with Sup35, dysfunction of this protein may lead to nonsense suppression. We sequenced the *SUP45* gene in the genome of the [*MCS*$^+$] strain, and there were no mutations present in the gene. Some other nuclear factor must be responsible for the [*MCS*$^+$] phenotype.

Table 4-5. Meiotic inheritance of [*MCS*$^+$] (data from tetrad analysis)

Diploid	No. of full tetrads with Ade$^+$: Ade$^-$ segregation					Total No. of spores	
	4:0	3:1	2:2	1:3	0:4	Ade$^+$	Ade$^-$
[*MCS*$^+$]/[*mcs*$^-$]	0	1	11	1	0	103	114
[*mcs*$^-$]/[*mcs*$^-$]	0	0	0	0	12	0	81

4-3-8 Synthetic Genetic Array (SGA) screening for the nuclear factor responsible for [*MCS*$^+$]

Synthetic lethality occurs when the combination of two mutations leads to an inviable organism. Mutants that are defective in the same essential pathway or in parallel nonessential pathways often display synthetic lethality (Tong et al., 2001). Dr. Boone's lab developed a synthetic genetic array (SGA) method to screen "synthetic lethal" double genetic mutations (Tong et al., 2001; Tong et al., 2006). They did this by incorporating a target gene deletion with ~5000 viable gene deletion mutants (about 80% of all yeast

genes) in *S. cerevisiae*. Since [*MCS*⁺] causes nonsense suppression, the nuclear element of [*MCS*⁺] (presumably a gene mutation) may also involve a translation termination process. As translation termination is an essential process, it is likely that a deletion of the gene will result in lethality or sublethality. Since [*MCS*⁺] only appears in the absence of Sup35N, a SGA screening in the *SUP35N*-deleted strain may provide us with a series of candidates for the nuclear element responsible for [*MCS*⁺].

The SGA screening was performed by Dr Boone's lab at the University of Toronto. The *SUP35* gene was deleted in the starting strain which contained a Sup35MC-expressing plasmid. 145 double deletions were screened for synthetic lethality at different levels. Then, we performed a small-scale SGA screening within the 145 candidate deletions following the protocol described in ref. Tong et al., 2006. We used another starting strain that expressed full-length Sup35as a control.. Ultimately, we found 6 double mutants with significant synthetic lethality effects in the strain expressing only Sup35MC, but with little or no lethality for the strain expressing Sup35 (Figure 4-5). The other mutants showed mild to no lethality, or the lethality wascomparable between the strains expressing Sup35MC or full length Sup35. The genes responsible for synthetic lethality are listed in Table 4- 6. These results suggested that the prion domain of Sup35 may be involved in various processes that regulate cellular functions. In order to further target the nuclear element of [*MCS*⁺], the nonsense suppression of the candidate double mutants can be checked by generating an *ade1* nonsense mutation in the strains.

|	I	II
	sup35Δ xxxΔ [*SUP35MC*]	*sup35Δ xxxΔ* [*SUP35*]
Synthetic lethal		
Non-lethal		
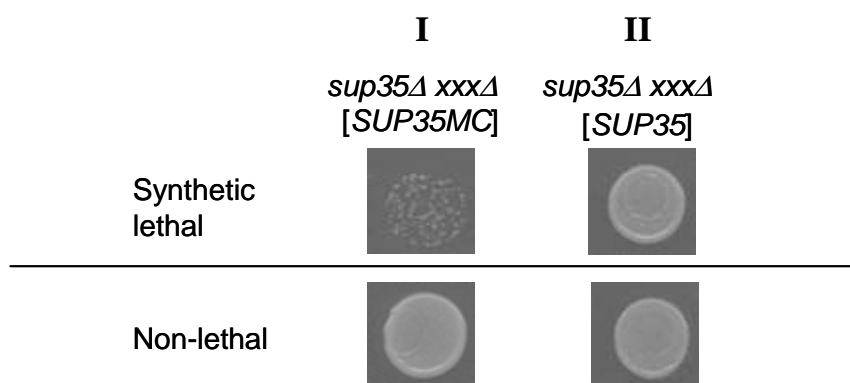
Figure 4-5. Detection of the synthetic lethality effect. The haploid spore with a double deletion of *SUP35* and the target gene (XXX) which contains a SUP35MC or full length Sup35 protein-expressing plasmid, was selected through the SGA screening. If the deleted gene had a synthetic lethal effect in the absence of Sup35N, it could be detected by weaker growth on the selective medium (e.g. *gsh1Δ,* panel I*)* as compared with the strain expressing full-length Sup35 (panel II). If the deleted gene had no synthetic lethal effect in the absence of Sup35N, then there was no difference between the growths in panels I and II.

Table 4-6. List of genes with synthetic lethal effect in the absence of Sup35N

Gene	Description
SUR4	Elongase, involved in fatty acid and sphingolipid biosynthesis
GSH1	Gamma glutamylcysteine synthetase, involved in glutathione biosynthesis
CDC73	Component of the Paf1p complex, modulates the activity of RNA polymerases I and II
SWS2	Putative mitochondrial ribosomal protein, participates in controlling sporulation efficiency
MKS1	Transcriptional regulator, involved in Ras-CAMP and lysine synthesis and nitrogen regulation
YOR059C	Uncharacterized

4-4 Discussions

We found a prion-like state termed [*MCS*[+]] that causes nonsense suppression in the absence of the Sup35 prion domain. [*MCS*[+]] showed some prion-like properties. [*MCS*[+]] could also be cured by the prion-eliminating agent GuHCl or by transient overproduction of Hsp104, suggesting the existence of a prion-like factor. However,

[MCS^+] followed a Mendelian pattern of inheritance, indicating the involvement of a nuclear element. It is possible that the prion factor and the nuclear factor coexist, and both may contribute to [MCS^+]; alternatively, the prion factor may be triggered by the nuclear factor. Thus, the prion factor would contribute to the prion-like properties of [MCS^+]. Interestingly, plasmid shuffle results showed that [MCS^+] existed in a strain expressing only Sup35C, suggesting that the Sup35M region did not significantly affect [MCS^+]. However, the [MCS^+] phenotype disappeared in the presence of full-length Sup35, and nonsense suppression was partially restored once Sup35 was removed from the cell. The presence of Sup35N may interact with the [MCS^+] prion factor and inhibit or "mask" it, resulting in a phenotypic elimination. However, the nuclear element of [MCS^+] would still exist, and the prion factor would be recovered by the nuclear factor upon removal of Sup35N. The infectivity of [MCS^+] was confirmed by transfection of yeast extract. However, our result also showed that [MCS^+] cannot be transmitted by cytoplasm transfer (cytoduction). The total yeast extract may contain some nuclear materials, so the prion factor and the nuclear factor responsible for [MCS^+] would have a chance to be transferred to the recipient cell. In contrast, there is only transfer of cytoplasm in cytoduction, so the nuclear factor can be transmitted to the recipient. Hsp104 was shown to modulate [MCS^+] propagation and excess Hsp104 cured [MCS^+]. However, the propagation of [MCS^+] was not Hsp104-dependent and [MCS^+] could be stably maintained by a *HSP104* deleted strain.

Interestingly, a new prion-like state termed [NSI^+] was recently described and only existed in the absence of Sup35N (Saifitdinova et al., 2010). [NSI^+] and [MCS^+] share several common features; notably, they both cause nonsense suppression that is curable by GuHCl. Introduction of full-length Sup35 eliminates the prion phenotype, and for both, the prion phenotype can be recovered by removal of the Sup35 protein. However, [NSI^+] follows a non-Mendelian pattern of inheritance and can be transmitted by cytoduction, indicating that no nuclear element is involved. Additionally, Hsp104 is required for [NSI^+] propagation, while [MCS^+] propagation is Hsp104-independent. The prion factors from [NSI+] and [MCS+] may, in fact, overlap. A study of one phenomenon may shed light on the other. Ultimately, the identification and further characterization of the [MCS^+] and the [NSI+] factors will help us understand prion-related phenomena, as well as nonsense suppression epigenetic control.

4-5 Conclusions:

- [MCS^+] causes nonsense suppression curable by GuHCl.
- The [MCS^+] phenotype disappeared in the presence of Sup35N.
- [MCS^+] is infectious.
- Propagation of [MCS^+] is not Hsp104-dependant.
- [MCS^+] follows a Mendelian pattern of inheritance.
- [MCS^+] is determined by both a prion factor and a nuclear factor.

APPENDIXES

APPENDIX A

S. cerevisiae strains containing [PIN$^+$] prion (Detected by "gel boiling" assay)

Strain	Geographic origin	Source	Provided by
S288c	California, USA	Rotting fig	Haber JE
YS2	Australia	Baker strain	Bell P
YS4	Netherlands	Baker strain	Bell P
YS9	Singapore	Baker strain	Bell P
PGL-1		laboratory strain of Petershoff Genetic Lines (PGL)	St. Petersburg University, Russia
PGL-2	NA		
Brewer yeast	NA	Mr. Beer Home brewery Systems	Mr Beer

S. cerevisiae strains of various origins
(No [*PIN*[+]], [*PSI*[+]] or [URE3] prions detected with "gel boiling" assay)

Strain	Geographic origin	Source	Provided by
SK1	USA	Soil	Haber JE
W303	Created by Rothstein R by multiple crossing	NA	EUROFAN
Y55	France	Grape	Haber JE
322134S	Royal Victoria Infirmary, Newcastle, UK	Clinical isolate (Throat)	Mackenzie D
378604X	Royal Victoria Infirmary, Newcastle, UK	Clinical isolate (Sputum)	Mackenzie D
273614N	Royal Victoria Infirmary, Newcastle, UK	Clinical isolate (Fecal)	Mackenzie D
UWOPS83-787.3	Great Inagua Island, Bahamas	Fruit, *Opuntia stricta*	Lachance M
UWOPS87-242.1	Puhelu Road, Maui, Hawaii,	Cladode, *Opuntia megacantha*	Lachance M
L-1374	Cauquenes, Chile	Fermentation from must pais	Martinez C
L-1528	Cauquenes, Chile	Fermentation from must Cabernet	Martinez C
BC187	Napa Valley, Bisson L, USA	Barrel fermentation	Gerke J
DBVPG1106	Australia	Grapes	Vaughan A
DBVPG1373	Netherlands	Soil	Vaughan A
DBVPG6765	Unknown	Unknown	Vaughan A
YIIc17_E5	Sauternes, France	Wine	Souciet JL
DBVPG6040	Netherlands	Fermenting fruit juice	Vaughan A
NCYC361	Ireland	Beer spoilage strain from wort	NCYC
DBVPG1788	Turku, Finland	Soil	Vaughan A
DBVPG1853	Ethiopia	White Teff	Vaughan A
YJM978		Isolated from vagina of patient suffering from vaginitis	
YJM981	Ospedali Riuniti di Bergamo, Italy		
YJM975			McCusker J

UWOPS03-461.4	Telok Senangin, Malaysia,	Nectar, Bertram palm	Lachance M
UWOPS05-217.3	Telok Senangin, Malaysia,	Nectar, Bertram palm	Lachance M
UWOPS05-227.2	Telok Senangin, Malaysia,	*Trigona* spp (Stingless bee)	Lachance M
K11	Japan	Shochu sake strain	Fay J
Y9	Indonesia	Ragi (similar to sake wine)	Fay J
Y12	Ivory Coast	Palm wine strain	Fay J
YPS606	Pennsylvania, USA,	Bark of *Q. rubra*	Gerke J
YPS128	Pennsylvania, USA,	Soil beneath *Q. alba*	Sniegowski P
NCYC110	West Africa	Ginger beer from *Z.officinale*	NCYC
DBVPG6044	West Africa	Bili wine, from *Osbeckia grandiflora*	Vaughan A

APPENDIX C

S. paradoxus strains of various origins
(No [*PIN*⁺], [*PSI*⁺] or [URE3] prions detected by "gel boiling" assay)

STRAIN	Geographic origin	Source	Provided by
Q31.4	Windsor Great Park, UK	Bark of *Quercus* spp	Koufopanou V
Q32.3	Windsor Great Park, UK	Bark of *Quercus* spp	Koufopanou V
Q59.1	Windsor Great Park, UK	Bark of *Quercus* spp	Koufopanou V
Q62.5	Windsor Great Park, UK	Bark of *Quercus* spp	Koufopanou V
Q69.8	Windsor Great Park, UK	Bark of *Quercus* spp	Koufopanou V
Q74.4	Windsor Great Park, UK	Bark of *Quercus* spp	Koufopanou V
Q89.8	Windsor Great Park, UK	Bark of *Quercus* spp	Koufopanou V
Q95.3	Windsor Great Park, UK	Bark of *Quercus* spp	Koufopanou V
S36.7	Silwood Park, UK,	Bark of *Quercus* spp	Koufopanou V
T21.4	Silwood Park, UK,	Bark of *Quercus* spp	Koufopanou V
W7	Silwood Park, UK,	Bark of *Quercus* spp	Koufopanou V
Y6.5	Silwood Park, UK,	Bark of *Quercus* spp	Koufopanou V
Y7	Silwood Park, UK,	Bark of *Quercus* spp	Koufopanou V
Y8.1	Silwood Park, UK,	Bark of *Quercus* spp	Koufopanou V
Y8.5	Silwood Park, UK,	Bark of *Quercus* spp	Koufopanou V
Y9.6	Silwood Park, UK,	Bark of *Quercus* spp	Koufopanou V
Z1	Silwood Park, UK,	Bark of *Quercus* spp	Koufopanou V
Z1.1	Silwood Park, UK,	Bark of *Quercus* spp	Koufopanou V
N-17	Tartastan, Russia	Exudate of *Q. robur*	Naumov G

CBS432	Moscow area, Russia	Bark of *Quercus* spp	Naumov G
CBS5829	Denmark	Mor soil, pH3.6	Naumov G
DBVPG4650	Marche, Italy	Fossilized guano in a cavern	Vaughan A
KPN3828	Novosibirsk, Siberia, Russia	Bark of *Q. robur*	Iurkow A
KPN3829	Novosibirsk, Siberia, Russia,	Bark of *Q. robur*	Iurkow A
N-43	Vladivostok, Russia	Exudate of *Q. mongolica*	Naumov G
N-44	Ternei, Russia	Exudate of *Q. mongolica*	Naumov G
N-45	Ternei, Russia	Exudate of *Q. mongolica*	Naumov G
IFO1804	Japan	Bark of *Quercus* spp	Pérez-Ortín J
YPS138	Pennsylvania, USA	Soil beneath *Q. velutina*	Sniegowski P
DBVPG6304	Yosemite, California, USA	*Drosophila pseudoobscura*	Vaughan A
A4	Mont St-Hilaire, Quebec, Canada	Bark of *Quercus rubra*	Koufopanou V
A12	Mont St-Hilaire, Quebec, Canada	Soil beneath *Q. rubra*	Koufopanou V
UFRJ50791	Catalao point, Rio de Janeiro, Brazil	*Drosophila spp*	Naumov G
UFRJ50816	Tijuca Forest, Rio de Janeiro, Brazil	*Drosophila spp*	Naumov G
UWOPS91-917.1	Saddle Road, Island of Hawaii,	Flux of *Myoporum sandwichense*	Lachance M

REFERENCES

Abramova N, Sertil O, Mehta S, Lowry CV. 2001. Reciprocal regulation of anaerobic and aerobic cell wall mannoprotein gene expression in Saccharomyces cerevisiae. *J Bacteriol.* 183(9):2881-7.

Aguzzi A, O'Connor T. Protein aggregation diseases: pathogenicity and therapeutic perspectives. *Nat Rev Drug Discov.* 2010 Mar;9(3):237-48.

Alberti, S., Halfmann, R., King, O., Kapila, A. and Lindquist, S. (2009). A systematic survey identifies prions and illuminates sequence features of prionogenic proteins. *Cell* 137, 146-158.

Bagriantsev S, Liebman SW. 2004. Specificity of prion assembly in vivo. [PSI+] and [PIN+] form separate structures in yeast. *J Biol Chem.* 279(49):51042-8.

Bagriantsev, S. & Liebman, S. 2006. Modulation of Aβ42 low-n oligomerization using a novel yeast reporter system. *BMC Biol.* 4, 32

Bailleul PA, Newnam GP, Steenbergen JN, Chernoff YO. 1999. Genetic study of interactions between the cytoskeletal assembly protein sla1 and prion-forming domain of the release factor Sup35 (eRF3) in Saccharomyces cerevisiae. Genetics. 153(1):81-94.

Borchsenius, A.S., et al., *Prion variant maintained only at high levels of the Hsp104 disaggregase.* Current genetics., 2006. 49(1): p. 21-9

Bradley, M.E., Edskes, H.K., Hong, J.Y., Wickner, R.B., and Liebman, S.W. 2002. Interactions among prions and prion'strains' in yeast. *Proc. Natl. Acad. Sci.* 99 (Suppl. 4): 16392–16399.

Brown P, Cathala F, Castaigne P, Gajdusek DC. 1986. Creutzfeldt–Jakob disease: clinical analysis of a consecutive series of 230 neuropathologically verified cases. *Ann Neurol.* 20: 597–602.

Brown JC, Lindquist S. 2009. A heritable switch in carbon source utilization driven by an unusual yeast prion. *Genes Dev.* 23(19):2320-32.

BuelerH,AguzziA, SailerA,GreinerRA,Autenried P, et al. 1993. Mice devoid of PrP are resistant to scrapie. *Cell* 73:1339–47

Caine, J. *et al. 2007.* Alzheimer's Aβ fused to green fluorescent protein induces growth stress and a heat shock response. *FEMS Yeast Res.* 7, 1230–1236.

Castilla J, Saá P, Hetz C, Soto C. In vitro generation of infectious scrapie prions. *Cell* 2005 Apr 22;121(2):195-206.

Caughey B, Kocisko DA, Raymond GJ, Lansbury PT Jr. Aggregates of scrapie-associated prion protein induce the cell-free conversion of protease-sensitive prion protein to the protease-resistant state. *Chem Biol.* 1995 Dec;2(12):807-17.

Chen B, Newnam GP, Chernoff YO. 2007. Prion species barrier between the closely related yeast proteins is detected despite coaggregation. Proc Natl Acad Sci U S A. 104(8):2791-6.

Chernoff, Y.O., Derkach, I.L., and Inge-Vechtomov, S.G. 1993.Multicopy SUP35 gene induces de-novo appearance of psi-like factors in the yeast Saccharomyces cerevisiae. *Curr. Genet.* 24: 268–270.

Chernoff YO, Lindquist SL, Ono B, Inge-Vechtomov SG, Liebman SW. 1995. Role of the chaperone protein Hsp104 in propagation of the yeast prion-like factor [psi+]. *Science.* 268(5212):880-4.

Chernoff YO, Galkin AP, Lewitin E, Chernova TA, Newnam GP, Belenkiy SM. 2000. Evolutionary conservation of prion-forming abilities of the yeast Sup35 protein. *Mol Microbiol.* 35(4):865-76.

Chernoff YO, Uptain SM, Lindquist SL. 2002. Analysis of prion factors in yeast. Methods Enzymol. 351:499-538.

Chernoff YO. 2004. Amyloidogenic domains, prions and structural inheritance: rudiments of early life or recent acquisition? *Curr Opin Chem Biol.* 8(6):665-71.

Chernoff YO. 2007. Stress and prions: lessons from the yeast model. *FEBS Lett.* 581(19):3695-701.

Chernoff YO. 2008. Prion: disease or relief? *Nat Cell Biol.* 10(9):1019-21.

Chien P, Weissman JS, DePace AH. 2004. Emerging principles of conformation-based prion inheritance. *Annu Rev Biochem* 73: 617–656.

Cobb NJ, Apetri AC, Surewicz WK. 2008. Prion protein amyloid formation under native-like conditions involves refolding of the C-terminal alpha-helical domain. *J Biol Chem.* 283(50):34704-11.

Collinge J, Hill AF, Ironside J, Zeidler M.1997. Diagnosis of new variant Creutzfeldt-Jakob disease by tonsil biopsy—authors'reply to Arya and Evans. *Lancet* 349:1322–23

Collinge J. 2001.Prion diseases of Humans and animals: Their Causes andMolecular Basis. *Annu. Rev. Neurosci.* 24:519–50

Conde, J. and G.R. Fink. 1976. *A mutant of* Saccharomyces cerevisiae *defective for nuclear fusion. Proceedings of the National Academy of Sciences of the United States of America.*, 73(10): p. 3651-5.

Couzin, J. (2002) Molecular biology. In yeast, prions' killer image doesn't apply. *Science* 297, 758–761

Cox BS, Tuite MF, Mundy CJ. 1980. Reversion from suppression to nonsuppression in SUQ5 [psi+] strains of yeast: the classificaion of mutations. *Genetics*. 95(3):589-609.

Dagkesamanskaya AR, Ter-Avanesyan MD. 1991. Interaction of the yeast omnipotent suppressors SUP1(SUP45) and SUP2(SUP35) with non-mendelian factors. *Genetics*. 128:513–520.

Derkatch IL, Chernoff YO, Kushnirov VV, Inge-Vechtomov SG, Liebman SW. 1996. Genesis andvariability of [*PSI*] prion factors in *Saccharomyces cerevisiae. Genetics*. 144:1375–1386.

Derkatch, I.L., Bradley, M.E., Zhou, P., Chernoff, Y.O., and Liebman, S.W. 1997. Genetic and environmental factors affecting the de novo appearance of the [PSI+] prion in Saccharomyces cerevisiae. *Genetics* 147: 507–519.

Derkatch IL, Bradley ME, Liebman SW. 1998. Overexpression of the *SUP45* gene encoding a Sup35pbinding protein inhibits the induction of the *de novo* appearance of the [*PSI+*] prion. *Proc Natl Acad Sci USA*. 95:2400–2405.

Derkatch, I.L., Bradley, M.E., Masse, S.V., Zadorsky, S.P., Polozkov, G.V., Inge-Vechtomov, S.G., and Liebman, S.W. 2000. Dependence and independence of [PSI+] and [PIN+]: A twoprion system in yeast? *EMBOJ*. 19: 1942–1952.

Derkatch IL, Bradley ME, Hong JY, Liebman SW. 2001. Prions affect the appearance of other prions: the story of [PIN(+)].*Cell*. 106(2):171-82.

Donne, D. G., J. H. Viles, D. Groth, I. Mehlhorn, T. L. James, F. E. Cohen, S. B. Prusiner, P. E. Wright, and H. J. Dyson. 1997. Structure of the recombinant full-length hamster prion protein PrP(29–231): the N terminus is highly flexible. *Proc. Natl. Acad. Sci. U.S.A.* 94:13452–13457.

Douglas PM, Treusch S, Ren HY, Halfmann R, Duennwald ML, Lindquist S, Cyr DM. 2008. Chaperone-dependent amyloid assembly protects cells from prion toxicity. *Proc Natl Acad Sci U S A*. 105(20):7206-11.

Du Z, Park KW, Yu H, Fan Q, Li L. 2008. Newly identified prion linked to the chromatin-remodeling factor Swi1 in Saccharomyces cerevisiae. *Nat Genet*. 40(4):460-5.

Fay JC, Benavides JA. 2005. Evidence for domesticated and wild populations of Saccharomyces cerevisiae. *PLoS Genet*. 1(1):66-71. Epub 2005 Jul 25.

Garrity SJ, Sivanathan V, Dong J, Lindquist S, Hochschild A. 2010. Conversion of a yeast prion protein to an infectious form in bacteria. *Proc Natl Acad Sci USA* [Epib ahead of print; doi: 10.1073/pnas.0913280107.]

Glover JR, Lum R. 2009. Remodeling of protein aggregates by Hsp104. *Protein Pept Lett*. 16(6):587-97.

Goedert, M. and M. G. Spillantini (2006) A century of Alzheimer's disease. *Science* 314(5800): 777-81.

Goehler, H., Droege, A., Lurz, R., Schnoegl, S., Chernoff, Y.O. and E.E. Wanker (2010) Pathogenic polyglutamine tracts are potent inducers of spontaneous Sup35 and Rnq1 amyloidogenesis. *PLoS One* 5(3):e9642.

Grimminger V, Richter K, Imhof A, Buchner J, Walter S. 2004. The prion curing agent guanidinium chloride specifically inhibits ATP hydrolysis by Hsp104. *J Biol Chem* 279:7378-7383.

Hardy J, Selkoe DJ. 2002. The amyloid hypothesis of Alzheimer's disease:
progress and problems on the road to therapeutics. *Science* 297:353-356.

Harrison PM, Gerstein M. 2003. A method to assess compositional bias in biological sequences and its application to prion-like glutamine/asparagine-rich domains in eukaryotic proteomes. *Genome Biol*. 4(6):R40.

Hilbich C, Kisters-Woike B, Reed J, Masters CL, Beyreuther K. 1992. Substitutions of hydrophobic amino acids reduce the amyloidogenicity of Alzheimer's disease beta A4 peptides. *J Mol Biol.* 228:460-473.

Hunt A, Schönknecht P, Henze M, Seidl U, Haberkorn U, Schröder J. 2007. Reduced cerebral glucose metabolism in patients at risk for Alzheimer's disease. *Psychiatry Res.* 155(2):147-54.

Ito, H., Y. Fukuda, K. Murata, and A. Kimura. (1983) Transformation of intact yeast cells treated with alkali cations. J. Bacteriol. 153: 163-168.

James, T. L., H. Liu, N. B. Ulyanov, S. Farr Jones, H. Zhang, D. G. Donne, K. Kaneko, D. Groth, I. Mehlhorn, S. B. Prusiner, and F. E. Cohen. 1997. Solution structure of a 142-residue recombinant prion protein corresponding to the infectious fragment of the scrapie isoform. *Proc.Natl. Acad. Sci. U.S.A.* 94:10086–10091.

Jeffrey M, Wells GA. 1988. Spongiform encephalopathy in a nyala (*Tragelaphus angasi*).*Vet. Pathol.* 25:398–99

Kalebina TS, Plotnikova TA, Gorkovskii AA, Selyakh IO, Galzitskaya OV, Bezsonov EE, Gellissen G, Kulaev IS. 2008. Amyloid-like properties of Saccharomyces cerevisiae cell wall glucantransferase Bgl2p: prediction and experimental evidences. *Prion*. 2(2):91-6.

Kaiser, C., S. Michaelis, and A. Mitchell (1994) Methods in yeast genetics: A Cold Spring Harbor Laboratory course manual. Cold Spring Harbor Laboratory Press, Cold Spring Harbor, New York.

Kane MD, Lipinski WJ, Callahan MJ, Bian F, Durham RA, Schwarz RD, Roher AE, Walker LC. 2000. Evidence for seeding of beta -amyloid by intracerebral infusion of Alzheimer brain extracts in beta -amyloid precursor protein-transgenic mice. *J Neurosci.* 20(10):3606-11

Kidd PM. 2008. Alzheimer's disease, amnestic mild cognitive impairment, and age-associated memory impairment: current understanding and progress toward integrative prevention. *Altern Med Rev.* 13(2):85-115.

Kimberlin RH. 1981. Scrapie. *Br Vet J.* 137: 105–112.

Kirkwood JK, Wells GA, Wilesmith JW,Cunningham AA, Jackson SI. 1990. Spongiform encephalopathy in an arabian oryx (*Oryx leucoryx*) and a greater kudu (*Tragelaphus strepsiceros*). *Vet. Rec.* 127:418–20

Kocisko DA, Caughey B. Searching for anti-prion compounds: cell-based high-throughput in vitro assays and animal testing strategies. *Methods Enzymol.* 2006;412:223-34.

Krammer C, Suhre MH, Kremmer E, Diemer C, Hess S, Schätzl HM, Scheibel T, Vorberg I. 2008. Prion protein/protein interactions: fusion with yeast Sup35p-NM modulates cytosolic PrP aggregation in mammalian cells. *FASEB J.* 22(3):762-73.

Krammer C, Kremmer E, Schätzl HM, Vorberg I. 2008. Dynamic interactions of Sup35p and PrP prion protein domains modulate aggregate nucleation and seeding. *Prion* 2(3):99-106

Krammer C, Kryndushkin D, Suhre MH, Kremmer E, Hofmann A, Pfeifer A, Scheibel T, Wickner RB, Schätzl HM, Vorberg I. 2009. The yeast Sup35NM domain propagates as a prion in mammalian cells. *Proc Natl Acad Sci USA* .106(2):462-7.

Krishnan R, Lindquist SL. 2005. Structural insights into a yeast prion illuminate nucleation and strain diversity. *Nature*. 435(7043):765-72.

Kryndushkin DS, Alexandrov IM, Ter-Avanesyan MD, Kushnirov VV. 2003. Yeast [PSI+] prion aggregates are formed by small Sup35 polymers fragmented by Hsp104. *J Biol Chem*. 278(49):49636-43.

Krobitsch, S. & Lindquist, S. 2000. Aggregation of huntingtin in yeast varies with the length of the polyglutamine expansion and the expression of chaperone proteins. *Proc. Natl Acad. Sci. USA* **97**, 1589–1594.

Kryndushkin DS, Alexandrov IM, Ter-Avanesyan MD, Kushnirov VV. 2003. Yeast [PSI+] prion aggregates are formed by small Sup35 polymers fragmented by Hsp104. *J Biol Chem*. 278(49):49636-43.

Kushnirov, V.V., and Ter-Avanesyan, M.D. 1998. Structure and replication of yeast prions. *Cell* 94, 13–16.

Kushnirov VV, Alexandrov IM, Mitkevich OV, Shkundina IS, Ter-Avanesyan MD. 2006. Purification and analysis of prion and amyloid aggregates. *Methods*. 39(1):50-5.

Kutzler MA, Cao C, Bai Y, Dong H, Choe PY, Saulino V, McLaughlin L, Whelan A, Choo AY, Weiner DB, Ugen KE. 2006. Mapping of immune responses following wild-type and mutant ABeta42 plasmid or peptide vaccination in different mouse haplotypes and HLA Class II transgenic mice. *Vaccine*. 24(21):4630-9

Lansbury, P.T. and B.S. Caughey (1995) The chemistry of scrapie infection: implications of the 'ice 9' metaphor. *Chem. Biol.* 2: 1-5.

LaFerla FM, Oddo S. 2005. Alzheimer's disease: Abeta, tau and synaptic dysfunction. *Trends Mol Med* 11:170-176.

Liti G, Carter DM, Moses AM, Warringer J, Parts L, James SA, Davey RP, Roberts IN, Burt A, Koufopanou V, Tsai IJ, Bergman CM, Bensasson D, O'Kelly MJ, van Oudenaarden A, Barton DB, Bailes E, Nguyen AN, Jones M, Quail MA, Goodhead I, Sims S, Smith F, Blomberg A, Durbin R, Louis EJ. (2009). Population genomics of domestic and wild yeasts. *Nature*.458(7236):337-41.

Liu JJ, Sondheimer N, Lindquist SL. 2002. Changes in the middle region of Sup35 profoundly alter the nature of epigenetic inheritance for the yeast prion [PSI+]. *Proc Natl Acad Sci USA* 99:16446–16453.

Ma, J. & Lindquist, S. 1999. *De novo* generation of a PrPSc like conformation in living cells. *Nature Cell Biol.* **1**, 358–361.

Malato L, Dos Reis S, Benkemoun L, Sabaté R, Saupe SJ. 2007. Role of Hsp104 in the propagation and inheritance of the [Het-s] prion. *Mol Biol Cell*. 18(12):4803-12.

Marsh RF. 1992. Transmissible mink encephalopathy. *Rev Sci Tech*. 11(2):539-50

Manson J, West JD, Thomson V, McBride P, Kaufman MH, Hope J. 1992. The prion protein gene: a role in mouse embryogenesis? *Development* 115:117–22

Meriin, A. B. *et al.*2002. Huntington toxicity in yeast model depends on polyglutamine aggregation mediated by a prion-like protein Rnq1. *J. Cell Biol.* **157**, 997–1004.

Moriyama, H., H.K. Edskes and R.B. Wickner (2000) [URE3] prion propagation in Saccharomyces cerevisiae: requirement for chaperone Hsp104 and curing by overexpressed chaperone Ydj1p. Mol. Cell Biol. 20, 8916-22.

Morimoto A, Irie K, Murakami K, Masuda Y, Ohigashi H, Nagao M, Fukuda H, Shimizu T, Shirasawa T. 2004. Analysis of the secondary structure of beta-amyloid (Abeta42) fibrils by systematic proline replacement. *J Biol Chem.* 279:52781-52788.

Morales R, Estrada LD, Diaz-Espinoza R, Morales-Scheihing D, Jara MC, Castilla J, Soto C. 2010. Molecular cross talk between misfolded proteins in animal models of Alzheimer's and prion diseases. *J Neurosci.* 30(13):4528-35.

Muramoto, T., Scott, M., Cohen, F. & Prusiner, S. B. (1996). Recombinant scrapie-like prion protein of 106 amino acids is soluble. Proc. Natl Acad. Sci. USA, 93, 15457-15462.

Nakayashiki T, Kurtzman CP, Edskes HK, Wickner RB. 2005. Yeast prions [URE3] and [PSI+] are diseases. *Proc Natl Acad Sci U S A.* 102(30):10575-80.

Nemecek J, Nakayashiki T, Wickner RB. 2009, A prion of yeast metacaspase homolog (Mca1p) detected by a genetic screen. *Proc Natl Acad Sci U S A.* 106(6):1892-6.

Nelson R, Sawaya MR, Balbirnie M, Madsen AØ, Riekel C, Grothe R, Eisenberg D. 2005. Structure of the cross-beta spine of amyloid-like fibrils. *Nature.* 435(7043):773-8.

Newnam GP, Wegrzyn RD, Lindquist SL, Chernoff YO. 1999. Antagonistic interactions between yeast chaperones Hsp104 and Hsp70 in prion curing. *Mol Cell Biol.* 19(2):1325-33.

Norstrom, E.M. and Mastrianni, J.A. (2005) The AGAAAAGA palindrome in PrP is required to generate a productive PrPSc–PrPC complex that leads to prion propagation. J. Biol. Chem. 280, 27236–27243.

Osherovich, L.Z. and J.S. Weissman (2001) Multiple Gln/Asn-rich prion domains confer susceptibility to induction of the yeast [*PSI*+] prion. *Cell* 106: 183-194.

Pan, K. M., Baldwin, M., Nguyen, J., Gasset, M., Serban, A., Groth, D., Mehlhorn, I., Huang, Z., Fletterick, R. J., Cohen, F. E. and et al. (1993) *Proc. Natl. Acad. Sci. USA* 90, 10962-6.

Patel BK, Gavin-Smyth J, Liebman SW. 2009. The yeast global transcriptional co-repressor protein Cyc8 can propagate as a prion. *Nat Cell Biol*. 11(3):344-9.

Paushkin SV, Kushnirov VV, Smirnov VN, Ter-Avanesyan MD. 1996. Propagation of the yeast prion-like [psi+] determinant is mediated by oligomerization of the SUP35-encoded polypeptide chain release factor. *EMBO J*. 15(12):3127-34.

Patino MM, Liu JJ, Glover JR, Lindquist S. 1996. Support for the prion hypothesis for inheritance of a phenotypic trait in yeast. *Science*. 273(5275):622-6.

Parsell, D.A., Kowal, A.S., Singer, M.A., and Lindquist, S. 1994. Protein disaggregation mediated by heat-shock protein Hsp104. *Nature* 372, 475–478.
Prusiner SB. 1998. Prions. Proc Natl Acad Sci U S A. 95(23):13363-83.

Peretz, D., R. A. Williamson, Y. Matsunaga, H. Serban, C. Pinilla, R. B. Bastidas, R. Rozenshteyn, T. L. James, R. A. Houghten, F. E. Cohen, S. B. Prusiner, and D. R. Burton. 1997. A conformational transition at the N-terminus of the prion protein features in formation of the scrapie isoform. *J. Mol. Biol.* 273:614–622.

Price NC, Stevens E. 1983. The denaturation of rabbit muscle phosphorylase b by guanidinium chloride. *Biochem J*. 213(3):595-602.
Prusiner SB. Novel proteinaceous infectious particles cause scrapie. *Science* 1982 Apr 9;216(4542):136-44.

Prusiner, S.B., M.R. Scott, S.J. De Armond and F.E. Cohen (1998) Prion protein biology. *Cell* 93: 337-348.

Prusiner, S. B. 1998. Prions. *Proc. Natl. Acad. Sci. U.S.A.* 95: 13363–13383.

Weissmann, C. Molecular biology of prion disease. *Trends Cell Biol.* **4,** 10 (1994).
Peretz, D., Williamson, R. A., Matsunaga, Y., Serban, H., Pinilla, C., Bastidas, R. B., Rozenshteyn, R., James, T. L., Houghten, R. A., Cohen, F. E., Prusiner, S. B., and Burton, D. R. 1997. A conformational transition at the N terminus of the prion protein features in formation of the scrapie isoform. J. Mol. Biol. 273, 614–622

Riek R, Hornemann S, Wider G, Billeter M,Glockshuber R, Wuthrich K. 1996. NMR structure of the mouse prion protein domain PrP (121-231). *Nature* 382:180–82

Roberson, E. D. and L. Mucke (2006) 100 years and counting: prospects for defeating Alzheimer's disease. *Science* **314**(5800): 781-4.

Ross ED, Edskes HK, Terry MJ, Wickner RB. 2005. Primary sequence independence for prion formation. *Proc Natl Acad Sci U S A*. 102(36):12825-30.

Saifitdinova AF, Nizhnikov AA, Lada AG, Rubel AA, Magomedova ZM, Ignatova VV, Inge-Vechtomov SG, Galkin AP. 2010. [NSI (+)]: a novel non-Mendelian nonsense suppressor determinant in Saccharomyces cerevisiae. *Curr Genet.* 56(5):467-78.

Sanchez Y, Lindquist SL. 1990. HSP104 required for induced thermotolerance. *Science.* 248(4959):1112-5.

Shao J, Diamond MI. Polyglutamine diseases: emerging concepts in pathogenesis and therapy. *Human Mol. Genet.* 2007 Spec No. 2: R115-R123.

Sambrook, J. and D.W. Russel, *Molecular Cloning: A laboratory Manual (3rd Edition)*, in *Cold Spring Harbor Laboratory Press*. 2001.

Shorter J, Lindquist S. 2005. Prions as adaptive conduits of memory and inheritance. *Nat Rev Genet.* 6(6):435-50.

Sondheimer N, Lindquist S. 2000. Rnq1: an epigenetic modifier of protein function in yeast. *Mol Cell.* 5(1):163-72.

Sondheimer N, Lindquist S. 2000. Rnq1: an epigenetic modifier of protein function in yeast. Mol Cell. 5(1):163-72.

Solomon IH, Schepker JA, Harris DA. 2009. Prion Neurotoxicity: insights from prion protein mutants. *Curr Issues Mol Biol.* 12(2):51-62.

Speransky VV, Taylor KL, Edskes HK, Wickner RB, Steven AC. 2001.Prion filament networks in [URE3] cells of Saccharomyces cerevisiae. *J Cell Biol.* 153(6):1327-36.

Tanaka M, Chien P, Naber N, Cooke R, Weissman JS. 2004. Conformational variations in an infectious protein determine prion strain differences. *Nature.* 428(6980):323-8.

Ter-Avanesyan MD, Dagkesamanskaya AR, Kushnirov VV, Smirnov VN. 1994. The SUP35 omnipotent suppressor gene is involved in the maintenance of the non-Mendelian determinant [psi+] in the yeast Saccharomyces cerevisiae. *Genetics.* 137(3):671-6.

Thal DR, Capetillo-Zarate E, Del Tredici K & Braak H (2006) The development of amyloid b protein deposits in the aged brain. *Sci Aging Knowledge Environ* 2006, re1.

Toombs JA, McCarty BR, Ross ED. 2010. Compositional determinants of prion formation in yeast. *Mol Cell Biol.* 30(1):319-32.

Tong AH, Evangelista M, Parsons AB, Xu H, Bader GD, Pagé N, Robinson M, Raghibizadeh S, Hogue CW, Bussey H, Andrews B, Tyers M, Boone C. 2001. Systematic genetic analysis with ordered arrays of yeast deletion mutants. *Science*. 294(5550):2364-8.

Tong AH, Boone C. 2006. Synthetic genetic array analysis in Saccharomyces cerevisiae. *Methods Mol Biol*. 313:171-92.

True,H.L.and Lindquist,S.L. (2000) A yeast prion provides a mechanism for genetic variation and phenotypic diversity. *Nature* 407, 477–483

Tuite MF, Mundy CR, Cox BS. 1981. Agents that cause a high frequency of genetic change from [psi+] to [psi-] in Saccharomyces cerevisiae. *Genetics* 98:691-711.

van der Kamp MW, Daggett V. 2009. The consequences of pathogenic mutations to the human prion protein. *Protein Eng Des Sel*. 22(8):461-8

Vishveshwara N, Bradley ME, Liebman SW. 2009. Sequestration of essential proteins causes prion associated toxicity in yeast. *Mol Microbiol*. 73(6):1101-14.

von der Haar, T., Jossé, L., Wright, P., Zenthon, J. & Tuite, M. F. 2007. Development of a novel yeast cell-based system for studying the aggregation of Alzheimer's disease-associated αβ peptides *in vivo*. *Neurodegener. Dis.* **4**, 136–147

Wang Y, Meriin AB, Zaarur N, Romanova NV, Chernoff YO, Costello CE, Sherman MY. 2009. Abnormal proteins can form aggresome in yeast: aggresome-targeting signals and components of the machinery. *FASEB J.* 23(2):451-63.

Wells GAH, Scott AC, Johnson CT, Gunning RF, Hancock RD, et al. 1987. A novel progressive spongiform encephalopathy in cattle.*Vet. Rec.* 31:419–20

Wickner RB. 1994. Evidence for a prion analog in *S. cerevisiae*: the [URE3] non-Mendelian genetic element as an altered *URE2* protein. *Science* 264:566–69

Wickner S, Maurizi MR, Gottesman S. 1999. Posttranslational quality control: folding, refolding, and degrading proteins. *Science*. 286(5446):1888-93.

Will RG. Surveillance of prion diseases in humans. In: Baker HF, Ridley RM, eds. Prion Diseases. Totawa, NJ: Humana Press, 1996; 119–137.

Wille, H., Michelitsch, M. D., Guenebaut, V., Supattapone, S., Serban, A., Cohen, F. E., Agard, D. A. and Prusiner, S. B. (2002) *Proc. Natl. Acad. Sci. USA* 99, 3563-8.

Williams ES, Young S. 1980. Chronic wasting disease of captive mule deer: a spongiform encephalopathy. *J. Wildl. Dis.* 16:89–98

Wyatt JM, Pearson GR, Smerdon TN, Gruffydd-Jones TJ, Wells GAH, Wilesmith JW. 1991. Naturally occurring scrapie-like spongiform encephalopathy in five domestic cats. *Vet. Rec.* 129:233–36

Yang, W., Yang, H. & Tien, P. 2006. *In vitro* self-propagation of recombinant PrPSc-like conformation generated in the yeast cytoplasm. *FEBS Lett.* 580, 4231–4235.

Zahn, R., A. Liu, T. Luhrs, R. Riek, C. von Schroetter, F. L. Garcia, M. Billeter, L. Calzolai, G. Wilder, and K. Wuthrich. 2000. NMR solution structure of the human prion protein. *Proc. Natl. Acad. Sci. U.S.A.* 97:145–150.

VITA

Meng Sun was born in Beijing, China on August 12th, 1983. He obtained his Bachelor's of Science in Life Sciences in June 2005 from Fudan University in Shanghai, China. He came to Georgia Institute of Technology in Atlanta, GA to pursue his Doctoral degree from August 2005 to August 2011.